SUPPLEMENTARY INFORMATION

Biosynthesis of Oxygenated Brasilane Terpene Glycosides Involves a Promiscuous *N*-Acetylglucosamine Transferase

Jin Feng[†], Frank Surup,[‡] Maurice Hauser,[†] Anna Miller,[†] Jan-Peer Wennrich, [‡] Marc Stadler,[‡] Russell J. Cox,[†] Eric Kuhnert[†,*]

[†]Institute for Organic Chemistry and Centre for Biomolecular Drug Research (BMWZ), Leibniz University Hannover, Schneiderberg 38, Hannover 30167, Germany

[‡]Department Microbial Drugs, Helmholtz Centre for Infection Research (HZI), Inhoffenstraße 7, 38124 Braunschweig, Germany

Table of Contents

S1. Experimental Details Page 1

S2. Structure elucidation Page 7

S3. Tables Page 10

S4. Figures Page 13

S5. HPLC chromatograms Page 14

S6. Compound **1 - 3, 5 - 7** physical data Page 26

References Page 87

S1 Experimental Details

S1.1 Reagents

Analytical grade chemicals and reagents were purchased from Sigma, Roth and Fischer. The solvents used for HPLC were analytical grade. Molecular biology kits were used according to the manufacturer's protocols. Analytical PCR was performed using OneTaq polymerase and preparative PCR was performed using Q5 polymerase. Restriction endonucleases were purchased from NEB or Thermofisher Scientific.

S1.2 Production and isolation of brasilane-type terpenoids

The ascospore-derived isolate *Annulohypoxylon truncatum* CBS 140778[1] was grown in a 500 mL Erlenmeyer flask containing 200 mL YMG medium (1.0 % malt extract, 0.4 % glucose, 0.4 % yeast extract, pH 6.3) as seed culture on a shaker for 5 days at 25°C and 140 rpm. Two 5 L Erlenmeyer flasks with 2 L YMG medium (total volume 4 L) were each inoculated with 10 mL of the homogenized seed culture and incubated for 9 days under the same conditions. Afterwards, the biomass was separated from the culture broth by vacuum filtration and the supernatant was incubated with 40 g Amberlite XAD-16N resin (Sigma-Aldrich) for 4 h under shaking conditions. The filtered absorber resin was then extracted with 1 L acetone and the organic solvent was evaporated to yield 1 g crude extract. The latter was pre-fractionated by flash chromatography using a Reveleris X2 purification system (Büchi, Flawil, Switzerland) equipped with a Reveleris Silica 40 g column and an ELS detector. A two-stage gradient (flowrate of 40 mL/min) with dichloromethane (DCM, solvent A1) and DCM/acetone (8:2,

solvent B1) in the first stage was applied going from 0 % to 20 % B in 9.5 min. For the second stage solvent B and DCM/acetone/methanol (8:2:3, solvent C) were used starting with a linear gradient from 20 % to 60 % C in 9.5 min, followed by 60 % to 100 % C in 5 min and finished with isocratic conditions (100 % C) for 5 min. Fractions between 16 and 20 min were combined (112 mg) and forwarded to a second round of flash chromatography using a Reveleris Silica 12 g column and a linear gradient (flowrate of 30 mL/min) with solvent A and B from 0 % to 100 % B in 25 min. Fractions between 10 and 15 min were combined (48 mg), which contained a mixture of brasilane A **1** and E **3**. Fractions between 15 and 18 min (37 mg combined) contained semi-pure quantities of brasilane D **2**. For final purification the mixture of 1 and 3 was separated on a preparative HPLC system (Gilson, Middleton, USA) equipped with a GX-271 Liquid Handler, a 172 DAD, a 305 and 306 pump (with 50SC Piston Pump Head). As stationary phase a VP 250/21 Nucleodur 100-5 C18 ec column (Macherey–Nagel) was used and the mobile phase was composed of deionized water with 0.5% acetic acid (solvent D) and acetonitrile with 0.5% acetic acid (solvent E). A linear gradient from 45 % to 80 % solvent E in 24 min with a flow rate set to 20 ml/min was applied to yield **3** at a retention time (R_t) of 8 min (7.3 mg) and **1** at R_t = 15 min (2.4 mg). To further purify **2** the same preparative HPLC conditions were used. **2** eluted after 6.2 min and 2.9 mg of pure compound was obtained.

S1.3 Genome sequencing and *bra* cluster identification

The genome of *A. truncatum* was sequenced with a combination of Oxford Nanopore and Illumina technology as previously published[2]. Gene prediction was performed by applying Augustus version 3.2[3] and GeneMark-ES 4.3.6.[4] using default settings. For Augustus, species parameter sets were established based on GeneMark-ES fungal version predictions. Predicted genes were functionally annotated using a modified version of the genome annotation platform GenDB 2.0[5] for eukaryotic genomes as previously described.[6]

Candidate gene clusters were preliminarily identified by manual blastp searches against an *A. truncatum* protein database using the Tvi09626[7] and TaTC6 brasilane synthase (LC484924)[8] as template. Nine terpene cyclases with homology to the latter were identified, but only one (*bra*) was associated with the predicted tailoring genes (glycosyl transferase and monooxygenase). We also found identical gene cluster in related genome-sequenced species of the Hypoxylaceae[2] (*Hypomontagnella monticulosa, Hypoxylon pulicicidum, Hypoxylon rubiginosum, Jackrogersella multiformis*) (Figure S2), some of which were able to produce compounds **1** – **3** (data not shown). The high similarity of the *bra* cluster sequences enabled us to validate the respective coding sequences from *A. truncatum* (Figure S2) due to the availability of transcriptome data for *Hypom. monticulosa*.[2] A sequence error (two missing nucleotides) at the beginning of the coding region of *braB* led to a substantial reading frame shift, which was confirmed by re-sequencing of the respective locus. The *braC* gene had a slightly shortened first exon due to an erroneous gene prediction, while the *braA* sequence was in accordance with the one from *Hypom. monticulosa*.

The re-annotated *A. truncatum bra* cluster was uploaded to GenBank and can be accessed under the accession number MT383109. Protein sequences of the respective enzymes are listed in Table S1.

S1.4 Heterologous Expression of the *bra* cluster in *Aspergillus oryzae*

A 5 days old liquid culture of *A. truncatum* grown in YMG medium was used for genomic DNA extraction. The mycelium was separated from the culture broth by vacuum filtration and ground to a fine powder in a mortar under liquid nitrogen. For the genomic DNA preparation, the GeneEluteTM Plant Genomic DNA Miniprep Kit (Sigma Life Science) was used following the manufacturer's

instructions. For the heterologous expression studies in *A. oryzae*, the genes of interest (*braA*, *braB*, *braC*) were directly amplified from the gDNA using the primer sets listed in Table S2. PCR was performed from gDNA using OneTaq DNA Polymerase (New England Biolabs) or Q5 DNA Polymerase (New England Biolabs) and sequences were checked by DNA sequencing (Mix2Seq kit, Eurofins). For vector construction the destination plasmid pTYGS-arg with *argB* as auxotropic marker was used.[9] Targeted genes in different combination were cloned into the vector by yeast homologous recombination applying previously described methods.[10] Plasmids were purified from yeast using the Zymoprep™ Yeast Plasmid Miniprep II kit (Zymo Research), transformed into *ccdB* Survival™ 2 T1R *E. coli* cells for amplification, screened by colony PCR and purified using the NucleoSpin™ Plasmid kit (Machery-Nagel). A list of the final vectors used in this study can be found in Table S3.

Transformation of the quadruple auxotrophic hosts *A. oryzae* NSAR1[11] was achieved by using previously described methods.[10] Transformation plates were composed of CZD/S bottom medium (3.5 % Czapek Dox broth, 1 M sorbitol, 0.05 % adenine, 0.15 % methionine, 0.1 % ammonium sulphate, 1.5 % agar) and CZD/S top medium (3.5 % Czapek Dox broth, 1 M sorbitol, 0.05 % adenine, 0.15 % methionine, 0.1 % ammonium sulphate, 0.8 % agar). Selection was performed on CZD medium (3.5 % Czapek Dox broth, 0.05 % adenine, 0.15 % methionine, 0.1 % ammonium sulphate, 1.5 % agar).

S1.5 Screening of transformants and isolation of brasilane-type terpenoids

After two rounds of selection, transformants were transferred to DPY (2.0 % dextrose from potato starch, 1.0 % polypeptone, 0.5 % yeast extract, 0.5 % monopotassium phosphate, 0.05 % magnesium sulfate hexahydrate) plates and grown for 5 – 7 days. Mycelia of the transformants was then scratched from the plates and mixed with 10 mL distilled water. Half of the suspension was transferred to 250 ml Erlenmeyer flasks containing 100 mL DPY liquid media and cultivated in a shaking incubator for 5 days at 28 °C and 110 rpm.

The culture broth of each transformant was filtered by vacuum filtration in a Büchner funnel to remove the mycelia and the remaining filtrate was extracted twice with the same volume of ethyl acetate. The organic phases were combined and evaporated to dryness. The crude extracts were dissolved in 1.5 mL methanol and centrifuged to remove the impurity for LCMS analysis.

For compound isolation the transformants (*A. oryzae braA*, *A. oryzae braAB*, *A. oryzae braABC*) were fermented in 1 L scale (10 flasks each containing 100 mL DPY media) under screening conditions. Culture filtrates were combined and extracted twice with equal amounts of ethyl acetate. The crude extracts were dissolved in methanol and centrifuged to remove the impurity prior to fractionation by preparative HPLC.

Fractionation of the *A. oryzae braAB* (90 mg) and *A. oryzae braABC* (78 mg) crude extracts was achieved by preparative reversed-phase HPLC using a Waters LCMS system comprised of a Waters 2767 autosampler, Waters 2545 pump, a Phenomenex Kinetex Axia column (5 µm, C18, 100 Å, 21.2 x 250 mm) equipped with a Phenomenex Security Guard precolumn (Luna, C5, 300 Å) and a flow rate of 20 mL/min. Detection was carried out by a diode array detector (Waters 2998) in the range of 210 to 600 nm and an ELSD detector (Waters 2424) together with a Waters SQD-2 mass spectrometer operating simultaneously in ES+ and ES− modes between 150 and 1000 m/z. The mobile phase was composed of HPLC-grade water mixed with 0.05 % formic acid (solvent A2) and HPLC-grade acetonitrile mixed with 0.045 % formic acid (solvent B2). For separation of the *A. oryzae braAB* crude extract a linear gradient was applied starting at 10 % B2 and ramping up to 90 % B2 in 15 min. Compound **1** (23 mg) eluted after 10 min. The same gradient was used for fractionation of the *A.*

oryzae braABC crude extract resulting in pure amounts of compound **2** (2 mg, R_t = 7.4 min) and compound **3** (8 mg, R_t = 7.9 min).

Fractionation of the *A. oryzae braA* crude extract was achieved by preparative reversed-phase HPLC on a Gilson PLC 2250. A VP Nucleodur® 100-5 C18ec column (250 x 21 mm, 5 µm) connected to a Kromasil® 100 C18 pre-column (50 x 20 mm, 7 µm; AkzoNobel, Bohus, Sweden) served as stationary phase. The mobile phase was composed of Milli-Q water (Millipore Schwalbach, Germany; solvent A3) supplemented with 0.05 % trifluoroacetic acid (TFA) and acetonitrile (HPLC-grade; solvent B3) supplemented with 0.05 % TFA. The yellowish extract (80 mg) was dissolved in 1.2 mL of methanol and separation was accomplished with the following elution conditions at a flow rate of 20 mL/min: isocratic conditions at 5 % solvent B3 for 5 min → linear gradient of B3 from 5 % to 25 % in 10 min → linear gradient of B2 from 25 % to 50% in 30 min → linear gradient of B3 from 50 % to 100 % in 10 min. UV detection was carried out at λ = 220, 280, 330 nm and with an additional scan from 200 to 600 nm. **5** (1.5 mg) was obtained at R_t = 40.2 min and **6** (3.2 mg) eluted after 37.2 min.

S1.6 Feeding of *A. oryzae braAC* transformants with 1

Aspergillus oryzae braAC was cultivated in 100 mL DPY media for 2 days under screening conditions and then 1.5 mg of brasilane A **1** dissolved in 100 µL methanol were fed to the culture. Incubation was continued for two more days before filtration and extraction of the supernatant with ethyl acetate. The crude extract was dissolved in methanol and analysed by LCMS (Figure S4).

S1.7 Expression and purification of BraA

For protein expression of the terpene cyclase BraA in *E. coli* BL21(DE3), the *braA* gene was amplified from *A. oryzae braA* cDNA. RNA was obtained by growing *A. oryzae braA* for 4 days in DPY liquid medium at 28 °C and 110 rpm and subsequent RNA extraction of the mycelia using the Quick-RNA Fungal/Bacterial Miniprep Kit (Zymo Research, Irvine, CA, USA). RNA was transcribed into cDNA applying the High Capacity RNA-to-DNA kit (Applied Biosystems, Foster City, CA, USA). The *braA* gene was cloned into the pET28a+ plasmid by yeast heterologous combination according to the literature[10]. The purified vector was transformed into *E. coli* BL21(DE3) by standard heat shock method. 5 mL of LB medium supplemented with 50 µg/mL kanamycin was inoculated with the transformed host and grown overnight at 37 °C and 200 rpm. 1 ml of the seed culture was transferred to 1 L LB medium (+ 50 µg/mL kanamycin) and equally distributed between 10 baffled 500 mL Erlenmeyer flasks. The cultures were cultivated at 37 °C and 200 rpm for 3 – 4 hours until the OD600 reached approximately 0.5. To induce the protein expression 0.5 mM IPTG was added to the flasks. After overnight growth at 16 °C and 200 rpm, the cells were harvested by centrifugation (9,000 g, 3 min, 4 °C). The cell pellet was resuspended in 40 mL lysis buffer (50 mM Tris/HCl pH 8.0, 150 mM NaCl, 10 % glycerol (v/v), 20 mM imidazole) and then lysed by sonication followed by centrifugation (10,000 g, 20 min, 4 °C) to remove the debris. All purification steps were carried out on an $ÄKTA_{FPLC}$ (GE Healthcare) with a 5 mL nickel affinity HisTrap FF column (GE Healthcare). The target protein was eluted of the column with elution buffer (50 mM Tris/HCl pH 8.0, 150 mM NaCl, 10 % glycerol (v/v), 500 mM imidazole) and detected by UV. Fractions with strong UV signals were combined and solution was replaced by storage buffer (50 mM Tris/HCl pH 7.5, 20 % glycerol (v/v)) using an Amicon Ultra-15 centrifugal filter (Millipore, 30K) and finally concentrated in 0.5 mL volumes. The protein concentration was assessed with a spectrophotometer and the protein was stored at -80 °C. Purified protein was analyzed by SDS-PAGE.

S1.8 Expression and purification of BraB

For protein expression of the *N*-acetylglucosamine transferase BraB in *E. coli* BL21(DE3) a commercially synthesized vector (BaseClear, Leiden, Netherlands) based on the pET28a+ plasmid was used. Therein, the codon-optimized gene sequence of *braB* was inserted downstream of the T7 promoter.

Transformation of the vector into *E. coli* BL21(DE3) and protein purification followed the method described in S1.7. The protein concentration was assessed with a spectrophotometer and the protein was stored at -80 °C. Purified protein was analyzed by SDS-PAGE.

S1.9 *In-vitro* enzyme assays with BraA

To identify the product of BraA, the enzyme was tested in 300 µL reaction volumes containing Tris/HCl buffer, 150 µg BraA, 500 µM FPP, 5 mM $MgCl_2$ and 5 mM DTT. The solution was incubated at 28 °C for 30 min and extracted with 300 µL pentane. The organic phase was analysed by GC-MS (Figure S5).

S1.10 *In-vitro* enzyme assays with BraB

Acceptor substrate specificity of BraB was assessed in 100 µL reaction volumes containing CutSmarter Buffer (NEB), 2 mM UDP-GlcNAc, 200 µg of purified enzyme and 0.5 mM substrate (geraniol, linalool, perillyl alcohol, menthol, benzyl alcohol, serine, serotonin, or 3,4-dichlorophenol). The reaction mixtures were incubated at 37 °C overnight and extracted by adding 200 µL ethyl acetate. The organic phase was dried and dissolved in 200 µL MeOH for LCMS analysis (Figure S10-S14). For negative control, the enzyme was deactivated by heat (95 °C for 5 min) prior to *in-vitro* reaction.

Donor substrate specificity of BraB was tested in 100 µL reaction volumes containing 10 µL 10x CutSmarter Buffer (NEB), 10 µM UDP-sugar (UDP-GlcNAc, UDP-glucose, or UDP-galactose), 100 µg of BraB, 150 µg of BraA, 100 µM FPP and 5 mM DTT. The reaction mixtures were incubated at 30 °C overnight and extracted by adding 200 µL ethyl acetate. The organic phase was dried and dissolved in 200 µL MeOH for LCMS analysis (Figure S6-S8).

In addition, donor substrate specificity of BraB was tested with perillyl alcohol as alternative acceptor substrate in 100 µL reaction volumes containing CutSmarter Buffer (NEB), 2 mM UDP-sugar (UDP-GlcNAc, UDP-glucose, or UDP-galactose), 200 µg of purified enzyme and 0.5 mM perillyl alcohol. The reaction mixtures were incubated at 37 °C overnight and extracted by adding 200 µL ethyl acetate. The organic phase was dried and dissolved in 200 µL MeOH for LCMS analysis (Figure S15).

To further assess the preferences of BraB for UDP-sugar, a competition assay was conducted. For this purpose, a reaction assay in triplicate was prepared with a mixtures of UDP-GlcNAc and UDP-Glc. The reaction mixtures were composed of 10 µL 10x CutSmarter Buffer (NEB), 200 µg of BraB, 150 µg of BraA, 200 µM FPP, 5 mM DTT and 100 µM of each UDP-sugar. The reaction mixtures were incubated at 30 °C for 10 h and extracted by adding 200 µL ethyl acetate. The organic phase was dried and dissolved in 200 µL MeOH for LCMS analysis (Figure S9).

S1.11 *In-vivo* enzyme assays with BraB

100 µL of *E. coli* pTYGS-arg-BraB seed culture was transferred to 100 mL LB medium (+ 50 µg/mL kanamycin) in a baffled 500 mL Erlenmeyer flask. The culture was cultivated at 37 °C and 200 rpm for 3 – 4 hours until the OD600 reached approximately 0.5. To induce the protein expression 0.5 mM IPTG was added to the flask and 5 mg perillyl alcohol dissolved in 100 µL methanol was fed to the culture simultaneously. After overnight growth at 16 °C and 200 rpm, the culture was extracted with two

volumes of ethyl acetate. The organic phase was concentrated to dryness and dissolved in methanol for LCMS analysis (Figure S13).
For compound isolation a large-scale fermentation (1 L) was conducted. The *E. coli* transformant was cultivated in 10 baffled 500 mL Erlenmeyer flasks. The induction, feeding (7.5 mg perillyl alcohol per flask) and extraction were performed with the same conditions as described before.

Fractionation of half of the crude extract was achieved by preparative reversed-phase HPLC (Gilson GX270, for specific instrumental data see S1.2). A VP Nucleodur® 100-5 C18ec column (250 x 21 mm, 5 µm) conntected to a Kromasil® 100 C18 pre-column (50 x 20 mm, 7 µm) served as stationary phase. The mobile phase was composed of Milli-Q water (Millipore Schwalbach, Germany; solvent A2) supplemented with 0.05 % trifluoroacetic acid (TFA) and acetonitrile (HPLC-grade; solvent B2) supplemented with 0.05 % TFA. The yellowish extract (89 mg) was dissolved in 1.2 mL of methanol. The separation was accomplished over two runs with the following elution conditions at a flow rate of 20 mL/min: isocratic conditions at 5 % solvent B2 for 5 min → linear gradient of B2 from 5 % to 25 % in 10 min → linear gradient of B2 from 25 % to 50% in 30 min → linear gradient of B2 from 50 % to 100 % in 10 min. UV detection was carried out at λ = 190, 200 and 220 nm. Compound **7** (5 mg) was obtained in pure amounts at a R_t of 28 min.

S1.12 Analytical HPLC-MS

Analytical LCMS data was obtained using a Waters LCMS system comprising of a Waters 2767 autosampler, Waters 2545 pump, a Phenomenex Kinetex column (2.6 µm, C18, 100 Å, 4.6 x 100 mm) equipped with a Phenomenex Security Guard precolumn (Luna, C5, 300 Å) and a flow rate of 1 mL/min. Detection was carried out by a diode array detector (Waters 2998) in the range of 210 to 600 nm and an ELSD detector (Waters 2424) together with a Waters SQD-2 mass spectrometer operating simultaneously in ES+ and ES− modes between 150 and 1000 m/z. The mobile phase was composed of HPLC-grade water mixed with 0.05 % formic acid (solvent A2) and HPLC-grade acetonitrile mixed with 0.045 % formic acid (solvent B2). A solvent gradient was run over 15 min starting at 10 % B2 and ramping up to 90 % B2. In case of the competition assay (S1.10) a shallower gradient was applied ramping from 10 to 50 % B2 in 15 min.

S1.12 GC-MS

GC-MS data were obtained on 6890N Network GC system (Agilent Technologies, Santa Clara, CA, USA) combined with a 5973 inert Mass Selective Detector (Agilent Technologies). The GC was equipped with an Agilent HP-5MS capillary column (30 m, 0.25 mm, 0.25 µm, 5% Diphenyl / 95% Dimethylpolysiloxan). The following GC parameters were used for analysis: inlet pressure 20.96 psi; split mode (5:1); split flow 10 mL/min; carrier gas helium; saver flow 30 mL/min; saver time 2 min; injection volume 1 µL; temperature gradient starting at 100 °C for 2 min, increasing at 2 °C/min to 180 °C, then increasing at 40 °C/min to 300 °C. Mass spectra were recorded under the following conditions: source temperature 230 °C, quadrupole temperature 150 °C, mass range 43.0 – 600.0

S1.13 HRMS and NMR Instrumentation

NMR data were recorded with a Bruker AVII-600 spectrometer equipped with a BBFO SmartProbe, a Bruker Avance III 500 MHz spectrometer equipped with a BBFO(plus) SmartProbe (^{1}H 500 MHz, ^{13}C 125 MHz), and a Bruker Avance III 700 MHz spectrometer equipped with a 5 mm TCI cryoprobe (^{1}H 700 MHz, ^{13}C 175 MHz). Chemical shifts δ were referenced to methanol-d_4 (^{1}H, δ = 3.31 ppm; ^{13}C, δ = 49.15 ppm), chloroform-*d* (^{1}H, δ = 7.27 ppm; ^{13}C, δ = 77.00 ppm), acetone-d_6 (^{1}H, δ = 2.05 ppm; ^{13}C, δ = 29.92 ppm), acetonitril-d_3 (^{1}H, δ = 1.94 ppm; ^{13}C, δ = 1.39 ppm), benzene-d_6 (^{1}H, δ = 7.16 ppm; ^{13}C, δ = 128.39 ppm), DMSO-d_6 (^{1}H, δ = 2.50 ppm; ^{13}C, δ = 39.51 ppm) and pyridin-d_5 (^{1}H, δ = 7.22 ppm; ^{13}C,

δ = 123.87 ppm). HR-ESI-MS measurements were conducted on a maXis ESI-TOF (Bruker Daltonics) mass spectrometer coupled to an Agilent 1200 Infinity Series HPLC system (Agilent Technologies). An Acquity UPLC BEH C18 column (Waters, Milford, USA; 2.1 x 50 mm, 1.7 µm) was used as stationary phase. Compounds were eluted with solvent A (Milli-Q water + 0.1% formic acid) and solvent B (HPLC-grade acetonitrile + 0.1% formic acid) using a flow rate of 0.6 mL/min and the following gradient: 5 % B for 0.5 min increasing to 100 % B in 19.5 min and then maintaining 100 % B for 5 min. UV/vis spectra was detected in the range of 200–600 nm. Mass spectra were recorded in positive ionisation mode (ESI+) with a scan range of 100–2500 m/z, a temperature of 200 °C and capillary voltage of 4500 V.

S2 Structure elucidation

Metabolite **1** was isolated as a colorless oil. Its molecular formula $C_{23}H_{39}NO_6$ was deduced from its pseudomolecular ion peak cluster at *m/z* 426.2840 in the HRESIMS spectrum. Its ^{1}H and HSQC spectra revealed the presence of five methyls, six aliphatic methylenes and eight methines. The ^{13}C spectrum indicated the additional existence of one carbonyl, one quaternary aliphatic and two olefinic carbon atoms. A database search with this data within the Chapman & Halls Dictionary of Natural Products on DVD suggested metabolite **1** being brasilane A, whose identity was confirmed by the comparison of ^{13}C NMR data obtained in methanol-d_4 with those of Hu et al.[12]

However, we carefully reinvestigated the stereochemistry of **1**. A strong overlap of signals was observed in methanol-d_4, which prevented the analysis of the coupling constants and ROESY correlations necessary for the stereo chemical assignment. Therefore, we measured ^{1}H, ^{13}C and HSQC NMR spectra of **1** in chloroform-*d*, acetonitril-d_3, DMSO-d_6, benzene-d_6, aceton-d_6 and pyridine-d_5 to find a solvent in which the signals are less overlaid. Pyridine-d_5 turned out to be the best solvent for this analysis, since the only overlap was observed between 1–H and 4–H_b. Strong NOESY correlations were observed between 15-H_3 (δ_H 0.77) and 6–H (δ_H 1.85) as well as 2–H_{ax} (δ_H 1.09), confirming these protons to be on the same side of the molecule. The expected ROESY correlation between 1–H (δ_H 1.59) and 14–H_3 (δ_H 0.86) could not be assigned unambiguously, since the shift of 1–H (δ_H 1.59) is nearly the same as of 4–H_{ax} (δ_H 1.59) in pyridin-d_5. However, this NOESY correlation between 14–H_3 (δ_H 0.93) and 1–H (δ_H 1.64) was observed in benzene-d_6, in which the signal of 1–H was sufficiently separated from that of 4–H_{ax} (δ_H 1.71). The NOESY spectrum measured in benzene-d_6 furthermore allowed the detection of 1,3 diaxial couplings between 6–H (δ_H 1.98) and 4–H_{ax} (δ_H 1.71), 6–H (δ_H 1.98) and 2–H_{ax} (δ_H 1.20), and 2–H_{ax} (δ_H 1.20) and 4–H_{ax} (δ_H 1.71). Additionally, the *trans* configuration of 1–H/6–H was confirmed by the large coupling constant between these protons of $^{3}J_{H1H6}$ = 12.0 Hz, which was observed in the signal pattern of 6–H, establishing a diaxial conformation of both protons. Thus, the stereochemistry of brasilane A **1** has to be revised to 1*S**, 6*S**, 9*S**.

The colorless oil brasilane D **2** was analyzed for a molecular formula of $C_{23}H_{39}NO_7$ based on its quasimolecular ion cluster at *m/z* 442.2830 in the HRESIMS spectrum, implying the formal addition of an oxygen atom compared to **1**. The NMR data of **2** were highly similar to those of **1**, with the key difference being the replacement of the methyl group 12–H_3 by an oxymethylene (δ_C 61.2; δ_H 4.26, 4.33). HMBC correlation of 12–H_a and 12–H_b to C–5, C–10 and C–11 confirmed this assignment. Since the chemical shifts and coupling constants of **2** are comparable with those of **1**, the common 1*S**, 6*S**, 9*S** configuration was assigned for **2**.

Brasilane C **3** was also isolated as a colorless oil. The HRESIMS spectrum showed a quasimolecular ion cluster at *m/z* 456.2599, implying the molecular formula $C_{23}H_{37}NO_8$. The NMR data of **3** were very similar to those of **1**. However, an aldehyde moiety was observed (δ_H 9.85, δ_C 201.7) instead of methyl 12–H_3. Furthermore, carbon atoms C–5 (δ_C 71.5) and C–10 (δ_C 33) were shifted significantly to high

field, suggesting the bonding of oxygen atoms to both in place of the $\Delta^{5,10}$ double bond. Due to the molecular formula, an epoxide moiety was deduced. Analogously to **1**, the ROESY correlation between 15–H_3 and 6–H/2–H_a in combination with the one from 14–H_3 and 1–H revealed the relative configuration as 1*S**, 6*S**, 9*S**. ROESY correlations further enabled us to assign the two additional stereo centers of **3**. Since 4-H_a and 4–H_b show ROESY correlations to 11–H_b, the C–10 is in equatorial position in contrast to the axial epoxide, and **3** has a 1*S**, 5*R**, 6*S**, 9*S**, 10*R** configuration.

For brasilane F **5** a molecular formula of $C_{15}H_{26}O_2$ was deduced based on its HRESIMS data. The ^{1}H and HSQC data of **5** were highly characteristic for the aglycon part of **1**. However, instead of methylene 7–H_2 an oxymethine was observed. HMBC correlations from 15–H_3 to C–7/C–8/C–1 and COSY correlations between 8–H and 7–H_2 as well as 9–H confirmed this assignment. The relative configuration was assigned by ROESY correlations in analogy to brasilane A (**1**). In addition, a series of 1D NOE experiments confirmed the 1*R**, 6*S**, 8*R**, 9*R** stereochemistry. Finally, the free hydroxyl function of 8–H was utilized to assign the absolute stereochemistry of the metabolite family by Mosher's method. Positive $\Delta\delta^{SR}$ values for 7–Ha, 7–H_b, 4–H_b and 12–H_3, but negative ones for 1–H, 2–H_a, 2–H_b and 9–H of the MTPA ester derivatives indicated an 8*R* absolute configuration (see Figure S1).

Metabolite **6** was analyzed for a molecular formula of $C_{15}H_{24}O_3$ based on its HRESIMS data. The ^{1}H and HSQC data of **6** were very similar to those of **5**. However, instead of oxymethylene 11–H_2 and methylene 7–H_2 a carboxylic acid moiety and an oxymethine were observed, respectively. HMBC correlations from 12–H_3 to C–6/C–10/C–11 and 15–H_3 to C–7/C–8/C–1 confirmed this assignment. Since metabolite **6** has similarities with the known metabolite xylarenic acid, it is designated as xylarenic acid B. The relative and absolute configuration of xylarenic acid B **6** was determined analogously to that of brasilane F **6** by ROESY correlations and Mosher's method, respectively.

Mosher`s ester analysis

For the preparation of the (*S*)-MTPA ester of brasilane F **5**, 0.5 mg of **5** were dissolved in 600 µL of pyridine-d_5, and 10 µL of (*R*)-MTPA chloride were added. The mixture was incubated at 25 °C for 30 min before the measurement of ^{1}H, COSY, TOCSY and HSQC NMR spectra: ^{1}H NMR (700 MHz, pyridine-d_5): similar to **5**, but δ_H 5.09 (11-H_a), 5.08 (8-H), 4.89 (11-H_b), 2.73 (7-H_a), 2.37 (4-H_a), 2.04 (6-H), 2.03 (9-H), 2.37 (4-H_a), 1.93 (7-H_b), 1.92 (1-H), 1.77 (12-H_3), 1.62 (4-H_b), 1.22 (2-H_a), 1.05 (2-H_b), 0.95 (15-H_3), 0.88 (13-H_3), 0.77 (14-H_3). The (*R*)-MTPA ester was prepared in the same manner by the addition of 10 µL of (*S*)-MTPA chloride to 0.35 mg of **5**: ^{1}H NMR (700 MHz, pyridine-d_5): similar to **5**, but δ_H 5.07 (11-H_a), 5.07 (8-H), 4.90 (11-H_b), 2.70 (7-H_a), 2.40 (4-H_a), 2.14 (9-H), 2.03 (6-H), 1.94 (1-H), 1.80 (7-H_b), 1.72 (12-H_3), 1.65 (4-H_b), 1.25 (2-H_a), 1.06 (2-H_b), 0.95 (15-H_3), 0.89 (13-H_3), 0.75 (14-H_3).

Analogously, the (*S*)-MTPA ester of xylarenic acid B **6** was prepared by the addition of 10 µL of (*R*)-MTPA chloride to 0.5 mg of **6** dissolved in 600 µL of pyridine-d_5. The mixture was incubated at 25 °C for 30 min before the measurement of ^{1}H, COSY, TOCSY and HSQC NMR spectra: ^{1}H NMR (700 MHz, pyridine-d_5): similar to **5**, but δ_H 5.10 (8-H), 2.72 (7-H_a), 2.60 (4-H_a), 2.15 (6-H), 2.06 (9-H), 1.99 (4-H_b), 1.90 (7-H_b), 2.00 (1-H), 1.87 (12-H_3), 1.62 (4-H_b), 1.22 (2-H_a), 1.05 (2-H_b), 0.95 (15-H_3), 0.86 (13-H_3), 0.82 (14-H_3). The (*R*)-MTPA ester was prepared in the same manner by the addition of 10 µL of (*S*)-MTPA chloride: ^{1}H NMR (700 MHz, pyridine-d_5): similar to **5**, but δ_H 5.07 (8-H), 2.68 (7-H_a), 2.60 (4-H_a), 2.17 (9-H), 2.15 (6-H), 2.03 (1-H), 1.77 (7-H_b), 1.82 (12-H_3), 1.97 (4-H_b), 1.25 (2-H_a), 1.06 (2-H_b), 0.95 (15-H_3), 0.84 (13-H_3), 0.79 (14-H_3).

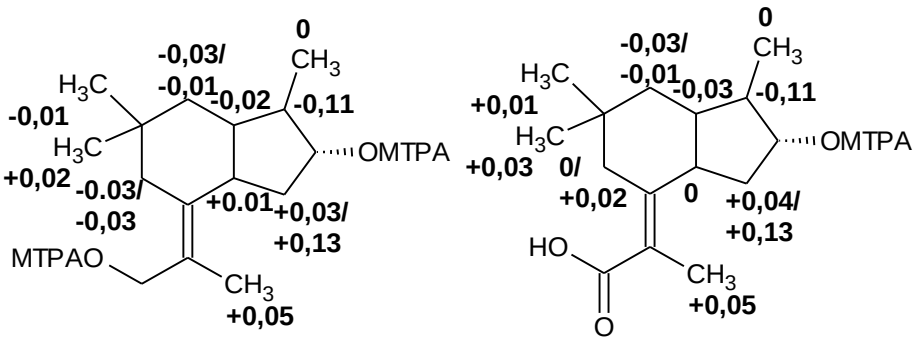

Figure S1 $\Delta\delta^{SR}$ values for MPTA esters of brasilane F **5** and xylarenic acid B **6**.

S3 Tables

Protein Name	Sequence
BraA	MAPDIDNIWSSTTDAAESPVDERRILLKRAVGQKILVPSILSLMPAWPSQVH PAVDEVNTEIDKWLPTVNVAEKKKAKHRARGNYAFLTAVYYPYCKETERLVV IAKFLYWIFFWDDEIDTGGELTEDEEGTIQCCEETNKCVDDCLGPNPNYNPP PNSRGTVEMFYPILRDFRAGLGPVSTERLRLELHDYINGVAKQQKVRQGERL PDPWYHFKIRSDDVGVIPSITQNEYAMKFELPEYVRRHEAMEEIVQECTKLT VLLNDVLSLQKEFRDSQLENLVLLFMNRYNLSLQAAVDKVLDLIREHYAICVA AEKRLPWSEDDEKLNDDIREYVRGCQRLATGTAYWSYSCERYFKQTQVNDK WEVLLDLSYVE
BraB	MVPSVMEGAPQLGITSTDTSSAGVPPGLKLIPTDRLDRRTDEEIAAWLQTRH PVTSDKNVWAFWHNGYTNMPPWVQRNIINWVRRLGPDWTVHLLDRVDG SATNVSHYVDSSFFPECFNNNTMDGPTVGQHSGDLVRLPLLWLYGGIWIDA GSFLFRHVEDICWNKIEDPESPYEMAGFVIEMRPGVEVMLNGFIAAKRGNP FIKRWLEIFKKLWDGATNVQGFHKHPLLRHLPMLCPPIDKLNLPPQGLNVV MEQFTDYMSQIMSFERLRKLVDPSDGFNGPEYYSNKMLLCSALQETFYFQL VTEWSGTKQFNLLSTKRKGEGVVKDENWHAAENFVHDALANTATMKLSHG PPGALDSFLADLWDSEEHHGKDNEDGTFAAYLRYGSVHFDQTREMVPIKM GWPDEEVLEAGVLEPKK
BraC	MASLYLPTIWASTLTAATIFIVAVLSKWLRKPRSFDVPIVGAESGDLNVLKARY VQEADALLREGYEKFKDAIFQVITPDGPRVFLPRKYAHDLKDYSRHEASGMK ALADRHIGHYTTIDHESDIMLGAIKIDLNRNLGTFVGDVEHEVAFCFETQF PACDDWTPIDLHDKLLRVVAQASARIFVGYPMCRNEEWLECSTKFALDVMT GGEKLKQWHPYLRPIAQYFVPEMTRIRGDHQRALELLLPELNRRLAEPADPD SSPHNDMIQWMQDRARKTGDNSFDNKELANLQMLTATAAIHTTRLAIIHAL YDLAARPEYVEPLRKEILEATKDSNGVLQKQHLTQMKMLDSFMKESQRHSP PSVATYQRKAMIPITLSNGFHIPAGTIVQCNTNILDETPPDWGDPHAFDGFR FYKLRNRTPDDINKFQFASPTYDSMQFGFGKDACPGRFFASNQIKIILAYILSH YDIKFEDSVVGRPKNFMFEVNVLADPTKMVLFKKIR
BraD	MSSDLVSKGMAQVFTGLGILLGAGRISSETHEEIMALLSADPGSNTGIMTGT NTGSTSIIPTQSKRVDMGDIPAGLPRPGKETPVSIQSHDLLGLGADLSTEAVQ PPETFRAQASPSAPSKELKIICPWWLTDGYSCREHDQGKCPFYHDNVAGGV KHPLICHFWADGGRCTKSQKDCRFAHYPAPHRVTAPMPSKKKSKKLRSSVA DDASHPDLGKARRHDPRDDEQNDEVWRNQGRARPGQEW

BraE	MLFSACADTNDQSLGPNVLGCRGDFDFTVKFEQLCFSLTPAAIFILASPWRV AHLVRKPTIVGAPLLRLAKLGVLVSYASLELSQLILITVLPFGASGIDIISSALRLA AALCMVGLSYFDHSKSPRPSIFLSAYLFFTLLFDIAQARTYWLASSTRPEIAFTA IFTAALAMKIAMLLLEAQRKTKWVAWDSKDHSPEETSGIYTLGVFSWLNKLF FDGYHKTLGIRDLYPLDQNLAATHLSERFSRHINEAKRKGHEIGLMEALAKTL YVPMILPIPAKLAAIGSFFCQPLFISSLTSRLSQSEPVPANIGYGFIGASICIYSVI AISQSLYWYFQQRLLYMMRACLATAIYTKTTEARAADEDENASLTLMSIDIER IMKGSLYMHELWGNVIEVALSAWLLYNLLGVAFIAPIVVVCICVGGVSFFMR FMGDSQRNWMAGIQKRVGLTSSVIGNMKNIKISGLTSPISRFVEKLRVDELQ AGSNFRLLMLTCSVFAYIPLLLSPPITFGVARRSLDATKLFTSLSYLLLMSTPLQ NLLETLPQMAAAVACLGRIQKFLQGEGRDDYRIFLAGSRRDPEKPSLDQLDK SPAVAIKDGSFGWKPDKMVLNNLDVEIPRGSLTIVVGPIASGKSSLCKALLGE MPHSQGTVTIATKFSCVGYCDQTPFLSNGSIRDNIIGYSPFDAQRYAEVVDG TMLGIDFETLPEADRTNIGSNGITLSGGQKQRVSLARCLYLQSDLLIMDDVFS GLDADTEDQVFQRVFGANGILKRRQATVVLCTHSVRHIPSATHVIALSTDGT VVEQGTFGDLVANQSYIHSLGVKAPSTSQADSEKIESDDSAIEPQINLIERAPT ETPEVGVNDKSRLSGDSAAYIVYMKSMGTMLPIAIFTSGLLYGFFYNFPTIWL TYWSADAVATNPSHSFGYYAAIYAVLEVCAMLSLIWLGVLLYITVLTRSGVSL HHAALRTLIHAPLRFFTTTDQGIITNLFSQDLSLIDNELPSALLNVIYMVFVGIG QAAVIASSSPYLAISYPFLFGMLYVVQKFYLRTSRQLRLLDLEAKSPLYTHFLDT SKGIVTLRAFGFVSEDRAKNAFLLDTSQRPAYLLAMIQQWLHFVLNVVVAIIA VMLTSLAVRLRSNSGFTGASLVTLMSFGEMLSGVVIYYTALETSLGAISRLKAF DKAAKTETKDGEDIVPPEEWPPRGEIILNNVSASYEYELPLFLSIRLTTNELSSN DTQPETPTLALKNLRLRIRPGEKIAICGRTGSGKSSLISLLLKLLDPIDETLDCVN IDNTPLSRIDRVTLRQRIIAIPQDIVFLPDGSTFQENLDPSNVSTAADAQAVLE AVDLWDFVRDKGGLEAGMTVSNLSQGQRQLFSLGRAVLRRRIRARSLGLGG GGSEGGILLLDEVSSSVDRETEKAMQEVIRVEFREYTVVAVSHRLDIIMDYDR VVVMEKGEIVEEGNPARLVEEPGTRFGELWSVGGN

Table S1 List of proteins encoded in the *bra* cluster and their respective protein sequences.

Name	5′-3′ Sequence	Application
AtBraA_1F	TCTTTCAACACAAGATCCCAAAGTCAAAGGATGGCTCCAGACATCGACAA	Vector construction
AtBraA_1R	CTATGCGTTATGAACATGTTCCCTGGCGCGTCATTCCACATATGACAAAT	
AtBraA_2F	ATGGCTCCAGACATCGACAA	Control PCR
AtBraA_2R	TCATTCCACATATGACAAAT	
AtBraB_1F	CGACTGACCAATTCCGCAGCTCGTCAAAGGATGGTACCTTCGGTAATGGA	Vector construction
AtBraB_1R	CTGGTAGACGTCATATAATCATACGGCGCGTTACTTCTTCGGCTCCAGAA	
AtBraB_2F	ATGGTACCTTCGGTAATGGA	Control PCR
AtBraB_2R	TTACTTCTTCGGCTCCAGAA	
AtBraC_1F	CAGCTACCCCGCTTGAGCAGACATCACCGGATGGCATCTCTTTACTTGCC	Vector construction
AtBraC_1R	ATGTCCATATCATCAATCATGACCGGCGCGCTATCGAATCTTCTTAAATA	
AtBraC_2F	ATGGCATCTCTTTACTTGCC	Control PCR
AtBraC_2R	CTATCGAATCTTCTTAAATA	

Table S2 List of primers used in this study.

Name	Expression Gene	Marker genes	Expression host
pTYGS-arg-BraA	*braA*	*ampR*, *URA3*, *argB*	*A. oryzae*
pTYGS-arg-BraC	*braC*	*ampR*, *URA3*, *argB*	*A. oryzae*
pTYGS-arg-BraAB	*braA*, *braB*	*ampR*, *URA3*, *argB*	*A. oryzae*
pTYGS-arg-BraAC	*braA*, *braC*	*ampR*, *URA3*, *argB*	*A. oryzae*
pTYGS-arg-BraABC	*braA*, *braB*, *braC*	*ampR*, *URA3*, *argB*	*A. oryzae*
pET-28a(+)-BraB	*braB*	*kan*	*E. coli*
pET-28a(+)-BraA	*braA*	*kan*	*E. coli*

Table S3 List of constructed vectors used in this study.

S4 Figures

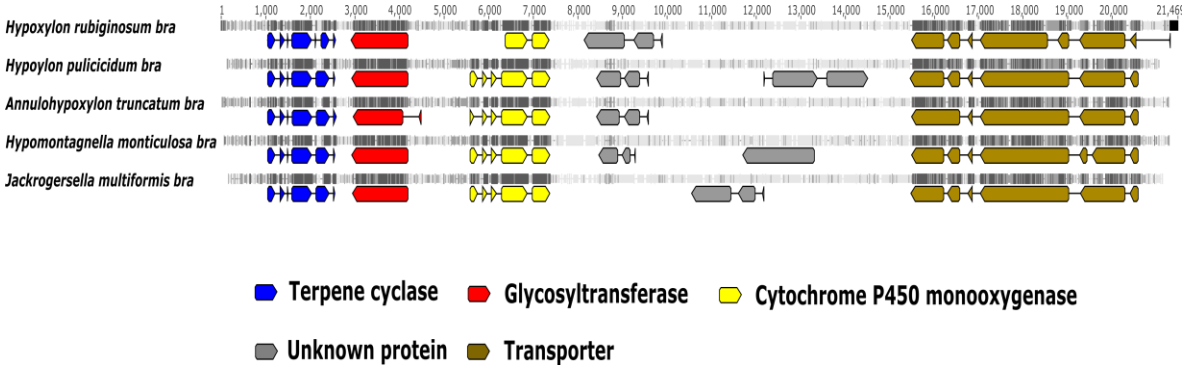

Figure S2 Alignment of the *bra* gene clusters found in different species of the Hypoxylaceae. Predicted coding regions of the different genes are shown below the sequences revealing putative erroneous gene predictions. Regions with high nucleotide similarity are shown in dark grey and indicate a high degree of gene conservation for the *bra* core genes.

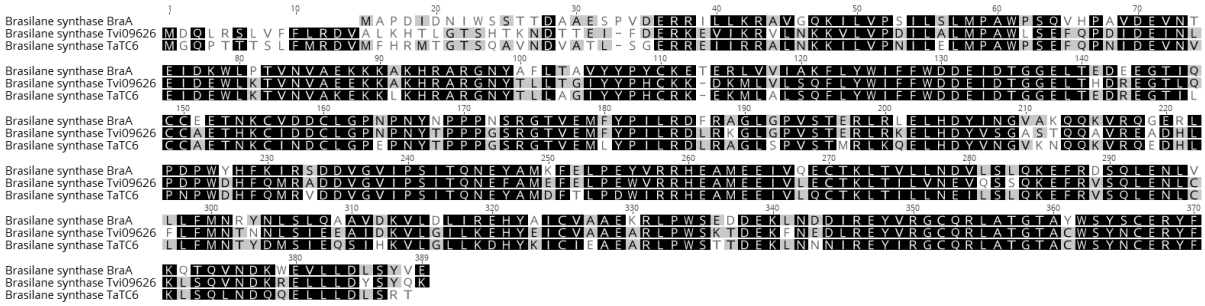

Figure S3 Alignment of the brasilane synthase protein sequences from *Annulohypoxylon truncatum* (BraA), *Trichoderma viride* (Tvi09626) and *T. atroviride* (TaTC6). Regions with high similarity across all sequences are highlighted in black.

S5 HPLC and GC Chromatograms from organic extracts

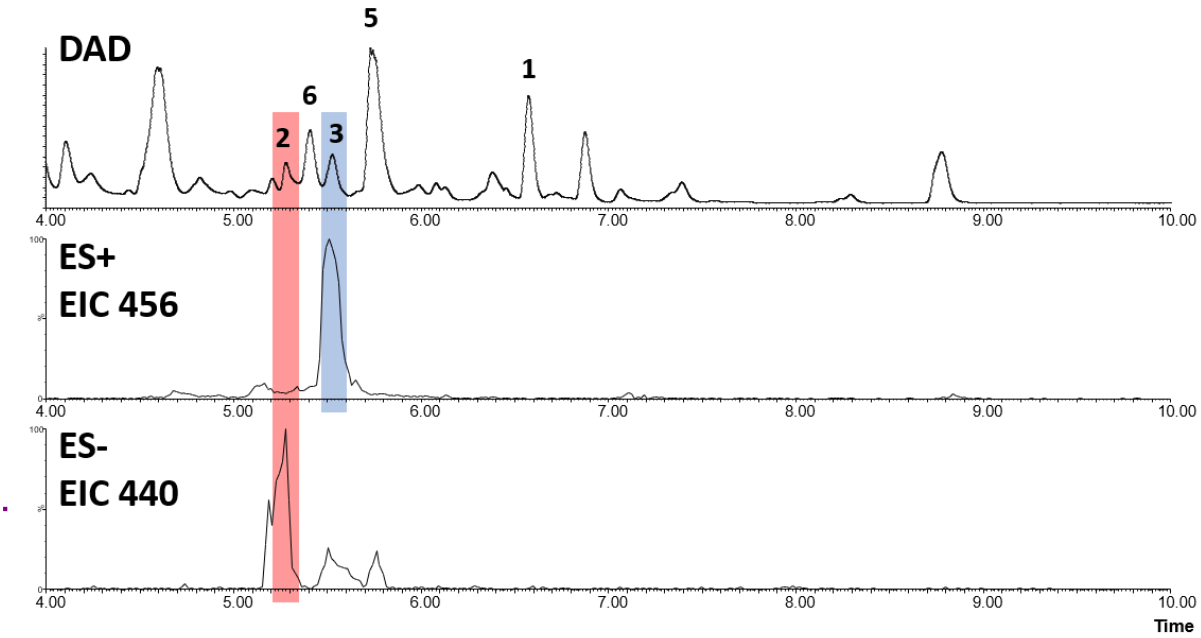

Figure S4 HPLC chromatogram of the crude extract obtained from *A. oryzae* BraAC fed with brasilane A **1**. The DAD (200-600 nm) chromatogram and the extracted ion chromatograms for brasilane D **2** (ES-, EIC 440) and brasilane E **3** (ES+, EIC 456) are depicted.

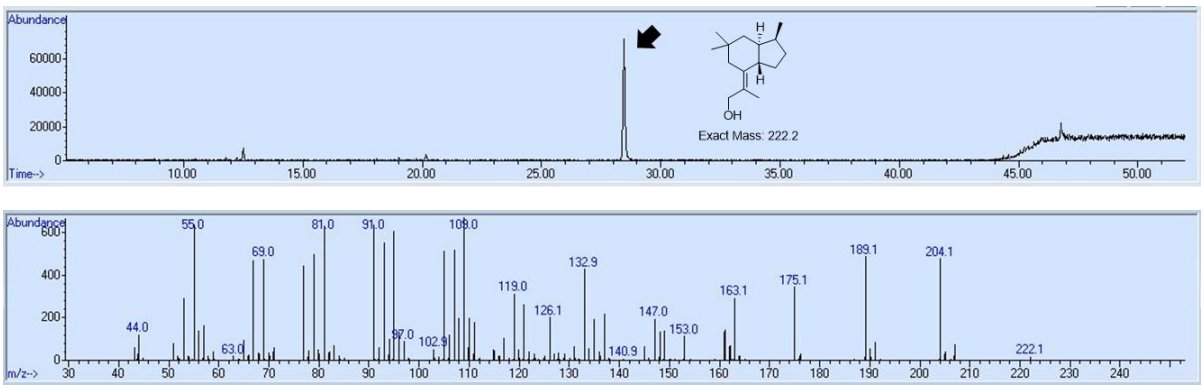

Figure S5 GC-MS chromatogram (top) of the crude extract obtained from the BraA *in-vitro* reaction with FPP. Mass fragmentation pattern (bottom) of the peak at 28.5 min identifies the compound as trichobrasilenol **4**.

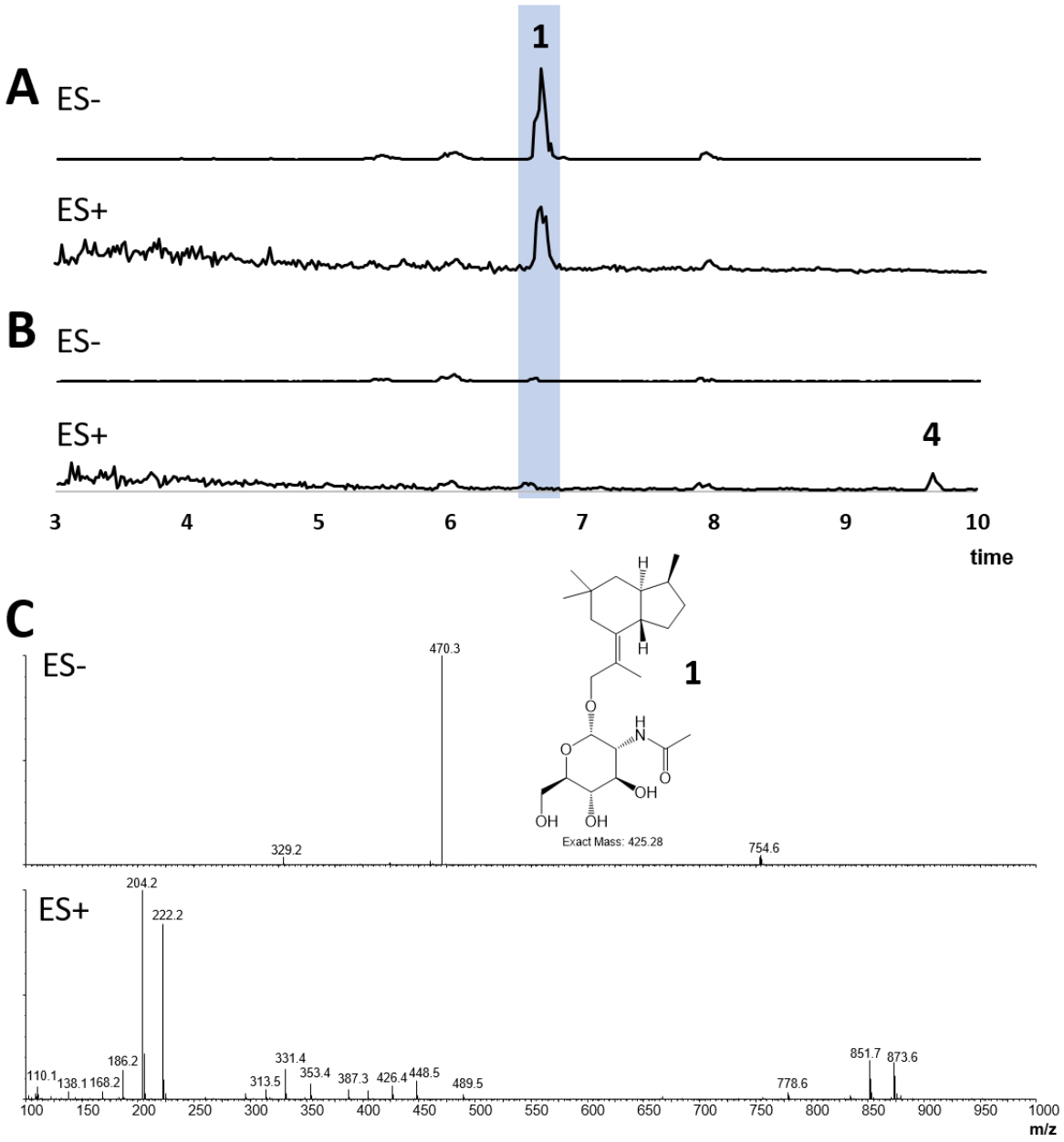

Figure S6 *In-vitro* reaction of BraA and BraB with FPP and UDP-GlcNAc. **A**, Base Peak Ion chromatogram in positive (ES+) and negative (ES-) ionisation mode are depicted showing the formation of brasilane A **1**; **B**, Reaction with heat-inactivated BraB. Base Peak Ion chromatogram in positive (ES+) and negative (ES-) ionisation mode are depicted showing traces of **1** (formed by spontaneous non-catalytic reaction of **4** with UDP-GlcNAc) and accumulation of **4**; **C**, mass spectra (ES+, ES-) of the reaction product **1**.

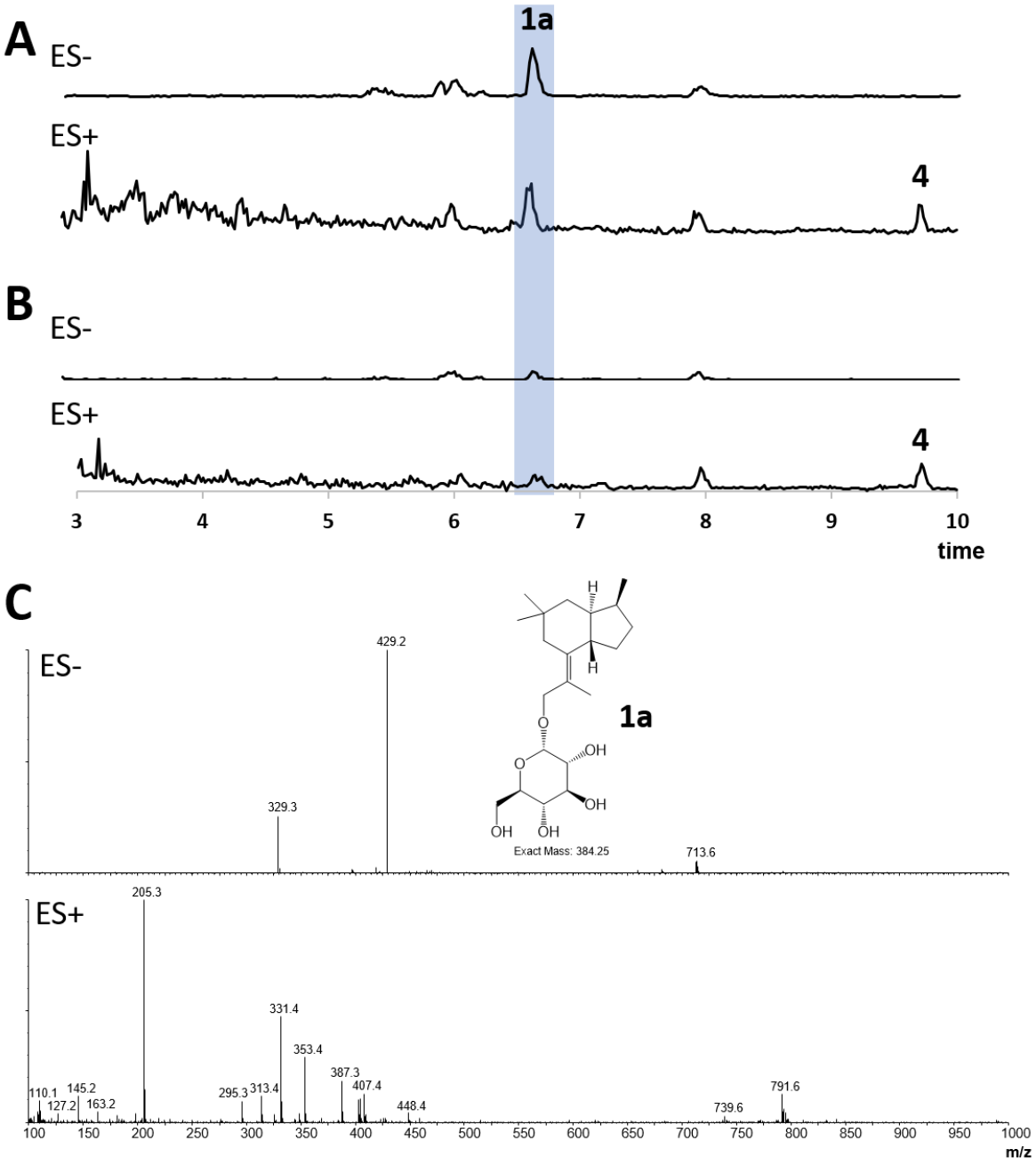

Figure S7 *In-vitro* reaction of BraA and BraB with FPP and UDP-Glc. **A**, Base Peak Ion chromatogram in positive (ES+) and negative (ES-) ionisation mode are depicted showing the formation of the brasilane glycoside **1a** (hypoxyside[13]) and the BraA product **4**; **B**, Reaction with heat-inactivated BraB. Base Peak Ion chromatogram in positive (ES+) and negative (ES-) ionisation mode are depicted showing traces of **1a** (formed by spontaneous non-catalytic reaction of **4** with UDP-Glc) and accumulation of **4**; **C**, mass spectra (ES+, ES-) of the reaction product **1a**.

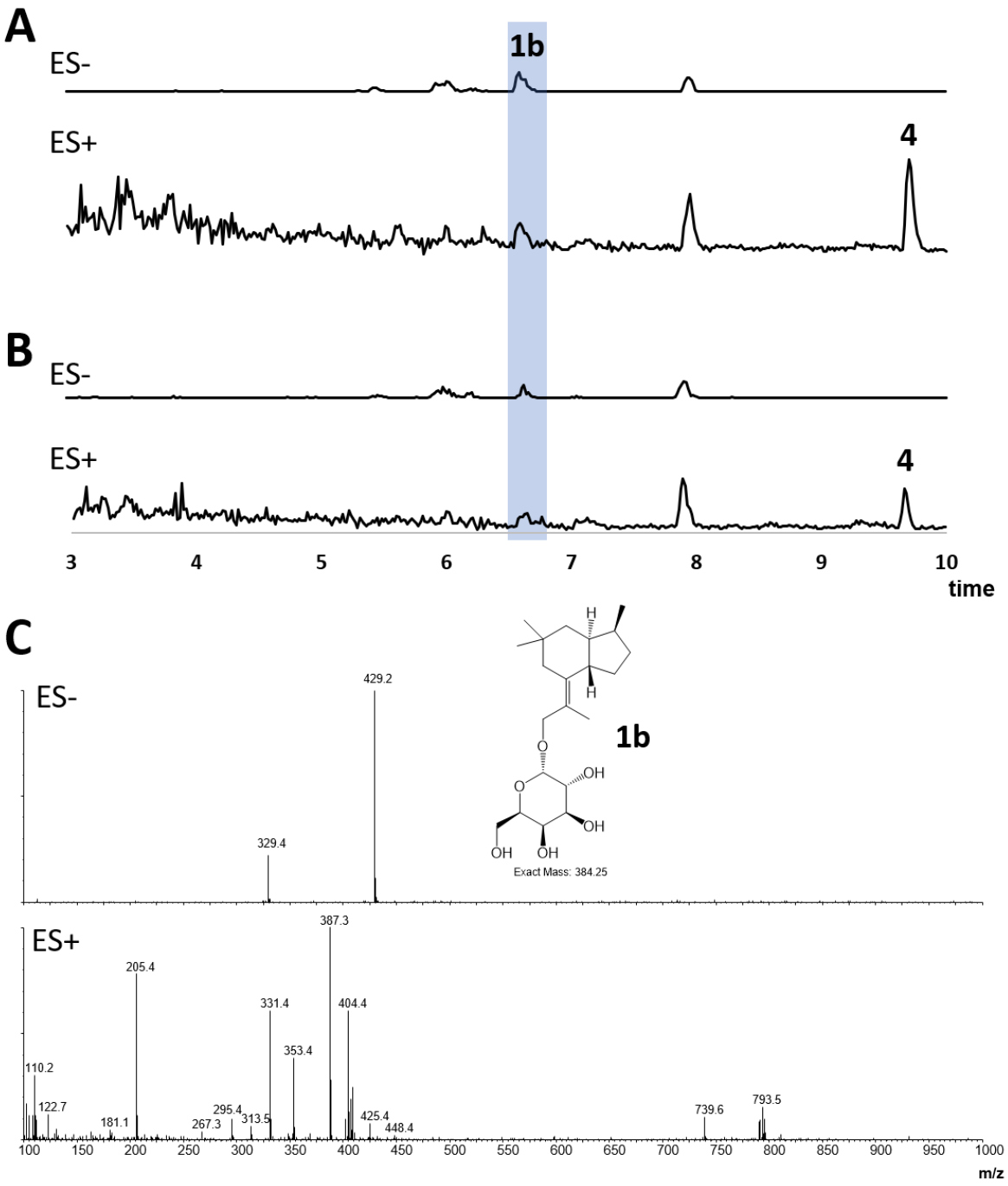

Figure S8 *In-vitro* reaction of BraA and BraB with FPP and UDP-Gal. **A**, Base Peak Ion chromatogram in positive (ES+) and negative (ES-) ionisation mode are depicted showing traces of a new brasilane glycoside **1b** and the BraA product **4**; **B**, Reaction with heat-inactivated BraB. Base Peak Ion chromatogram in positive (ES+) and negative (ES-) ionisation mode are depicted showing also traces of **1b** (formed by spontaneous non-catalytic reaction of **4** with UDP-Glc) and accumulation of **4**; **C**, mass spectra (ES+, ES-) of the reaction product **1b**.

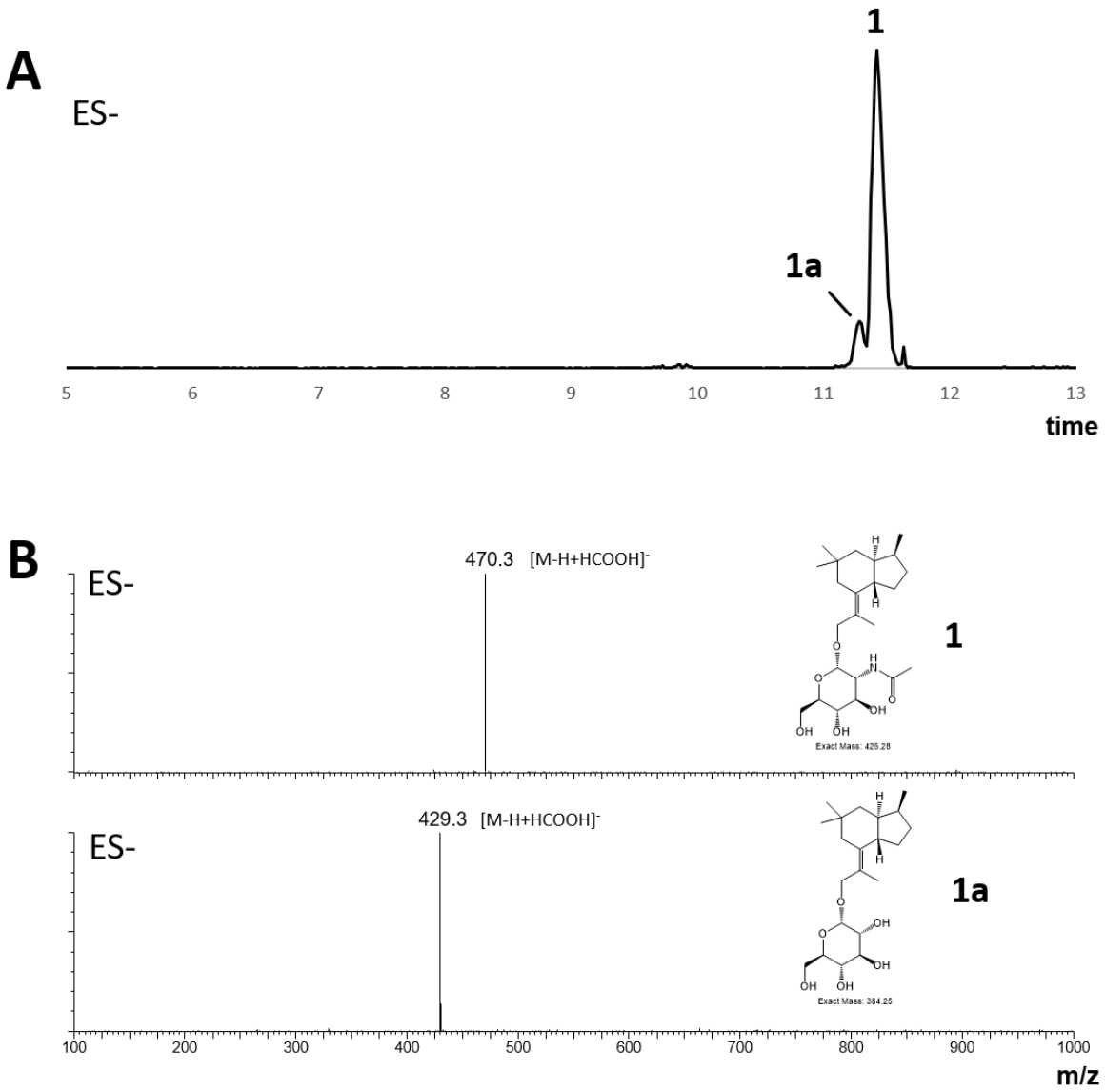

Figure S9 *In-vitro* competition assay of BraA and BraB with FPP and UDP-GlcNAc/UDP-Glc mixture. **A**, Base Peak Ion chromatogram in negative (ES-) ionisation mode showing the formation of **1** as predominant product and **1a** as minor compound; **B**, mass fragmentation spectra (ES-) of the products.

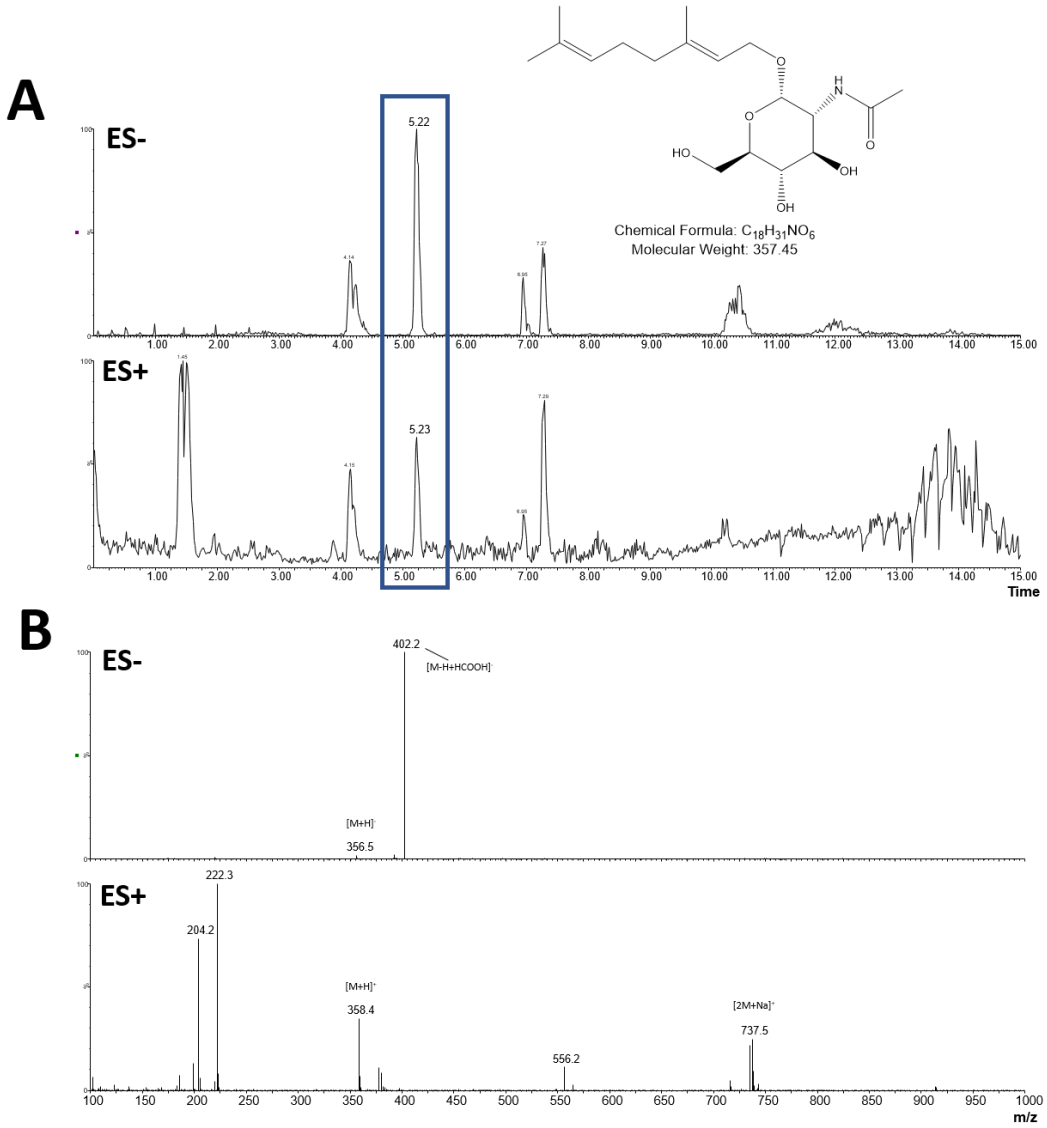

Figure S10 *In-vitro* reaction of BraB with geraniol and UDP-GlcNAc. **A**, Base Peak Ion chromatogram in positive (ES+) and negative (ES-) ionisation mode. Structure of the most likely reaction product is depicted; **B**, mass fragmentation spectra of the peak eluted after 5.2 min. The masses 222.3 and 204.2 in ES+ mode are in accordance with *N*-acetylglucosamine fragments.

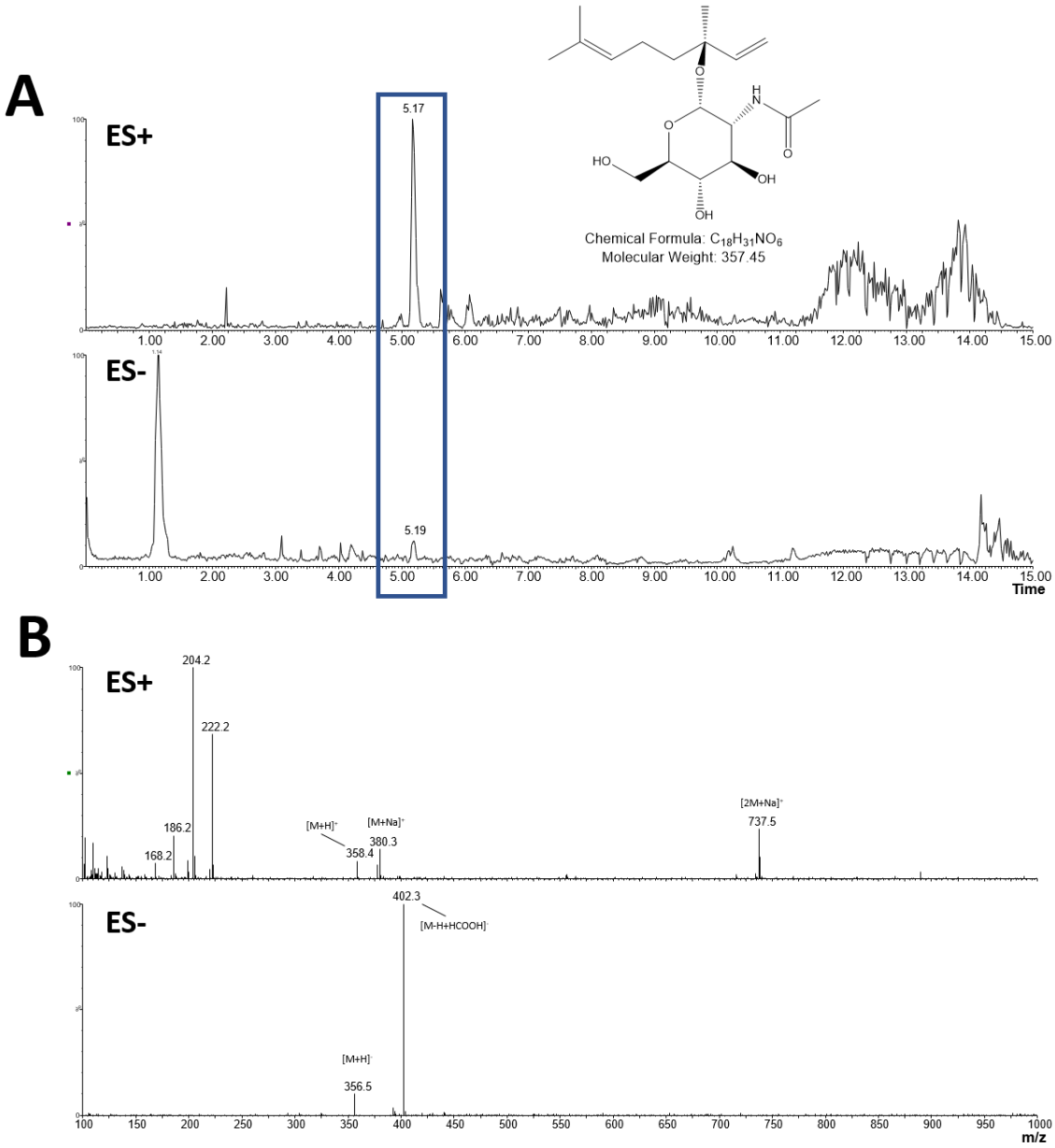

Figure S11 *In-vitro* reaction of BraB with linalool and UDP-GlcNAc. **A**, Base Peak Ion chromatogram in positive (ES+) and negative (ES-) ionisation mode. Structure of the most likely reaction product is depicted; **B**, mass fragmentation spectra of the peak eluted after 5.2 min. The masses 222.3 and 204.2 in ES+ mode are in accordance with *N*-acetylglucosamine fragments.

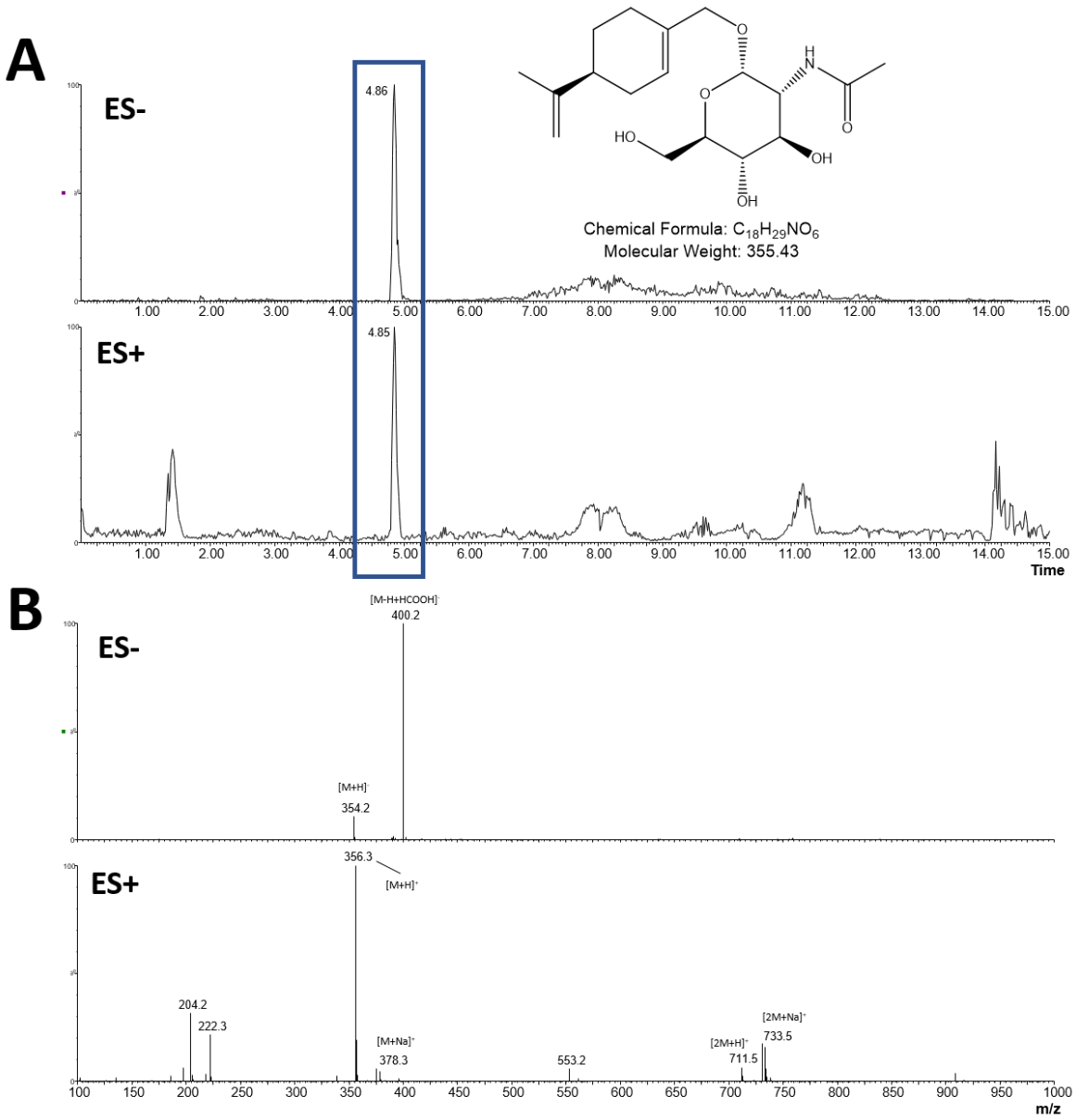

Figure S12 *In-vitro* reaction of BraB with perillyl alcohol and UDP-GlcNAc. **A**, Base Peak Ion chromatogram in positive (ES+) and negative (ES-) ionisation mode. Structure of the most likely reaction product is depicted; **B**, mass fragmentation spectra of the peak eluted after 4.8 min. The masses 222.3 and 204.2 in ES+ mode are in accordance with *N*-acetylglucosamine fragments.

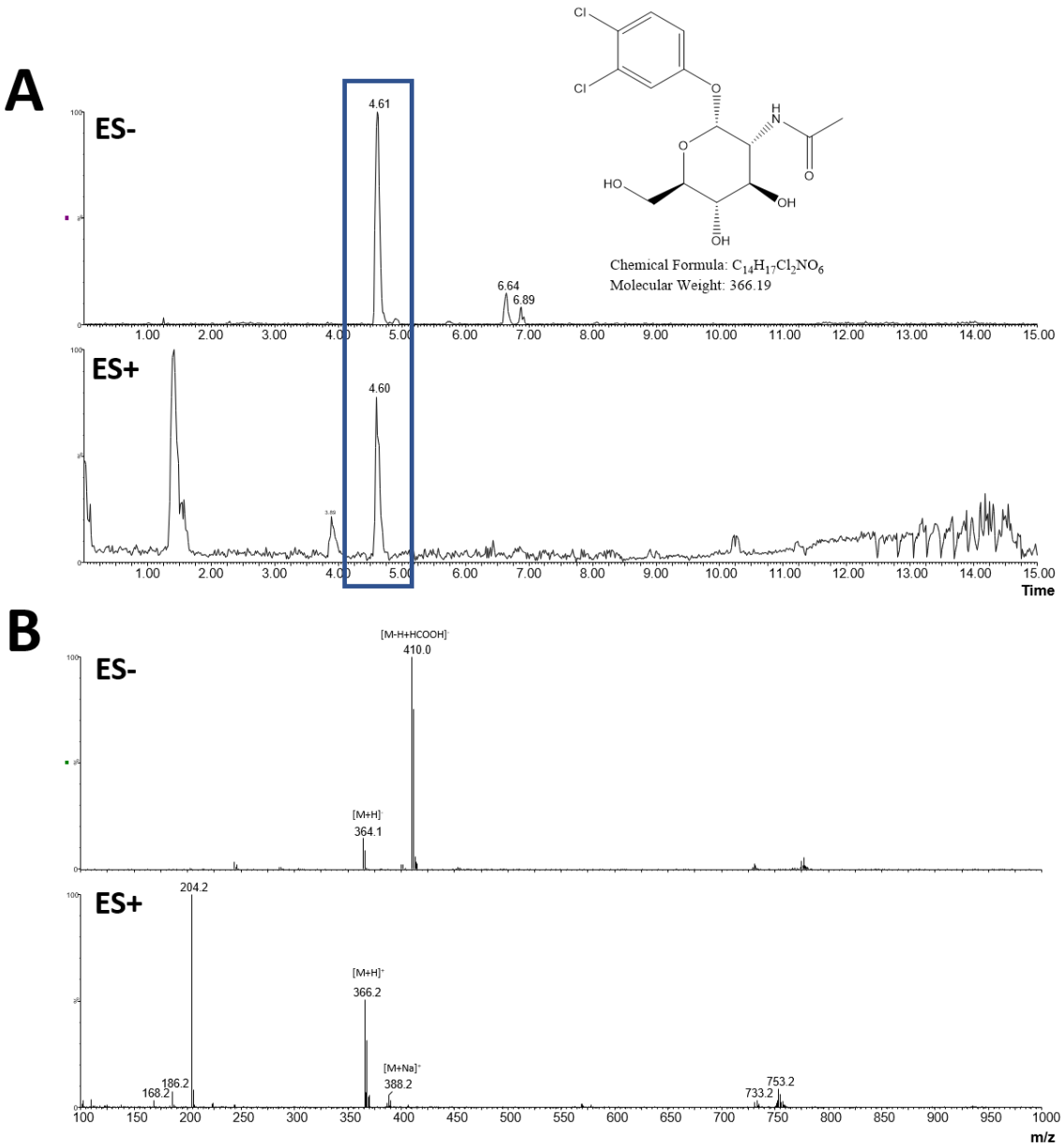

Figure S13 *In-vitro* reaction of BraB with 3,4-dichlorophenol and UDP-GlcNAc. **A**, Base Peak Ion chromatogram in positive (ES+) and negative (ES-) ionisation mode. Structure of the most likely reaction product is depicted. 3,4-dichlorophenol can be seen at 6.6 min; **B**, mass fragmentation spectra of the peak eluted after 4.6 min. The masses 204.2 and 186.2 in ES+ mode are in accordance with *N*-acetylglucosamine fragments.

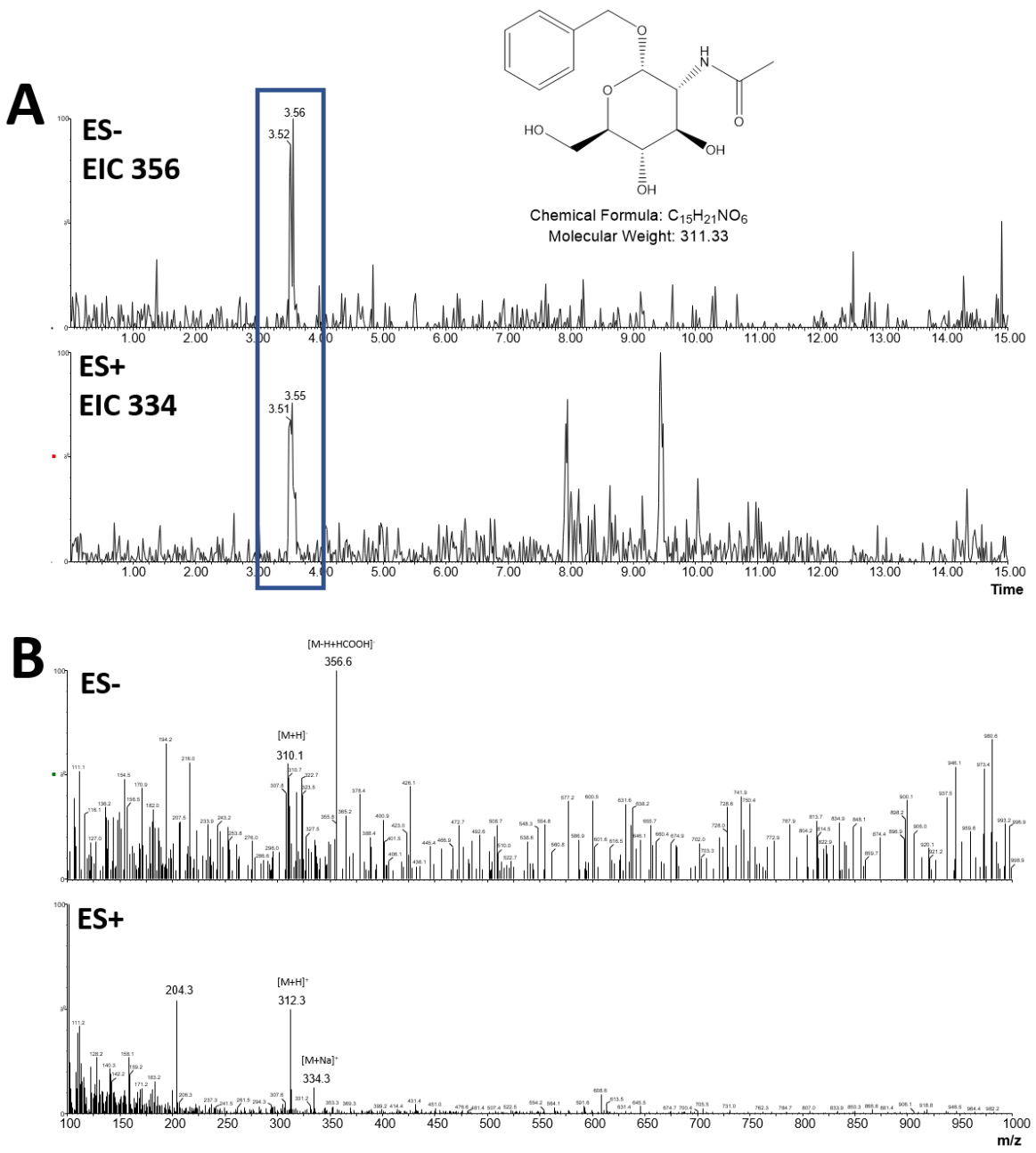

Figure S14 *In-vitro* reaction of BraB with benzyl alcohol and UDP-GlcNAc. **A**, Extracted Ion chromatogram (EIC) in positive [ES+, m/z = 334 $(M+Na)^+$] and negative [ES-, m/z = 356 $(M-H+HCOOH)^-$] ionisation mode. Structure of the most likely reaction product is depicted; **B**, mass fragmentation spectra of the peak eluted after 3.5 min. The mass 204.2 in ES+ mode is in accordance with *N*-acetylglucosamine fragments.

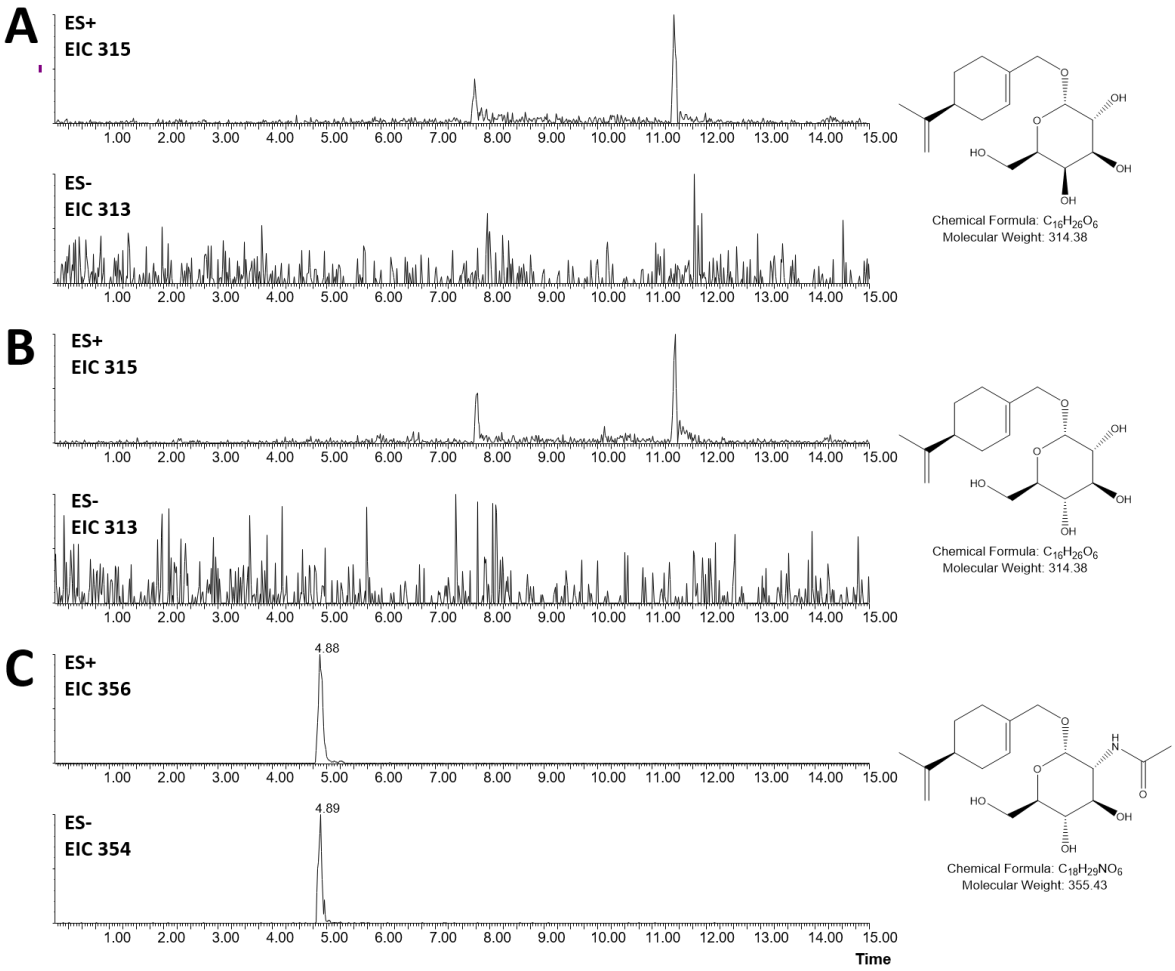

Figure S15 *In-vitro* reaction of BraB with perillyl alcohol and different UDP-sugars. **A**, reaction with UDP-galactose. Extracted Ion chromatogram (EIC) in positive [ES+, m/z = 315 $(M+H)^+$] and negative [ES-, m/z = 313 $(M-H)^-$] ionisation mode. Structure of the most likely reaction product is depicted. **B**, reaction with UDP-glucose. Extracted Ion chromatogram (EIC) in positive [ES+, m/z = 315 $(M+H)^+$] and negative [ES-, m/z = 313 $(M-H)^-$] ionisation mode. Structure of the most likely reaction product is depicted. Weak signals can be observed for EIC of m/z = 337 $(M+Na)^+$ and m/z = 359 $(M-H+HCOOH)^-$ at a retention time of 4.7 min (data not shown). **C**, control reaction with UDP-GlcNAc. Extracted Ion chromatogram (EIC) in positive [ES+, m/z = 356 $(M+H)^+$] and negative [ES-, m/z = 354 $(M-H)^-$] ionisation mode. Structure of the reaction product is depicted.

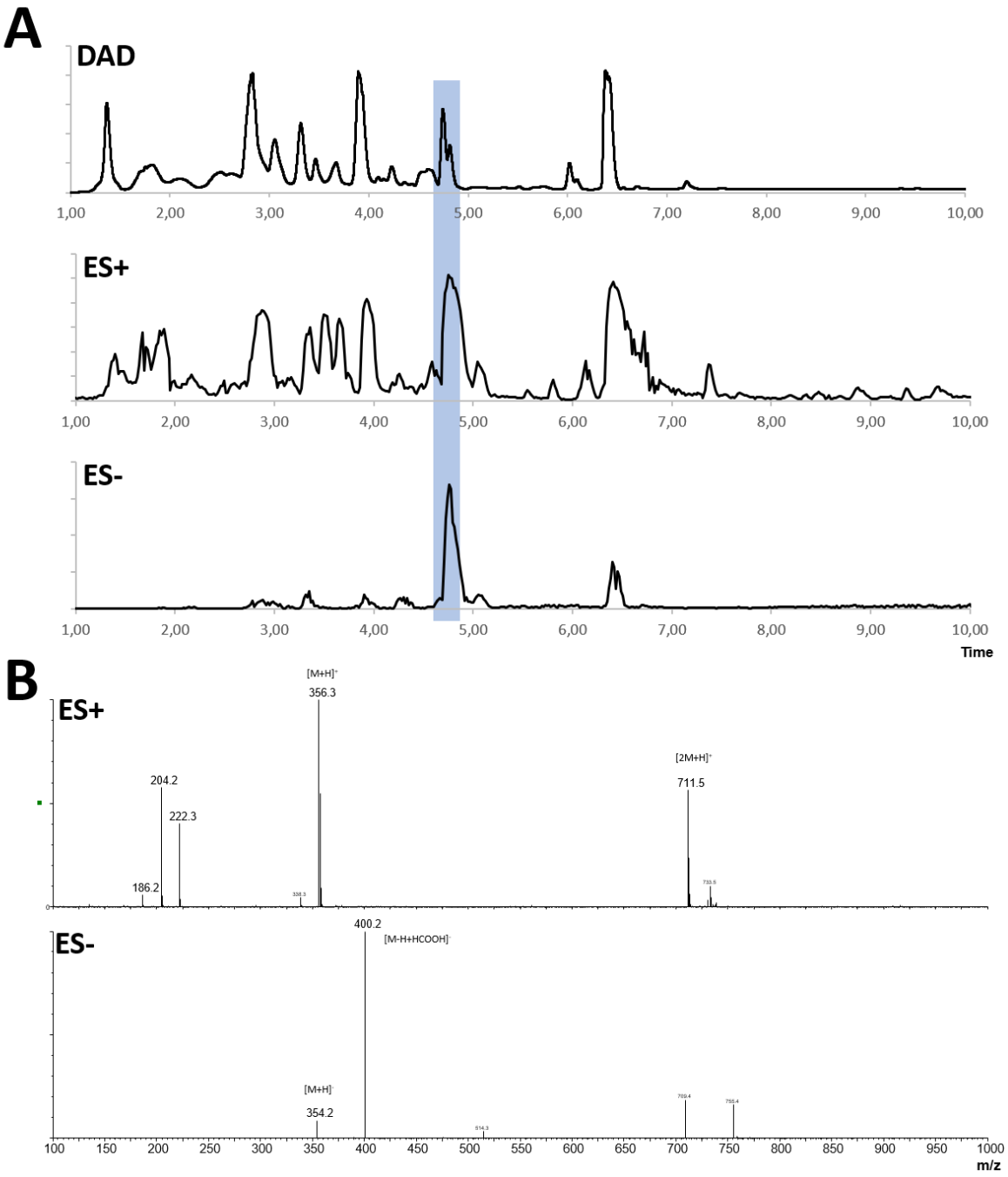

Figure S16 HPLC chromatogram of the crude extract obtained from *E. coli* BraB fed with perillyl alcohol. **A**, Base peak chromatograms of the DAD detector and mass spectrometer in positive (ES+) and negative (ES-) ionisation mode. **B**, mass fragmentation spectra of the highlighted peak (perillyl glycoside **7**). The mass 204.2 in ES+ mode is in accordance with *N*-acetylglucosamine fragments.

S6 Compound Physical Data

S6.1 UV/vis and mass spectra of compounds isolated in this study

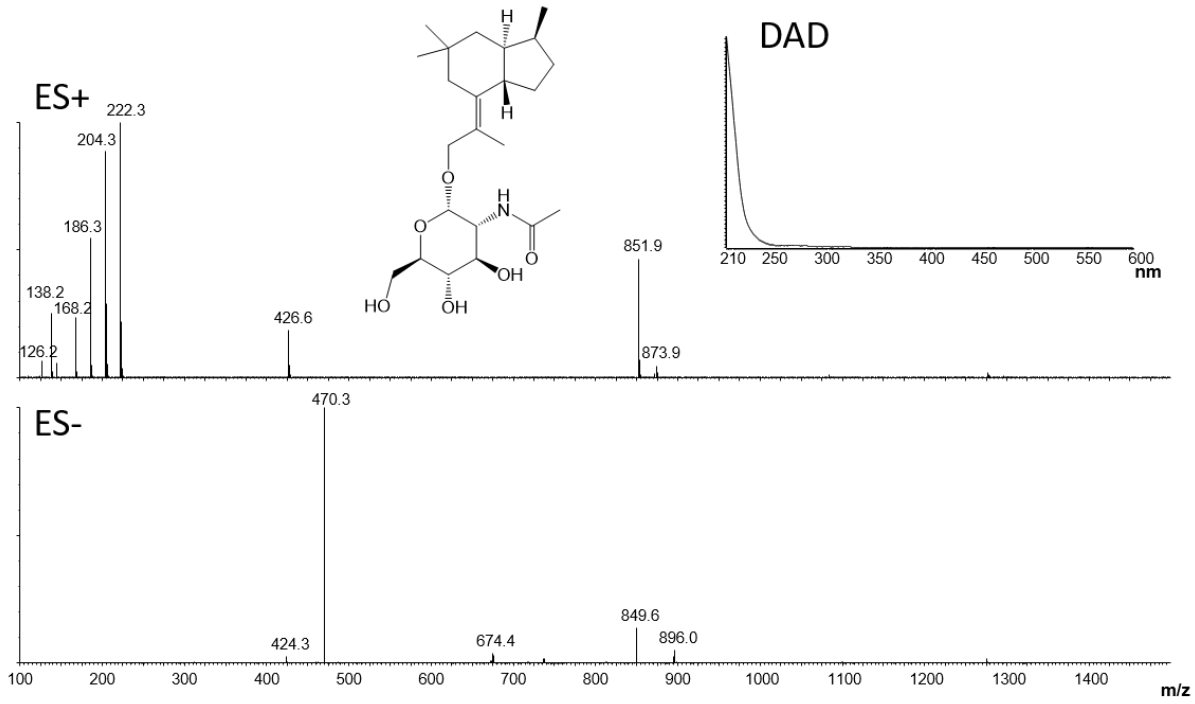

Figure S17 Mass (ES+, ES-) and UV/vis (DAD) spectrum of brasilane A **1**.

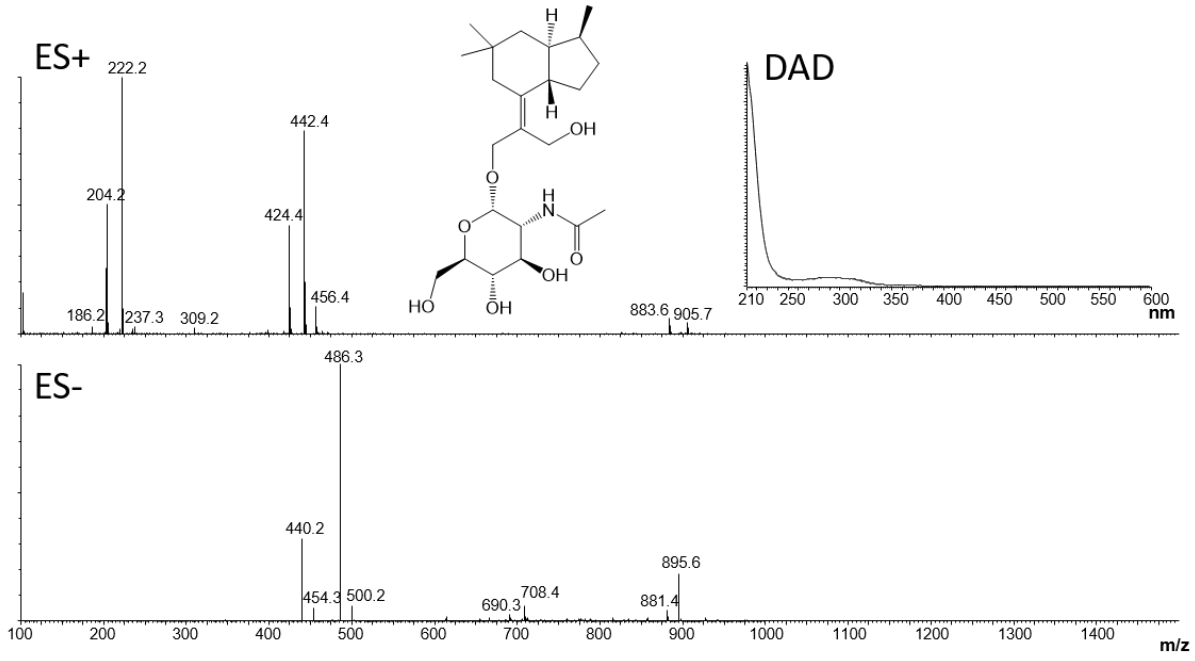

Figure S18 Mass (ES+, ES-) and UV/vis (DAD) spectrum of brasilane D **2**.

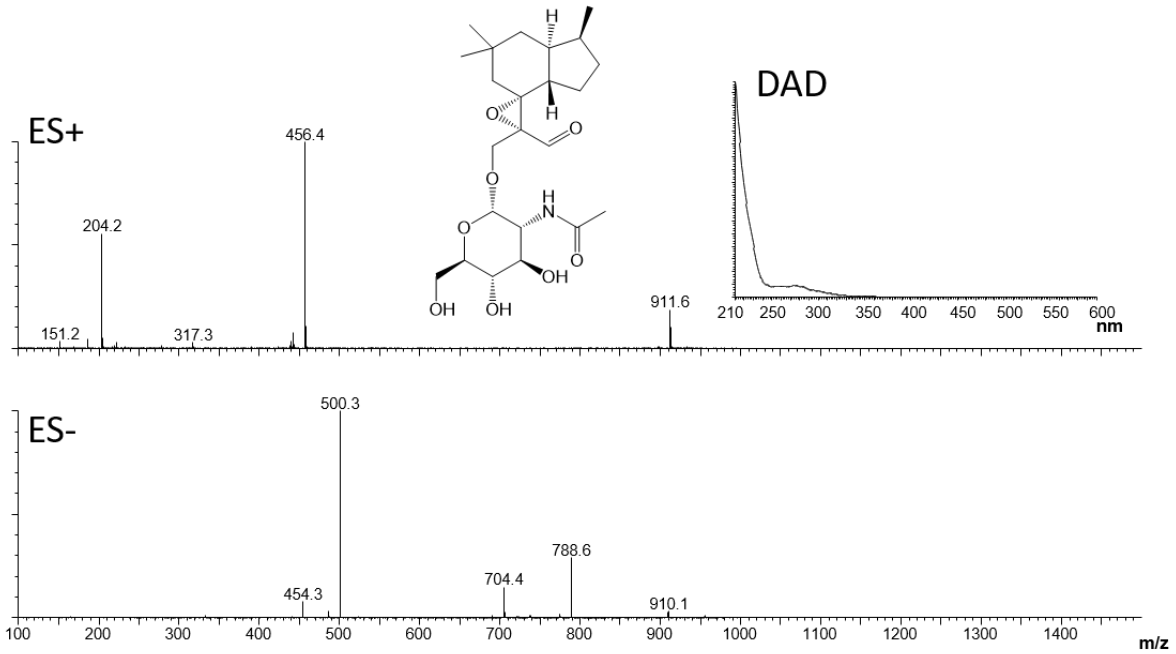

Figure S19 Mass (ES+, ES-) and UV/vis (DAD) spectrum of brasilane E **3**.

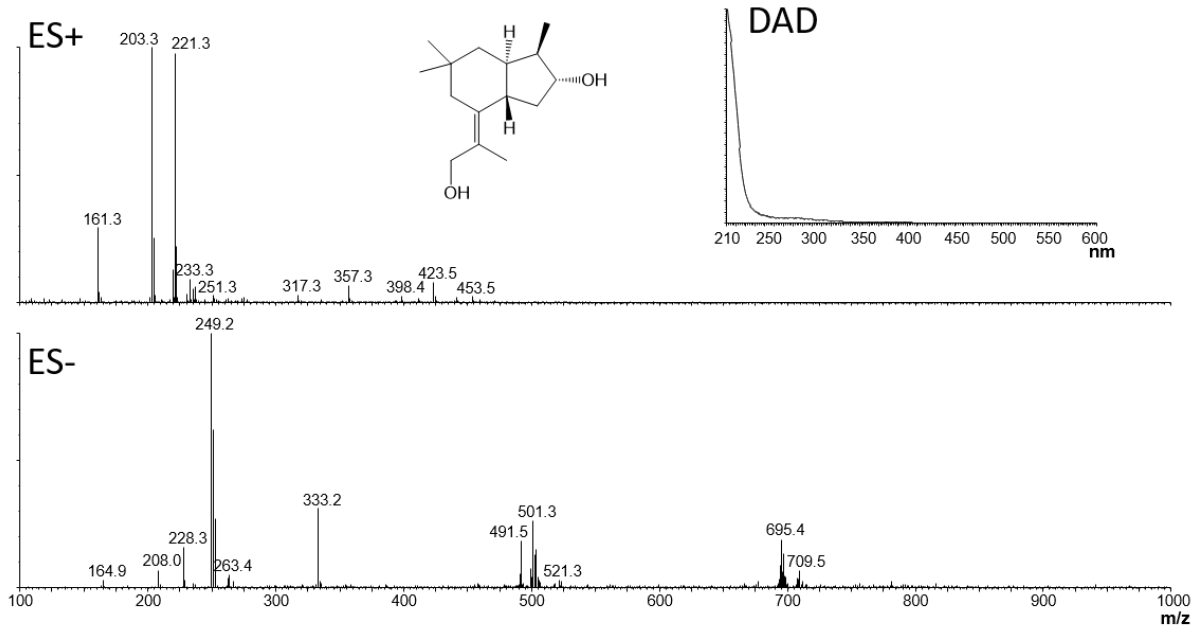

Figure S20 Mass (ES+, ES-) and UV/vis (DAD) spectrum of brasilane F **5**.

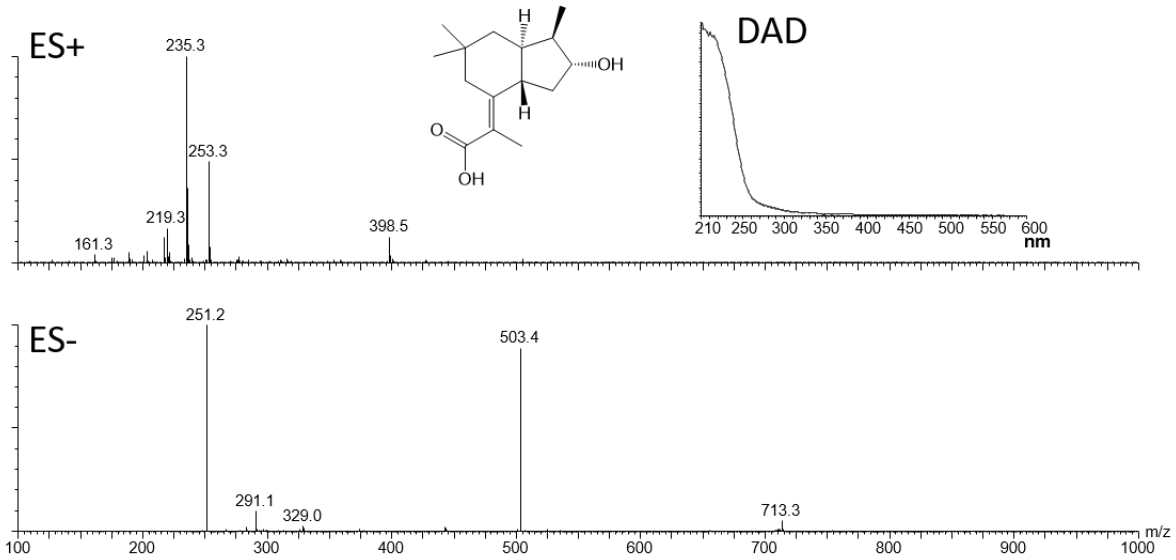

Figure S21 Mass (ES+, ES-) and UV/vis (DAD) spectrum of xylarenic acid B **6**.

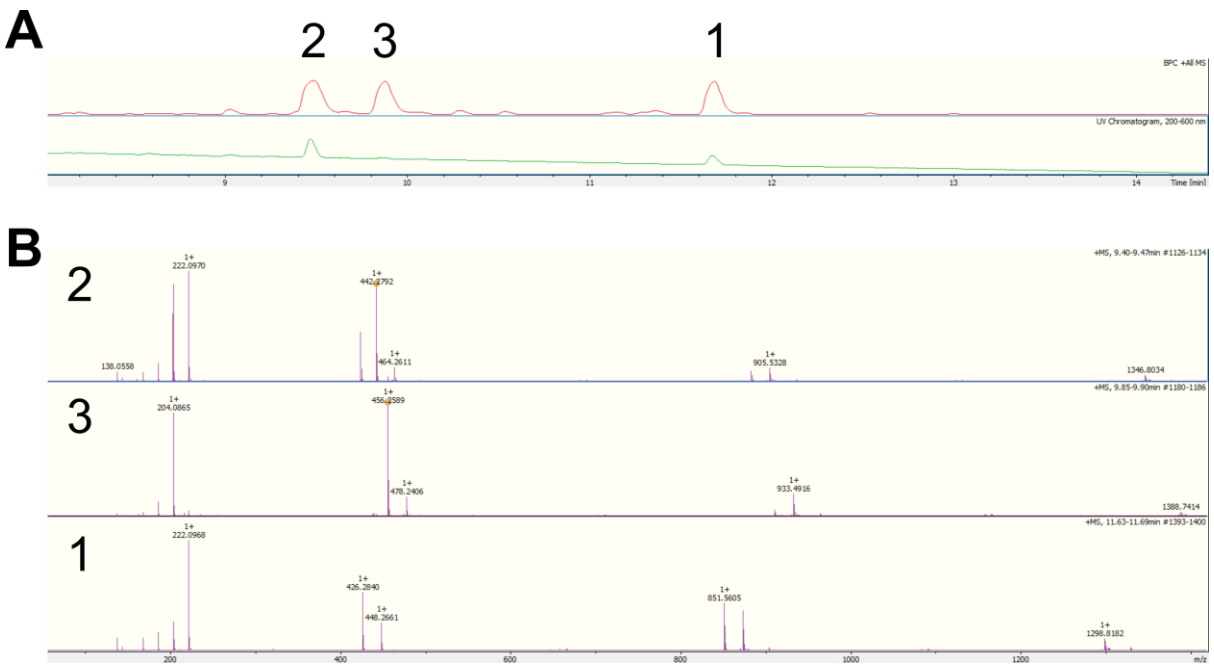

Figure S22 HPLC chromatogram of a fraction containing **1** – **3**. **A**, LC-MS (base peak, ESIMS in positive mode) and UV/Vis (200-600nm) chromatogram. **B**, HRESIMS spectra in positive ionisation mode for **1** – **3**.

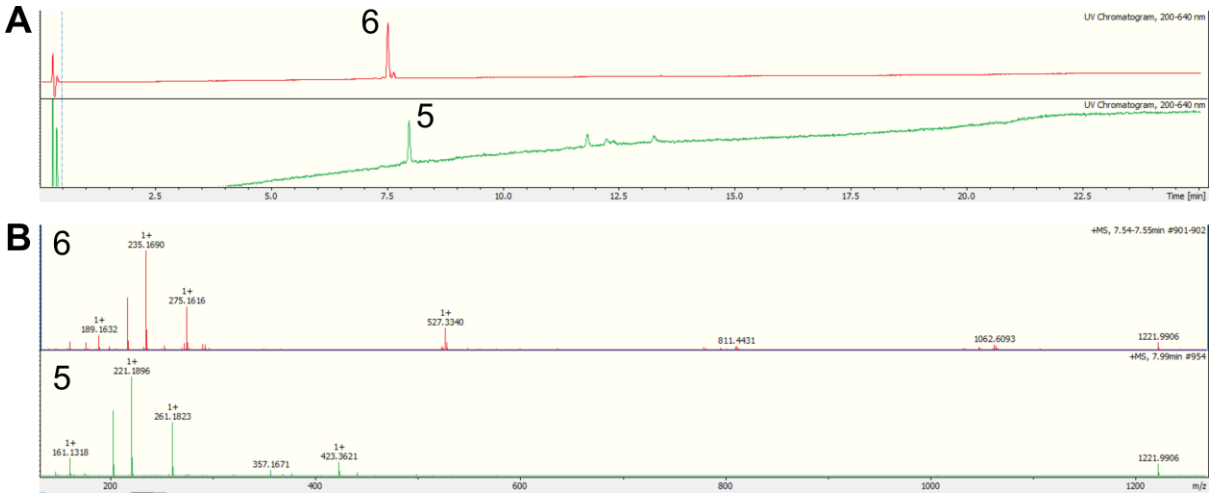

Figure S23 HPLC chromatogram of brasilane F **5** and xylarenic acid B **6**. **A**, UV/Vis (200-600nm) chromatogram. **B**, HRESIMS spectra in positive ionisation mode for compound **5** and **6**.

S6.2 Brasilane A

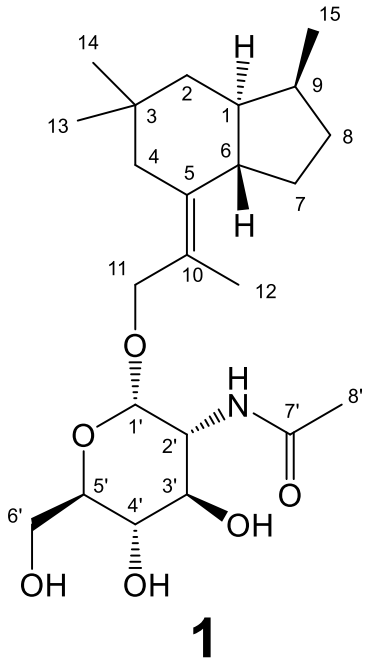

1

amorphous solid; $[\alpha]^{20}_{D}$ +107.0 (c = 0.1, CH_3OH); CD (CH_3OH) λ_{max} (Δ_ε): 194 nm (+2.0), 214 nm (-3.3); ^{13}C NMR data (CH_3OH-d_4, 125 MHz): δ_c 171.6 (C, C–7'), 140.5 (C, C–5), 124.9 (C, C–10), 96.9 (CH, C–1'), 73.9 (CH, C–5'), 72.8 (CH, C–3'), 72.6 (CH, C–4'), 70.2 (CH_2, C–11), 62.9 (CH_2, C–6'), 55.8 (CH, C–2'), 43.3 (CH, C–6, chemical shift extracted from HSQC spectrum), 47.0 (CH, C–1), 45.3 (CH_2, C–4), 42.2 (CH_2, C–2), 34.7 (CH_2, C–8), 34.4 (C, C–3), 33.3 (CH, C–9), 32.9 (CH_3, C–13), 32.5 (CH_2, C–7), 26.9 (CH_3, C–14), 22.7 (CH_3, C–8'), 18.5 (CH_3, C–15), 18.2 (CH_3, C–12), data are consistent with those previously reported by Hu at al., ^1H NMR (pyridin-d_5; 700 MHz), ^{13}C NMR (pyridin-d_5; 175 MHz) see table S1; ESI-MS *m/z* 448.29 $[M+Na]^+$, 873.57 $[2M+Na]^+$, 424.32 $[M-H]^-$, 470.33 $[M+HCOO]^-$; HR-ESI-MS *m/z* 426.2840 $[M+H]^+$ (calcd. for $C_{23}H_{40}NO_6$, 426.2850), 448.2661 $[M+Na]^+$ (calcd. for $C_{23}H_{39}NO_6Na$, 448.2670).

Atom#	C Shift	H Shift	COSY	N/ROESY	C to H HMBC
1	46.053, CH	1.589, m	6, 9	14, 2a, 2b, 9	
2a	41.547, CH_2	1.090, dd (12.8, 12.6)	2b, 4b	15, 13, 2b, 1, 4b, 6	14, 13, 3, 1, 6
2b	41.547, CH_2	1.293, br dd (12.5, 2.6)	2a	15, 14, 13, 2a, 1	3, 4, 6
3	33.848, C				
4a	44.830, CH_2	2.574, d (14.0)	4b	14, 13, 4b, 11, 11	14, 13, 3, 2, 6, 10, 5
4b	44.830, CH_2	1.593, m	2a, 4a	14, 13, 2a, 6, 4a	14, 3, 6, 10, 5
5	139.301, C				
6	48.591, CH	1.846, ddd (12.5, 11.5, 5.2)	7b, 1, 7a	15, 8a, 2a, 4b, 7a	10, 5
7a	31.880, CH_2	2.020, m	8a, 7b, 6	7b, 6	9, 1, 6
7b	31.880, CH_2	1.535, m	8a, 6, 7a	12, 8b, 7a	5
8a	34.145, CH_2	1.018, m	7b, 8b, 7a	15, 6, 8b	9
8b	34.145, CH_2	1.983, m	8a, 9	8a, 7b	
9	32.473, CH	1.914, m	15, 1, 8b	15, 1	
10	124.519, C				
11a	69.962, CH_2	4.273, d (10.8)	11	12, 4a, 1'	1', 10, 5
11b	69.962, CH_2	4.345, d (10.8)	11	4a, 1'	12, 1', 10, 5
12	18.428, CH_3	1.926, s		7b, 11	11, 10, 5
13	32.784, CH_3	0.944, s		14, 2a, 2b, 4b, 4a	14, 3, 2, 4, 5
14	26.659, CH_3	0.859, s		13, 2b, 1, 4b, 4a	13, 3, 2, 4
15	18.573, CH_3	0.773, d (7.1)	9	8a, 2a, 2b, 6, 9	9, 8, 1
1'	97.769, CH	5.414, d (3.7)	2'	11, 11, 2', 2'NH	11, 3', 5'
2'	55.849, CH	4.895, ddd (10.8, 8.6, 3.7)	3', 1', 2'NH	4', 1', 2'NH	3', 7'
2'NH	NH	8.985, br d (8.6)	2'	8', 3', 2', 1'	2', 3', 7'
3'	73.397, CH	4.520, m	4', 2'	2'NH	2'
4'	73.518, CH	4.257, m	5', 3'	2'	6', 3', 5'
5'	74.985, CH	4.395, m	4'		6', 4'
6'a	63.373, CH_2	4.400, m	6'	6'	5'
6'b	63.373, CH_2	4.541, m	6'	6'	4'
7'	170.824, C				
8'	23.695, CH_3	2.211, s		2'NH	7'

Table S4 NMR data (^{1}H 700MHz, ^{13}C 125 MHz) of brasilane A **1** in pyridine-d_5.

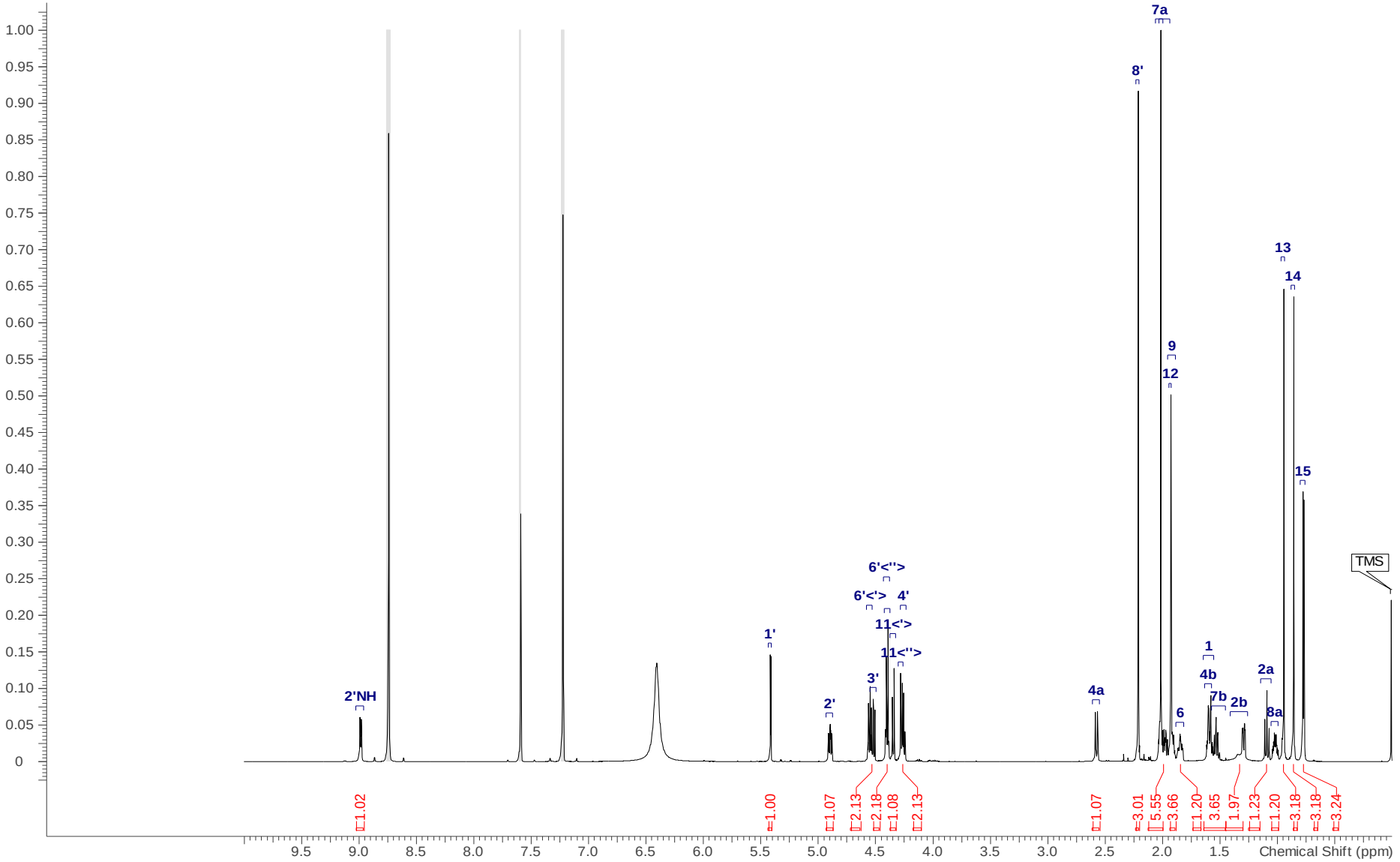

Figure S24 ^{1}H NMR spectrum (700 MHz, pyridine-d_5) of brasilane A **1**.

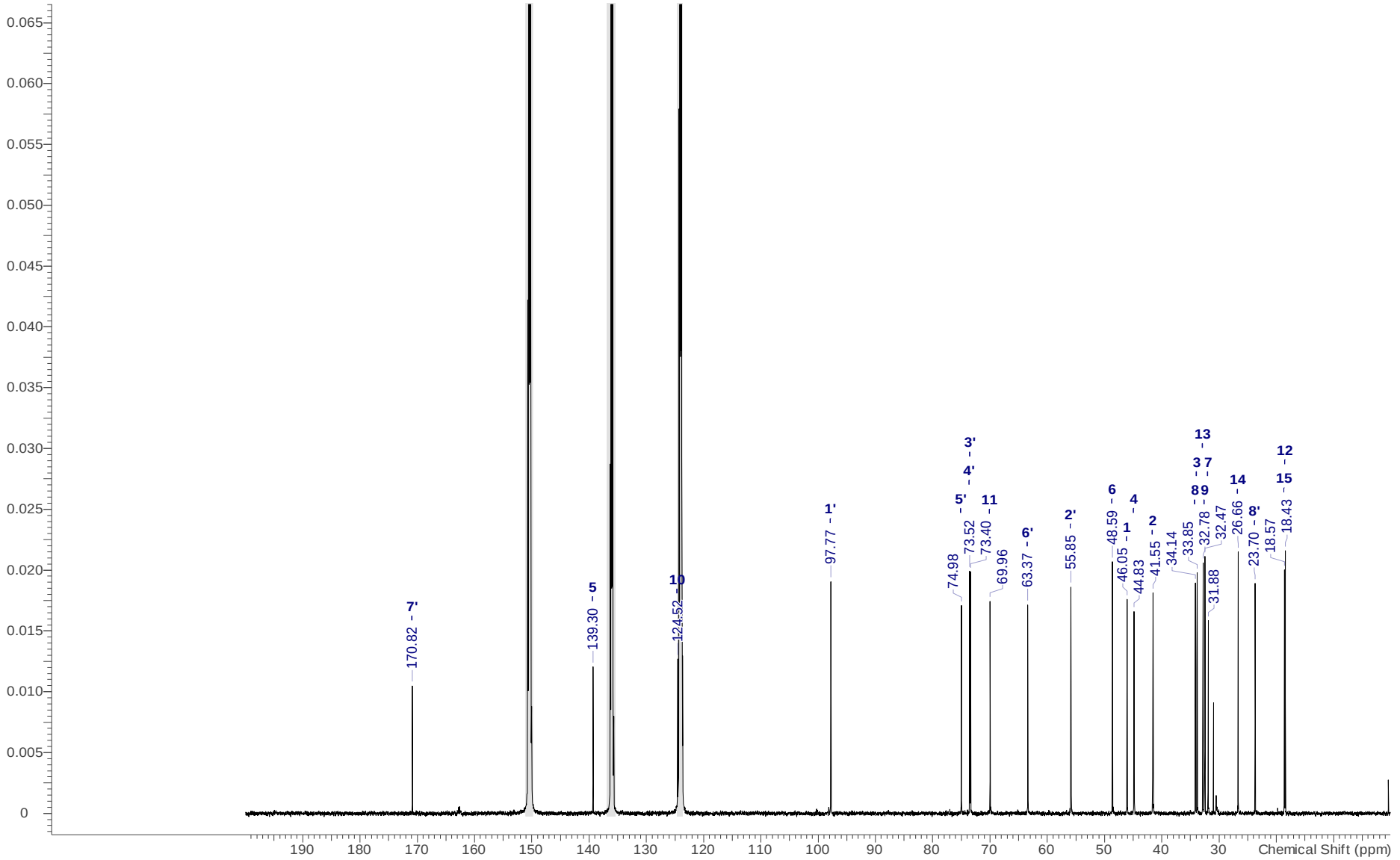

Figure S25 ^{13}C NMR spectrum (125 MHz, pyridine-d_5) of brasilane A **1**.

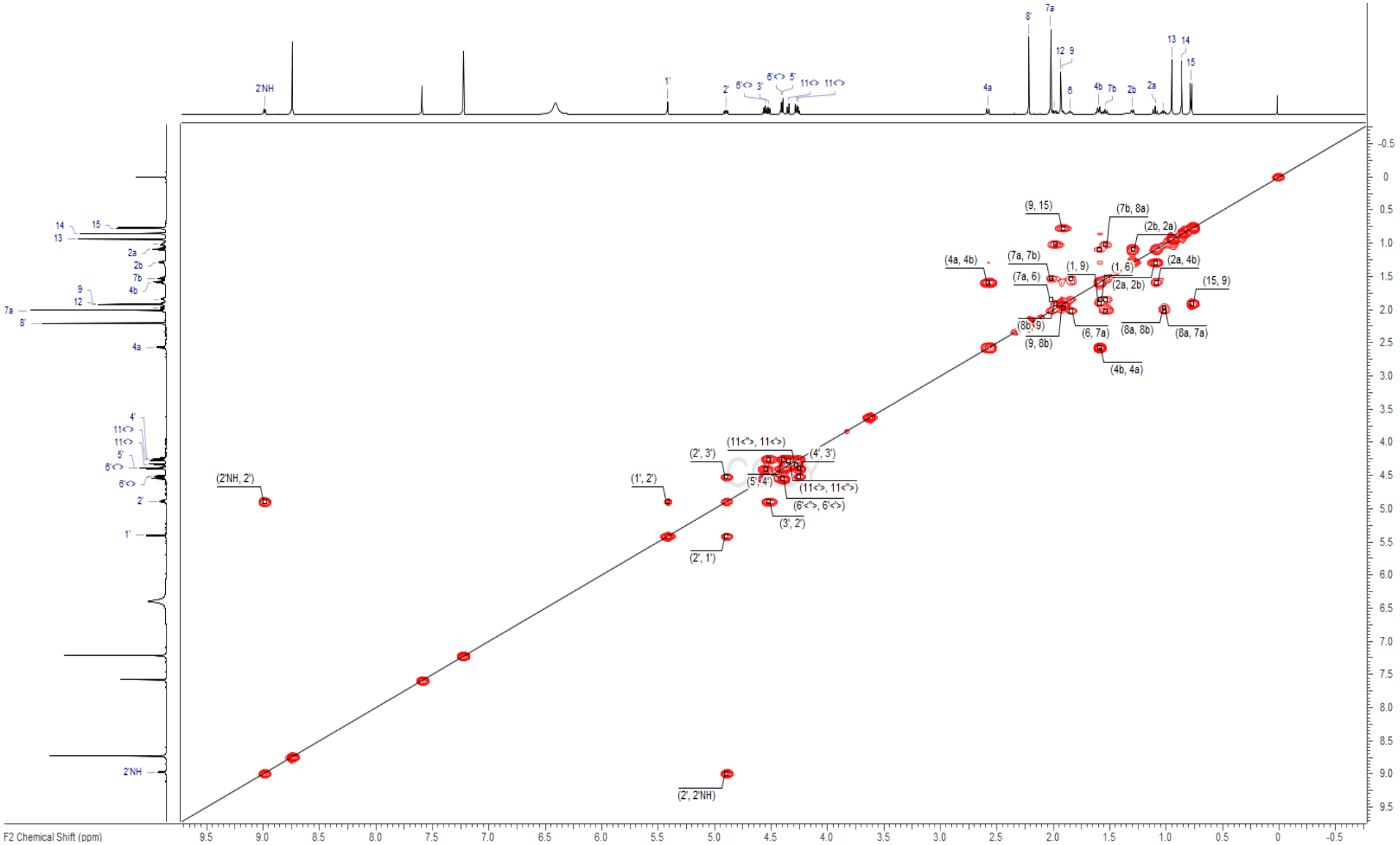

Figure S26 COSY NMR spectrum (700 MHz, pyridine-d_5) of brasilane A **1**.

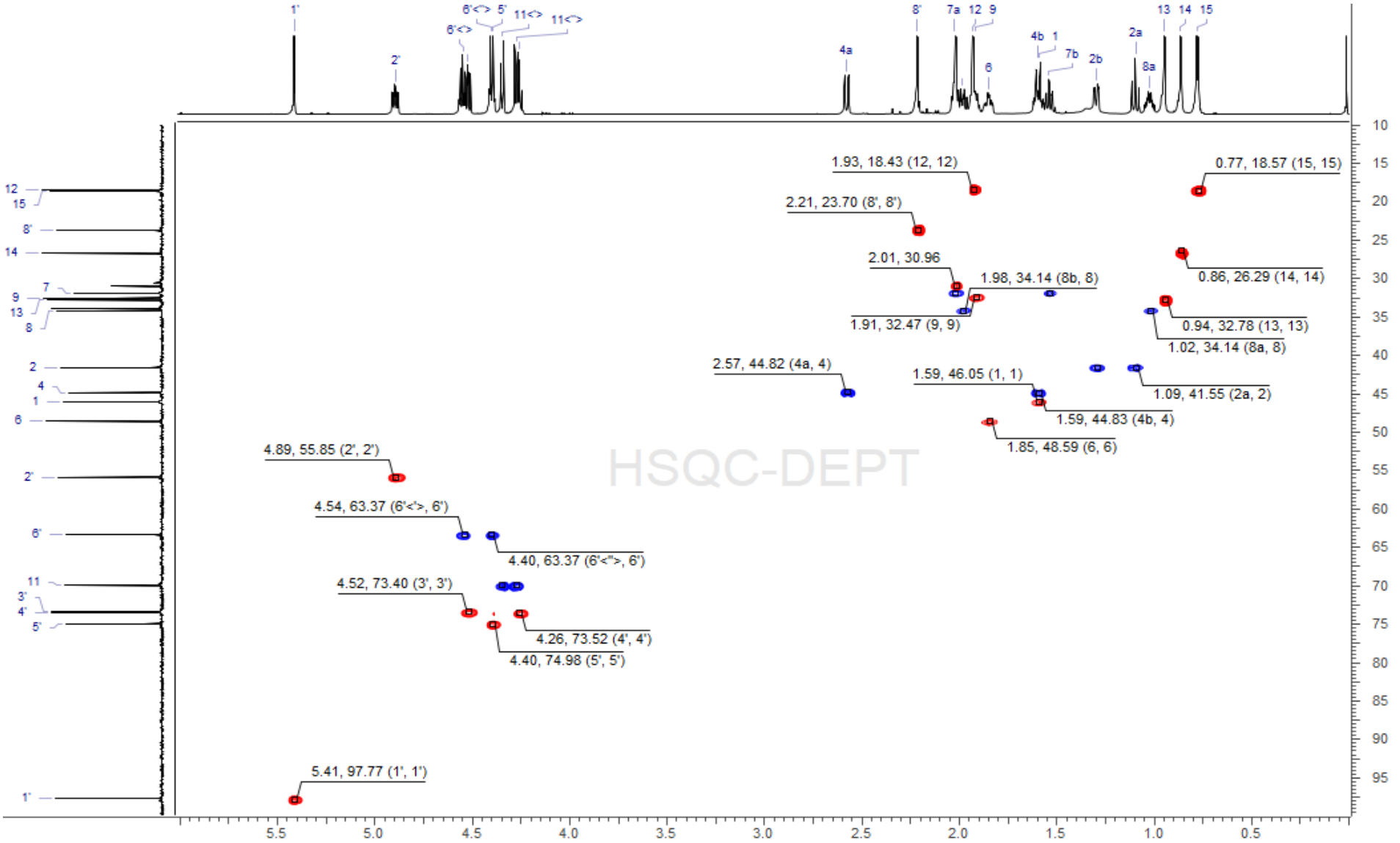

Figure S27 HSQC NMR spectrum (500 MHz, pyridin-d_5) of brasilane A **1**.

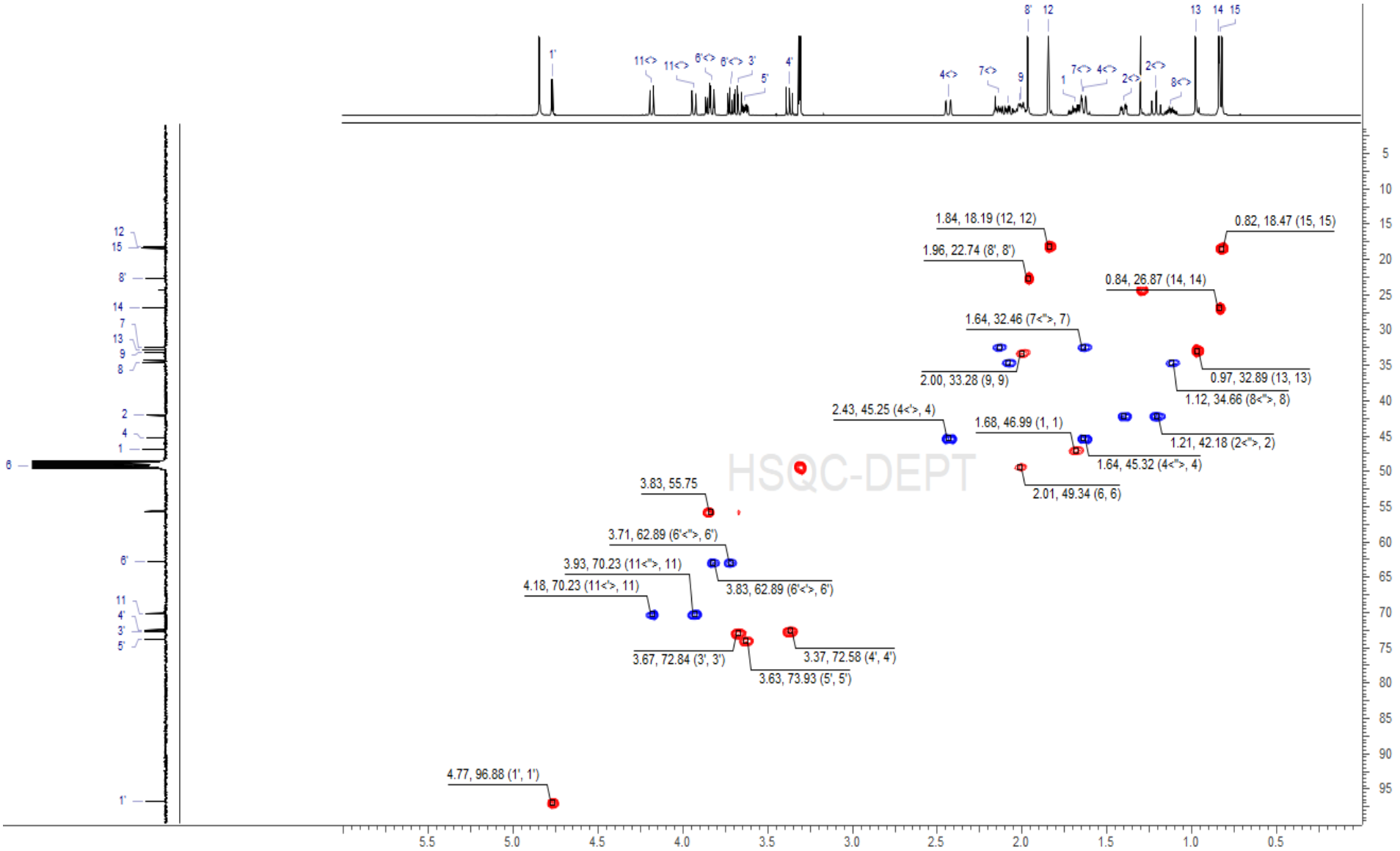

Figure S28 HSQC NMR spectrum (500 MHz, methanol-d_4) of brasilane A **1**.

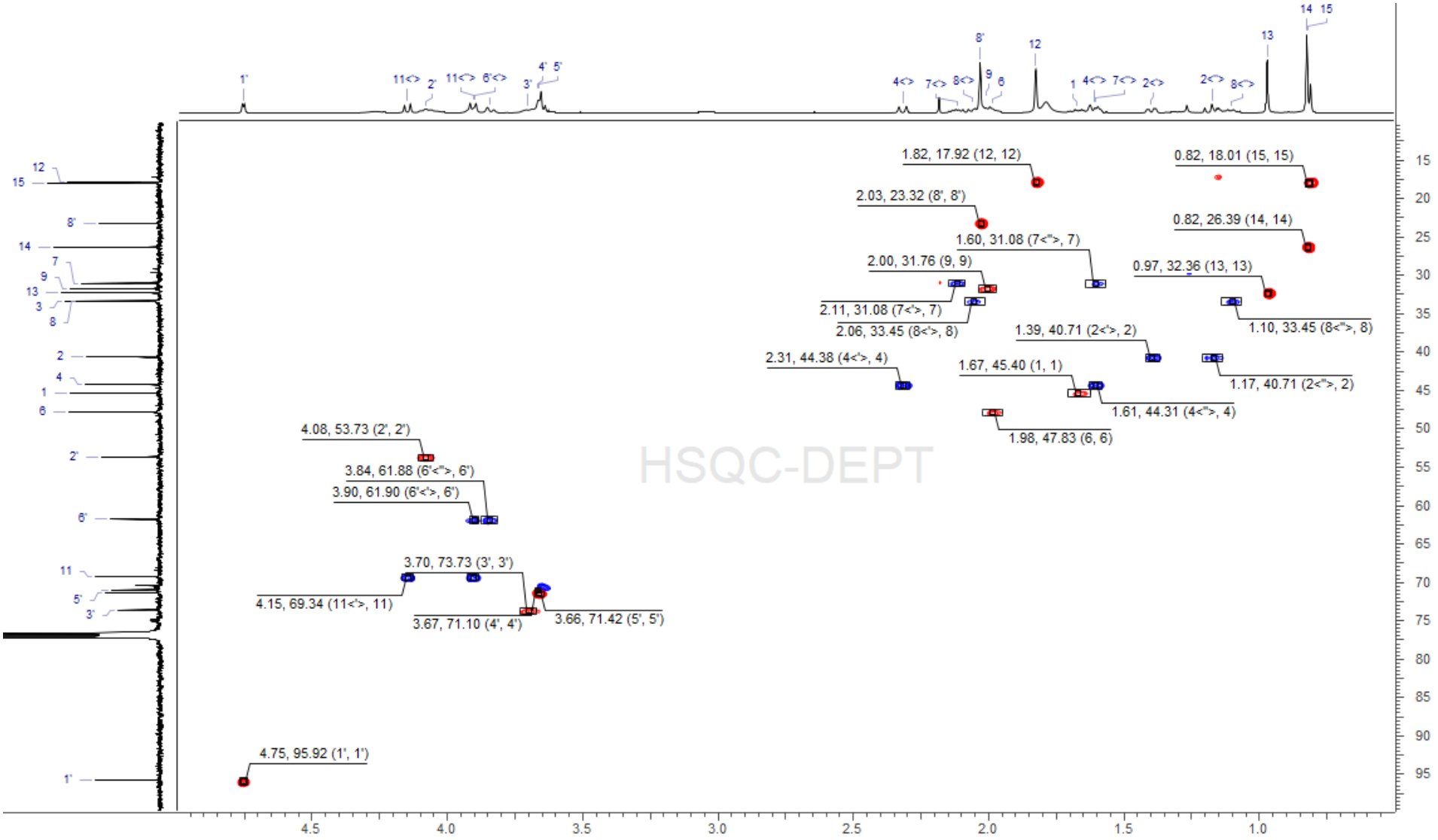

Figure S29 HSQC NMR spectrum (500 MHz, chloroform-*d*) of brasilane A **1**.

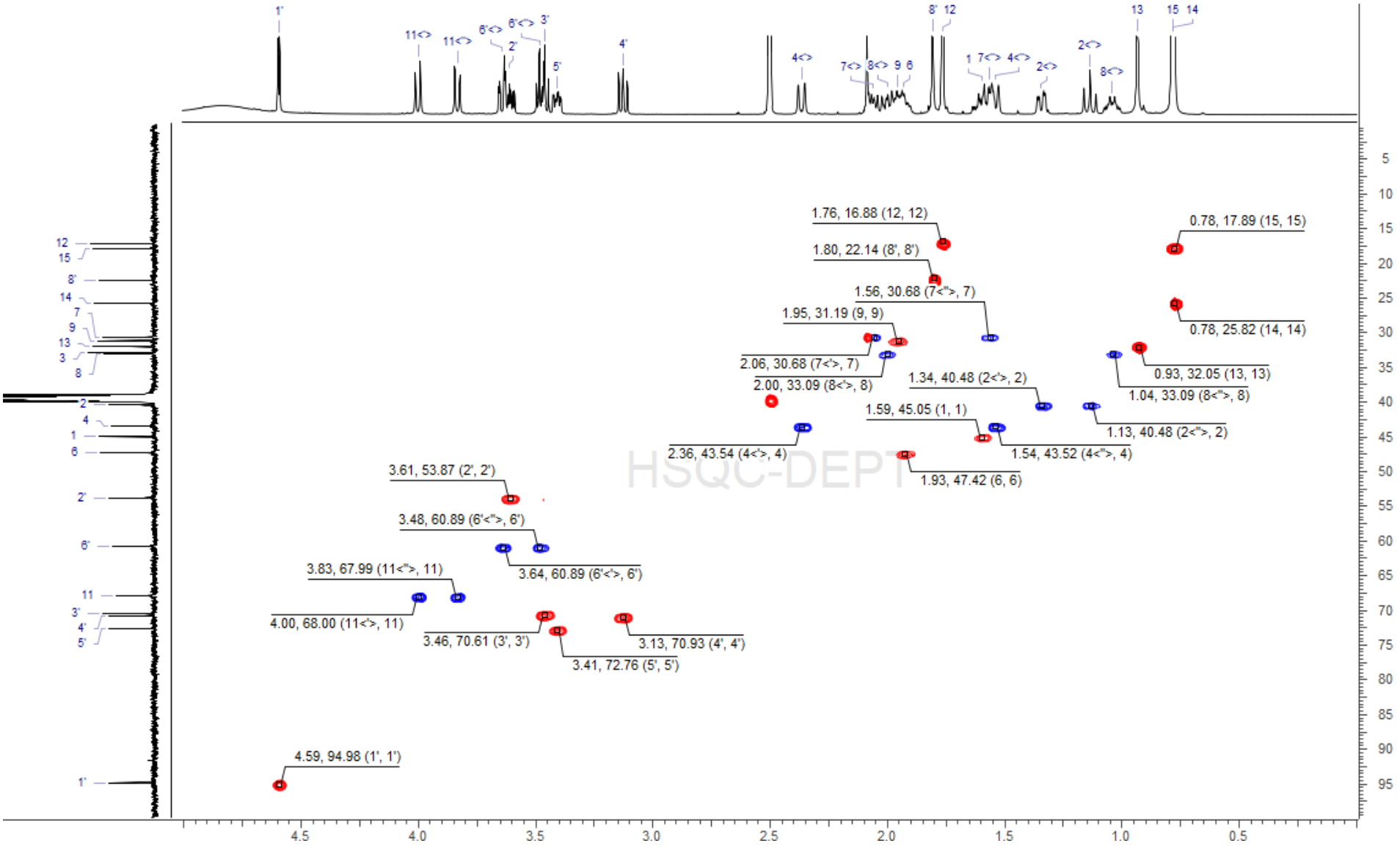

Figure S30 HSQC NMR spectrum (500 MHz, DMSO-d_6) of brasilane A **1**.

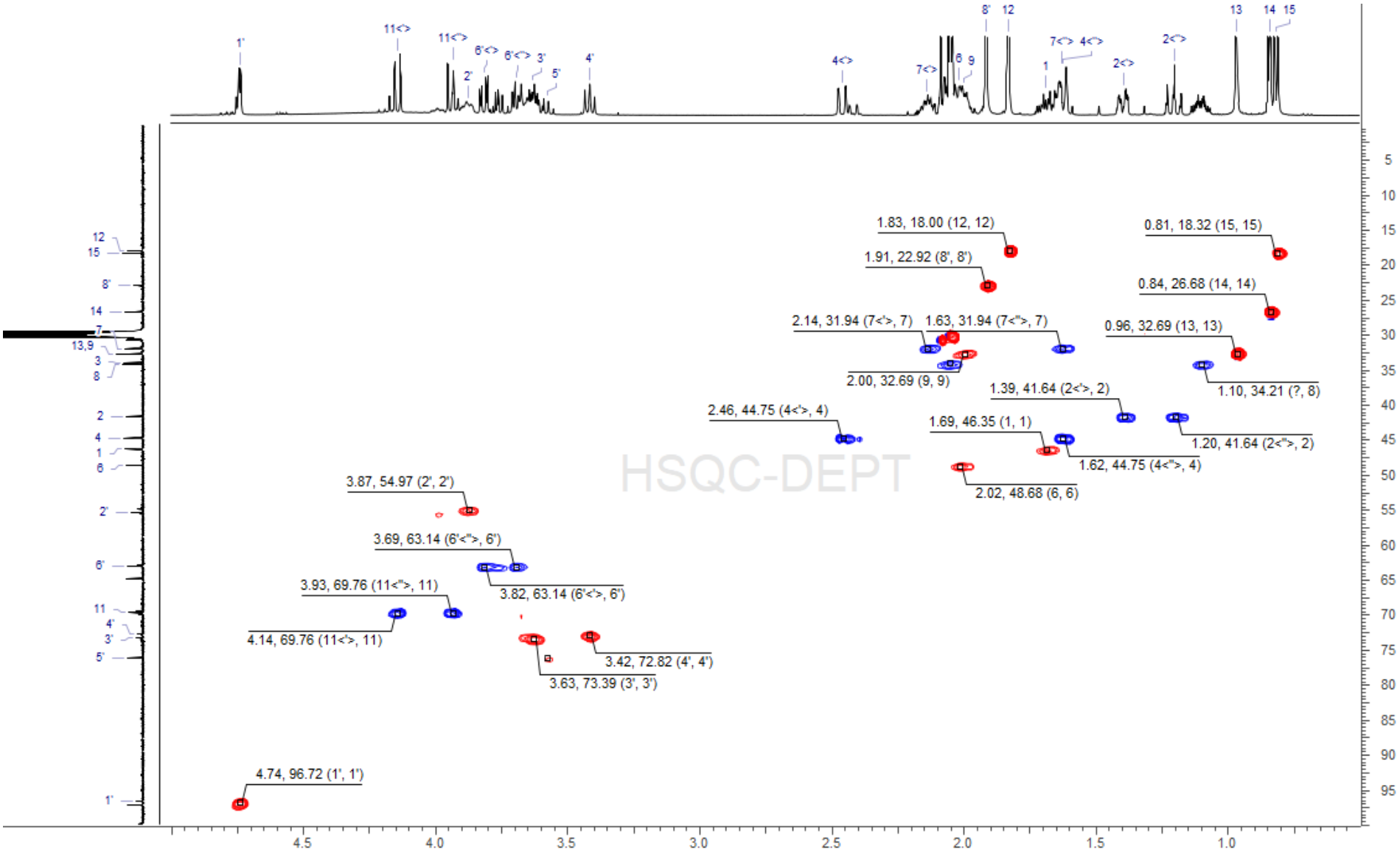

Figure S31 HSQC NMR spectrum (500 MHz, acetone-d_6) of brasilane A **1**.

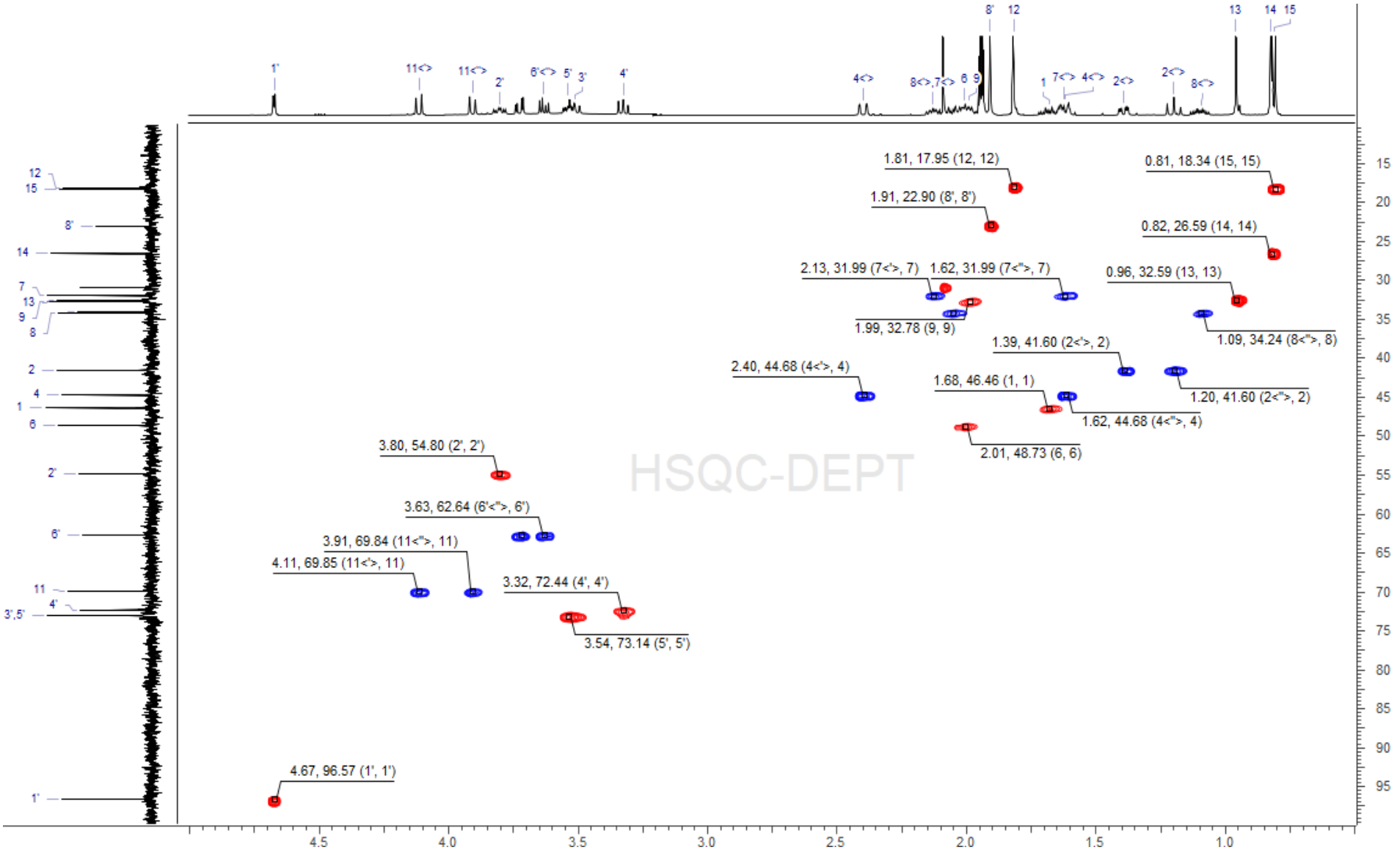

Figure S32 HSQC NMR spectrum (500 MHz, acetonitrile-d_3) of brasilane A **1**.

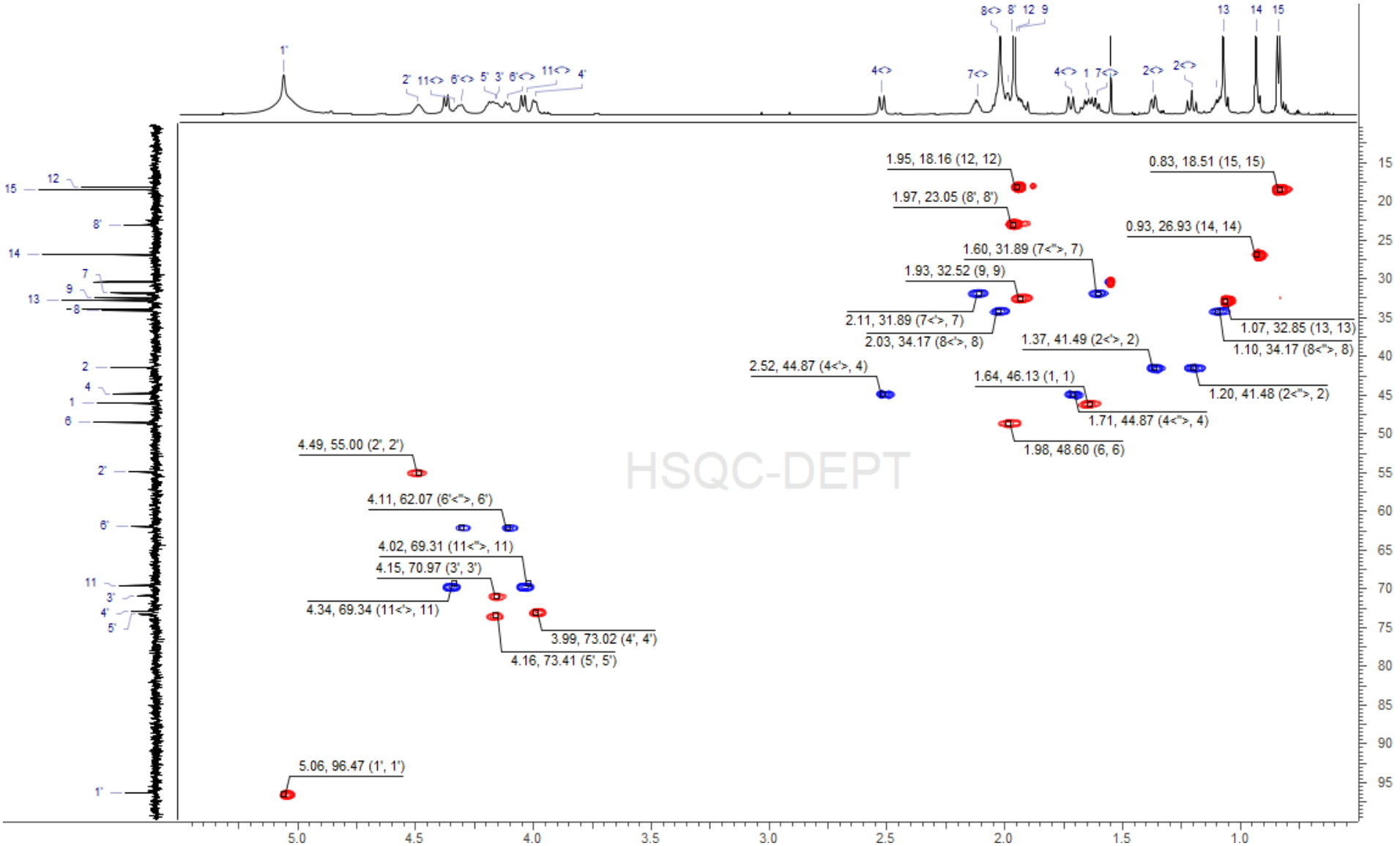

Figure S33 HSQC NMR spectrum (500 MHz, benzene-d_6) of brasilane A **1**.

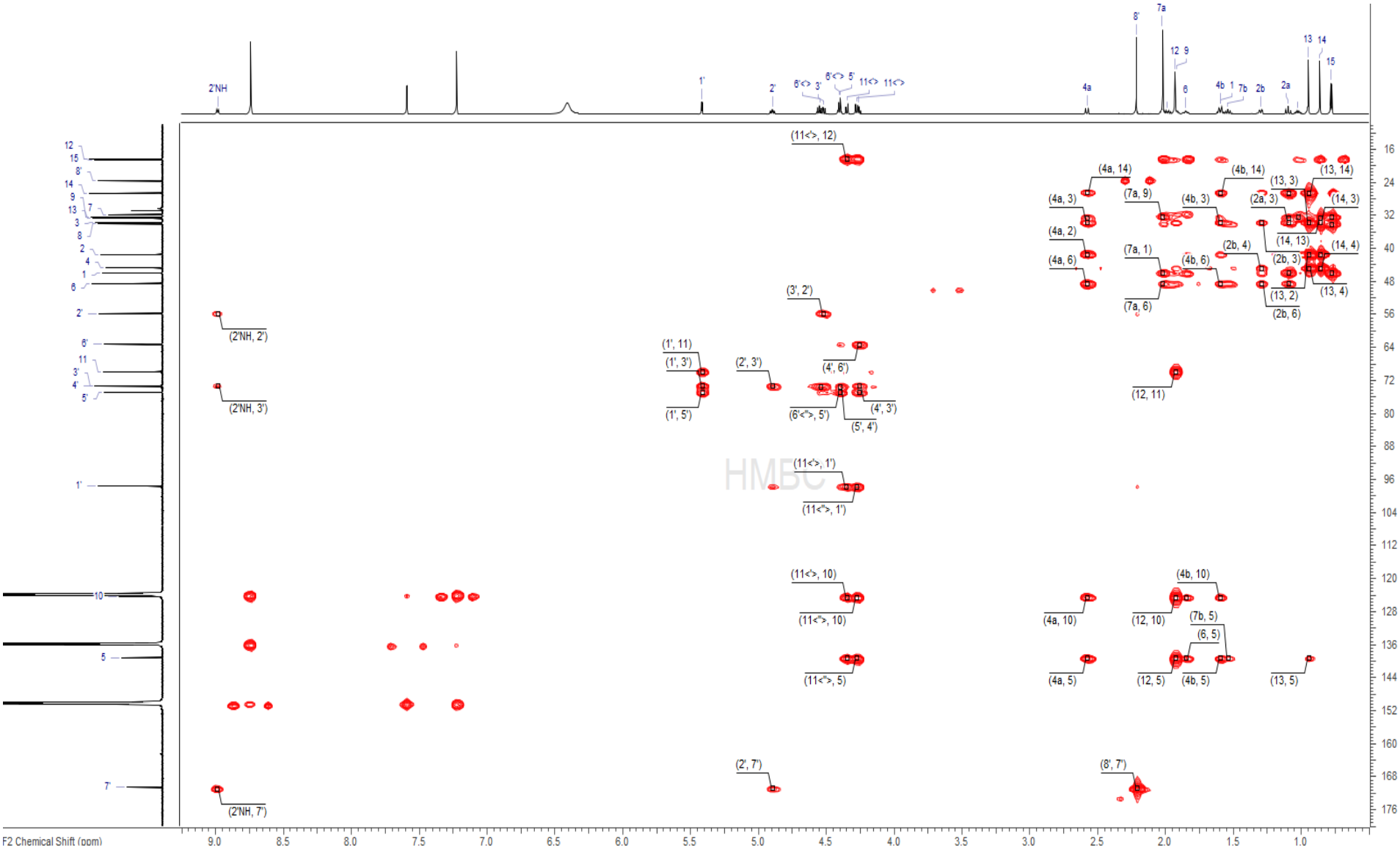

Figure S34 HMBC NMR spectrum (700 MHz, pyridine-d_5) of brasilane A **1**.

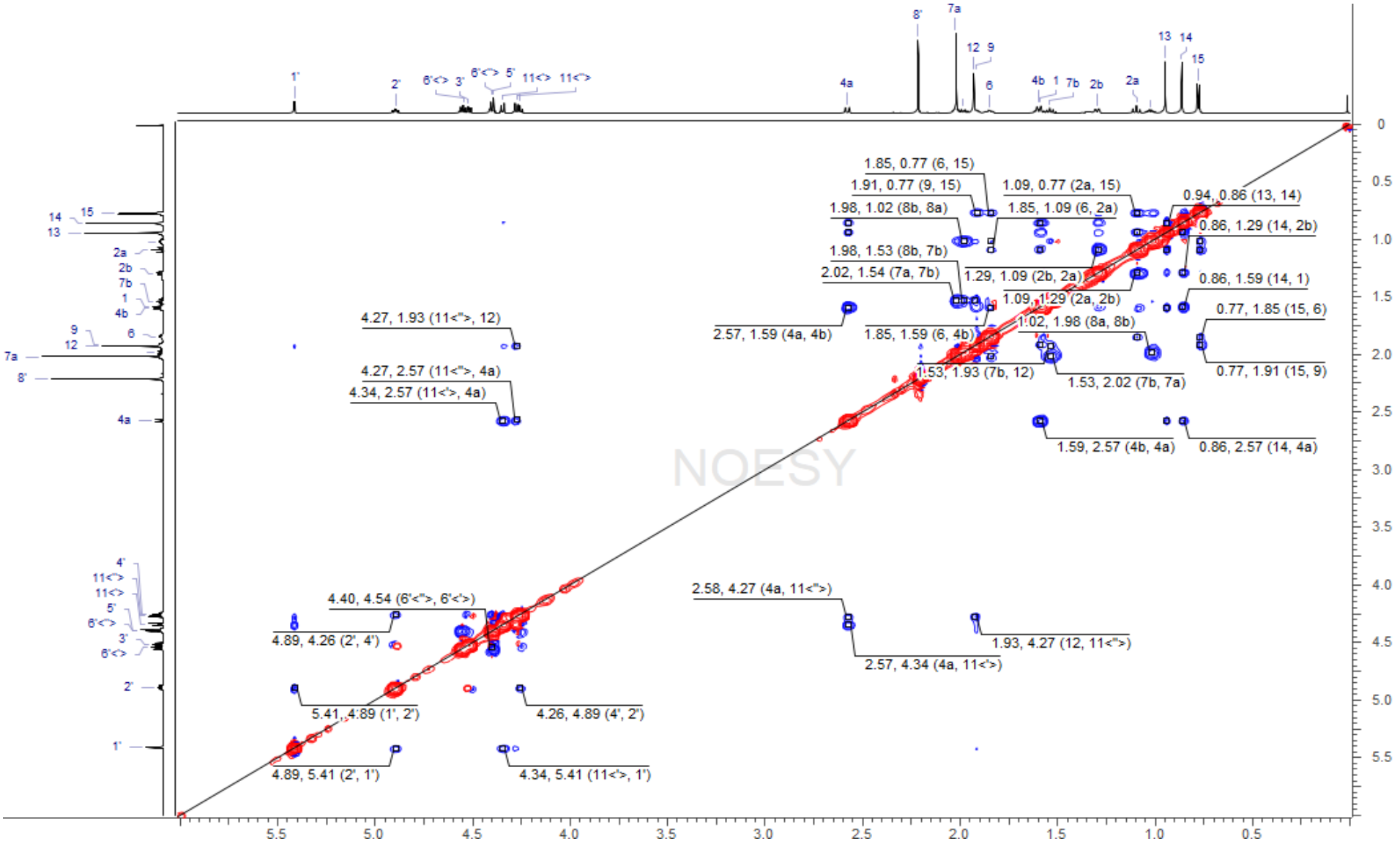

Figure S35 NOESY NMR spectrum (700 MHz, pyridin-d_5) of brasilane A **1**.

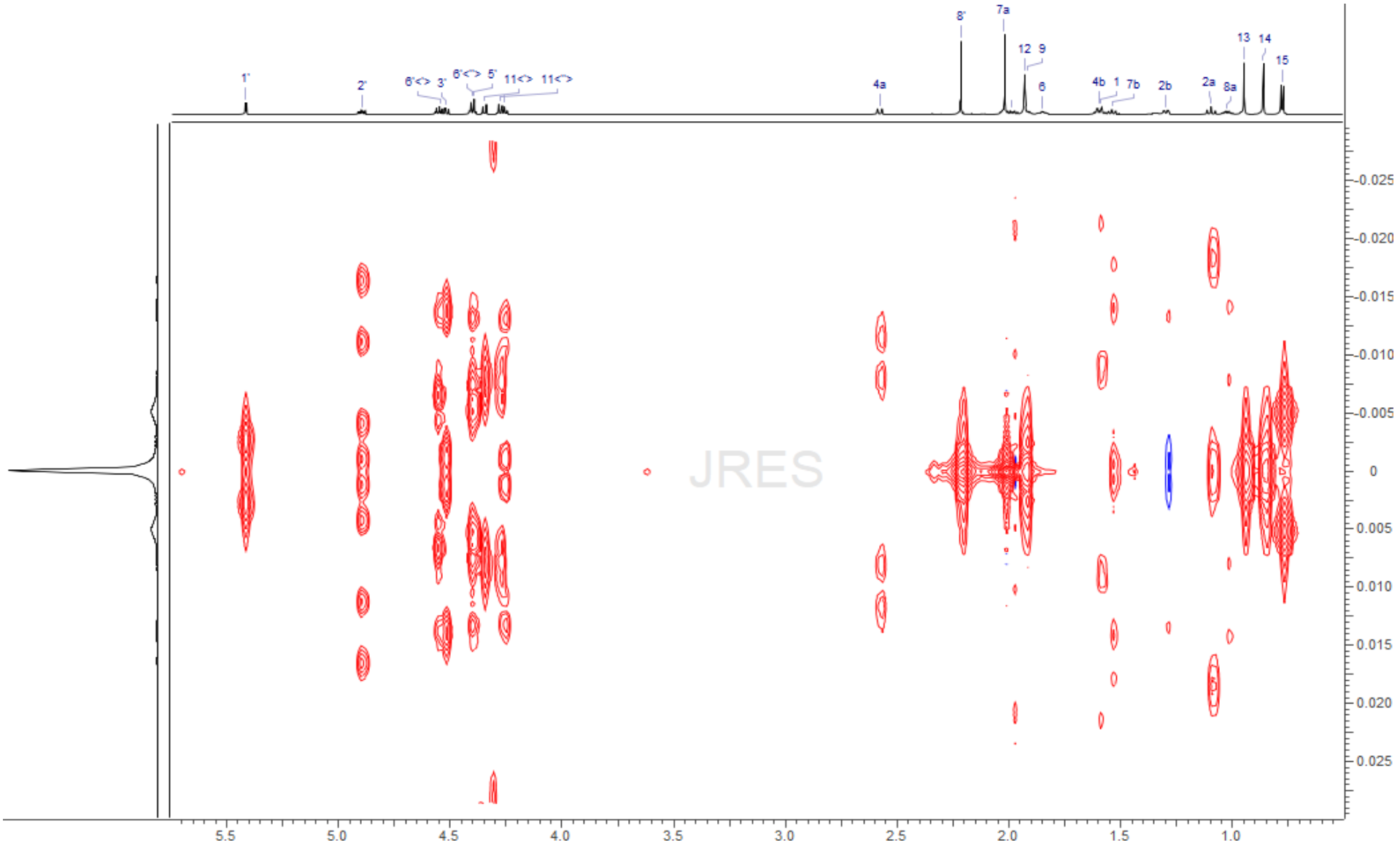

Figure S36 Jres NMR spectrum (700 MHz, pyridin-d_5) of brasilane A **1**.

S6.3 Brasilane D

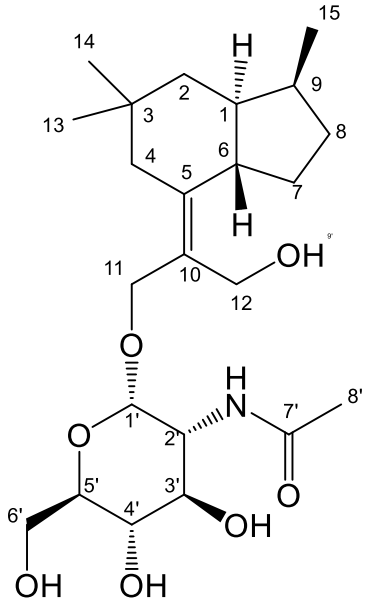

2

amorphous solid; $[\alpha]^{20}_{D}$ +46.0 (c = 0.1, CH_3OH); CD (CH_3OH) λ_{max} (Δ_ε): 195 nm (+1.8), 211 nm (-3.1); ^{1}H NMR (DMSO-d_6; 500 MHz), ^{13}C NMR (DMSO-d_6; 125 MHz) see table S2; ESI-MS *m/z* 424.27 $[M+H-H_2O]^+$, 442.26 $[M+H]^+$, 464.28 $[M+Na]^+$, 905.53 $[2M+Na]^+$, 440.33 $[M-H]^-$, 486.33 $[M+HCOO]^-$; HR-ESI-MS *m/z* 442.2792 $[M+H]^+$ (calcd. for $C_{23}H_{40}NO_7$, 442.2799), 464.2611 $[M+Na]^+$ (calcd. for $C_{23}H_{39}NO_7Na$, 464.2619).

Atom#	C Shift	dH, mult	COSY	N/ROESY	C to H HMBC
1	45.3, CH	1.63, m	2, 2, 6	14, 15, 8	
2	40.7, CH_2	1.17, m	2, 1	14, 13, 2	14, 13, 3, 1, 6
		1.34, m	2, 1	14, 2	6
3	33.5, C				
4a	44.0, CH_2	1.54, br d (13.7)	4	13, 4	14, 3, 2, 6, 10, 5
4b		2.40, dd (14.0, 1.4)	4	14, 13, 4, 11	3, 2, 6, 10, 5
5	142.5, C				
6	47.7, CH	1.93, s	1, 7		1, 10, 5
7a	29.5, CH_2	1.8, br s	8, 6, 7	12	
7b		2.01, m	8, 7	12	9, 1, 6
8a	33.1, CH_2	2.00, m	8	15, 8, 1, 12	
8b		1.05, br s	7, 8, 7	15, 8	9
9	31.4, CH	1.96, br d (4.43)	15	15	
10	128.3, C				
11a	65.2, CH_2	4.06, d (10.8)	11	11	12, 1', 10, 5
11b		3.97, d (10.8)	11	4, 11, 1'	12, 1', 10, 5
12a	58.2, CH_2	3.84, d (11.3)	12	12	11, 10, 5
12b		4.11, d (11.3)	12	7, 8, 7, 12	11, 10, 5
13	32.2, CH_3	0.95, s		14, 2, 4, 4	14, 3, 2, 4
14	25.3, CH_3	0.78, s		13, 2, 2, 1, 4	3, 2, 4
15	17.9, CH_3	0.79, m	9	8, 1, 9, 8	9, 8, 1
1'	95.3, CH	4.60, d (3.5)	2'	3', 2', 11	11, 3', 5'
2'NH		7.62, d (7.9)	2'	8', 3', 2'	7'
2'	53.9, CH	3.60, ddd (10.8, 7.9, 3.5)	3', 1', 1'NH	4', 1', 1'NH	3', 7'
3'	70.7, CH	3.44, dd (10.8, 8.5)	4', 2'	1', 1'NH	2', 4'
4'	70.8, CH	3.14, dd (9.5, 8.5)	5', 3'	2'	2', 6', 3', 5'
5'	72.7, CH	3.42, m	4', 6', 6'	6'	
6'a	60.8, CH_2	3.63, dd (11.6, 2.0)	5', 6'	5', 6'	
6'b		3.50, br dd (11.6, 5.3)	5', 6'	6'	5'
7'	169.2, C				
8'	22.5, CH_3	1.80, s		1'NH	7'

Table S5 NMR data (^{1}H 500MHz, ^{13}C 125 MHz) of brasilane D **2** in DMSO-d_6.

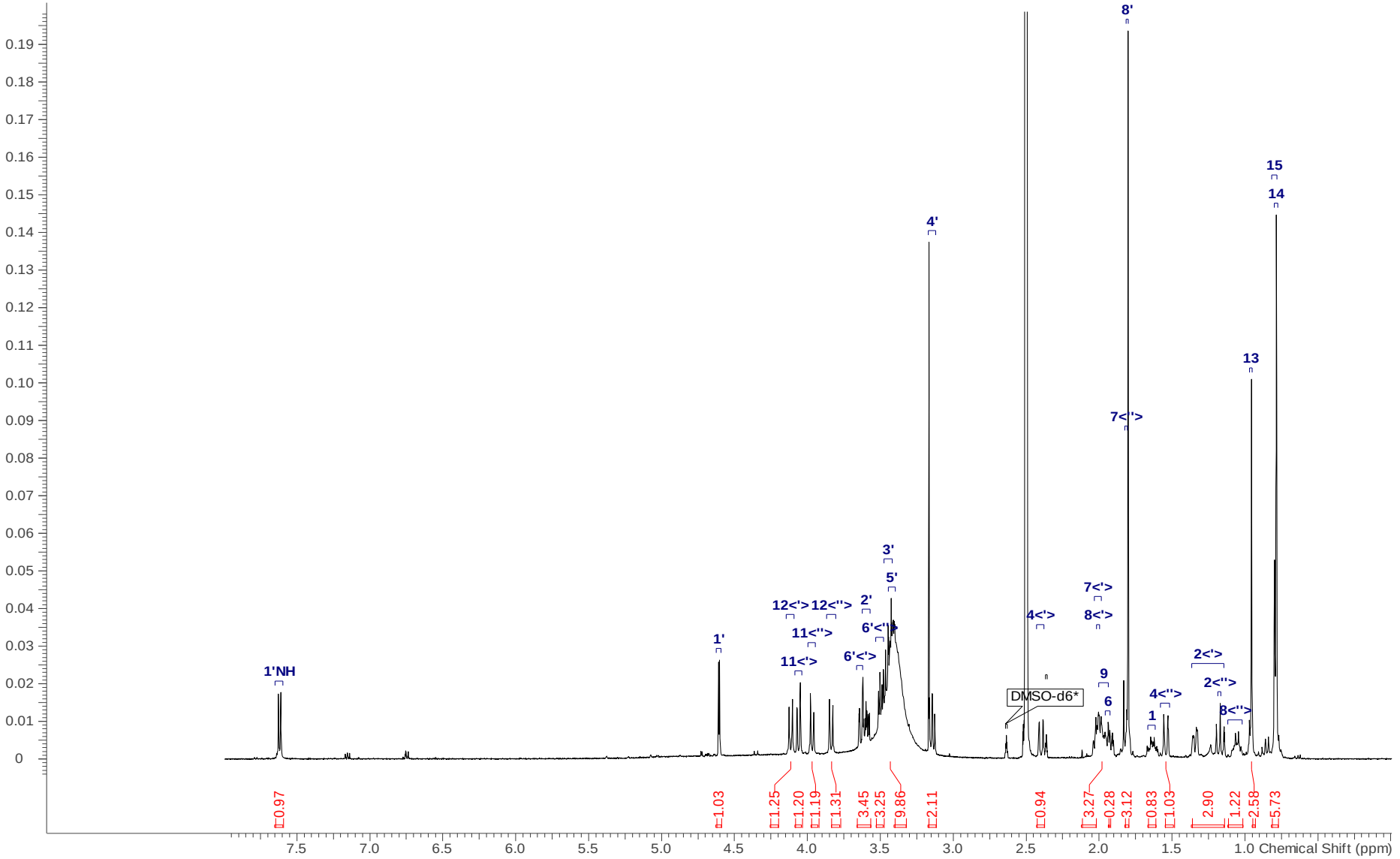

Figure S37 ^{1}H NMR spectrum (500 MHz, DMSO-d_6) of brasilane D **2**.

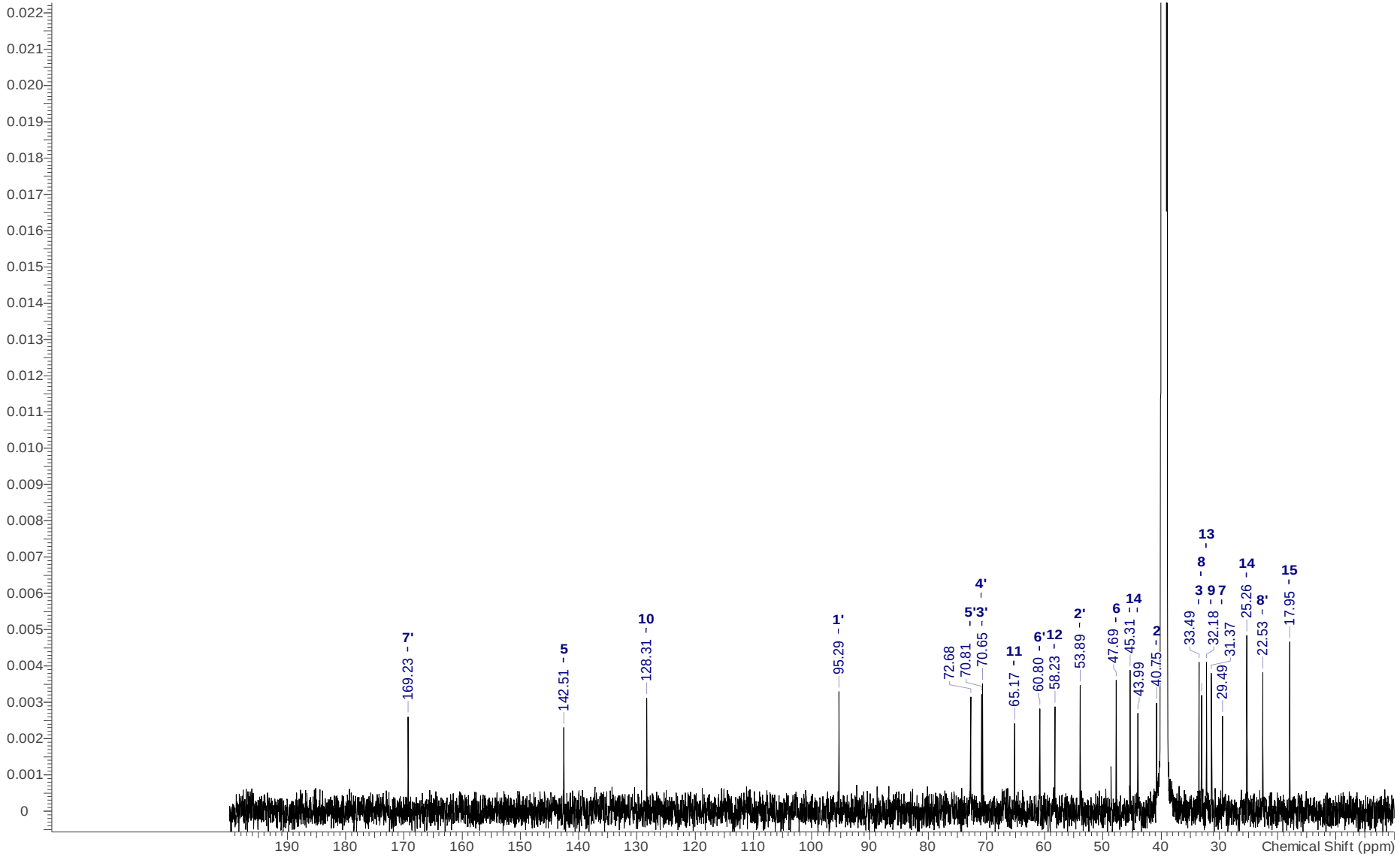

Figure S38 ^{13}C NMR spectrum (125 MHz, DMSO-d_6) of brasilane D **2**.

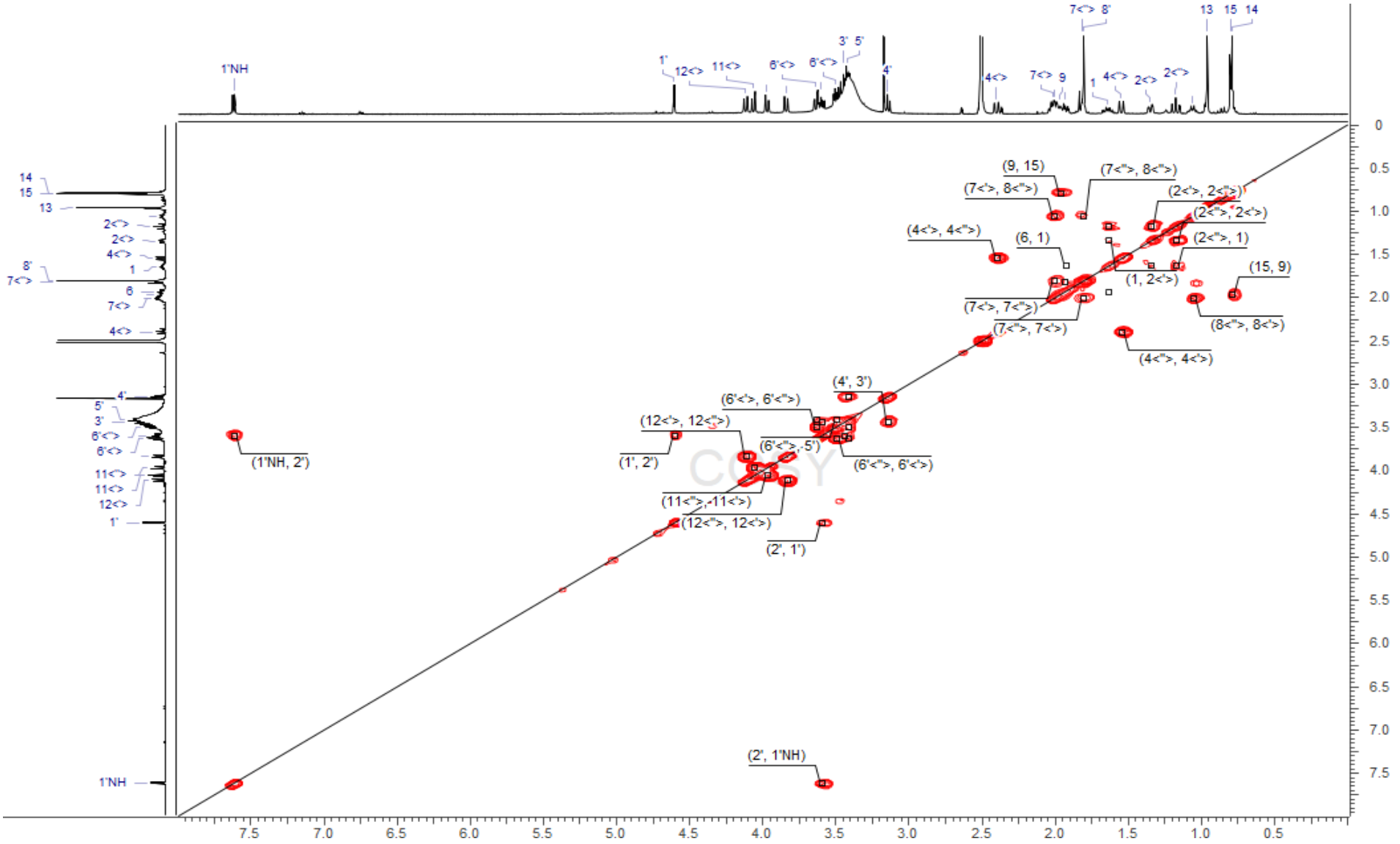

Figure S39 COSY NMR spectrum (500 MHz, DMSO-d_6) of brasilane D **2**.

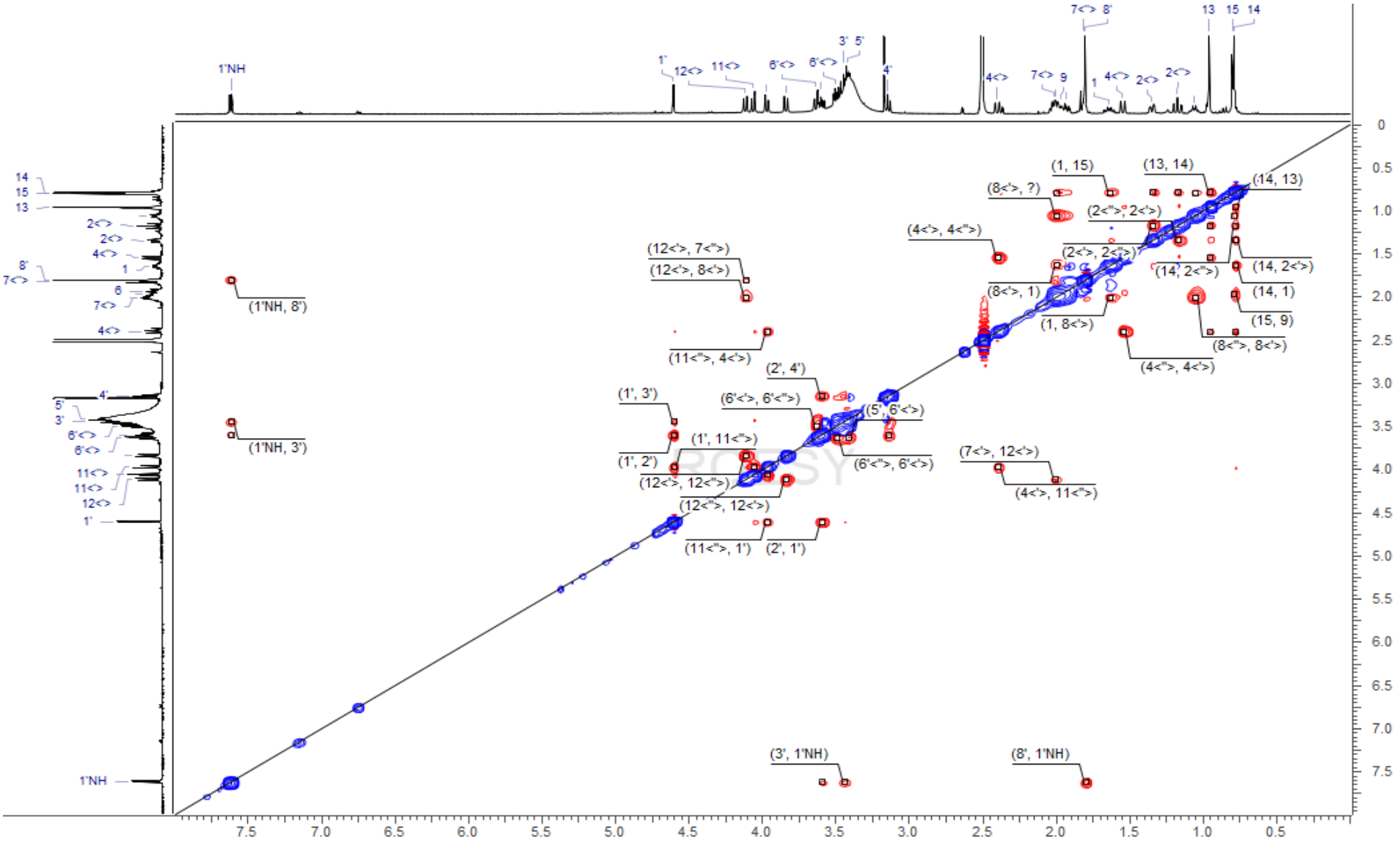

Figure S40 ROESY NMR spectrum (500 MHz, DMSO-d_6) of brasilane D **2**.

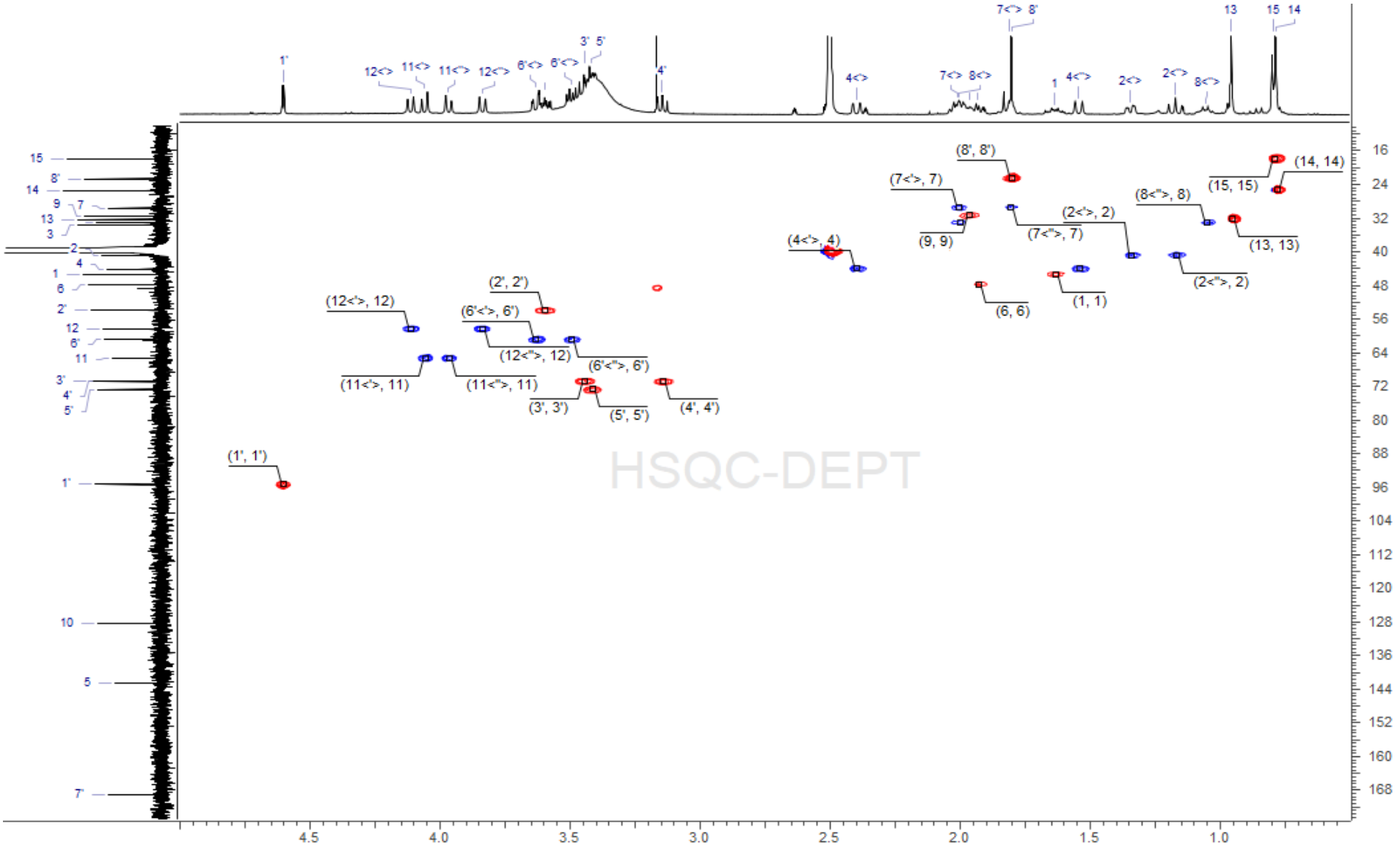

Figure S41 HSQC NMR spectrum (500 MHz, DMSO-d_6) of brasilane D **2**.

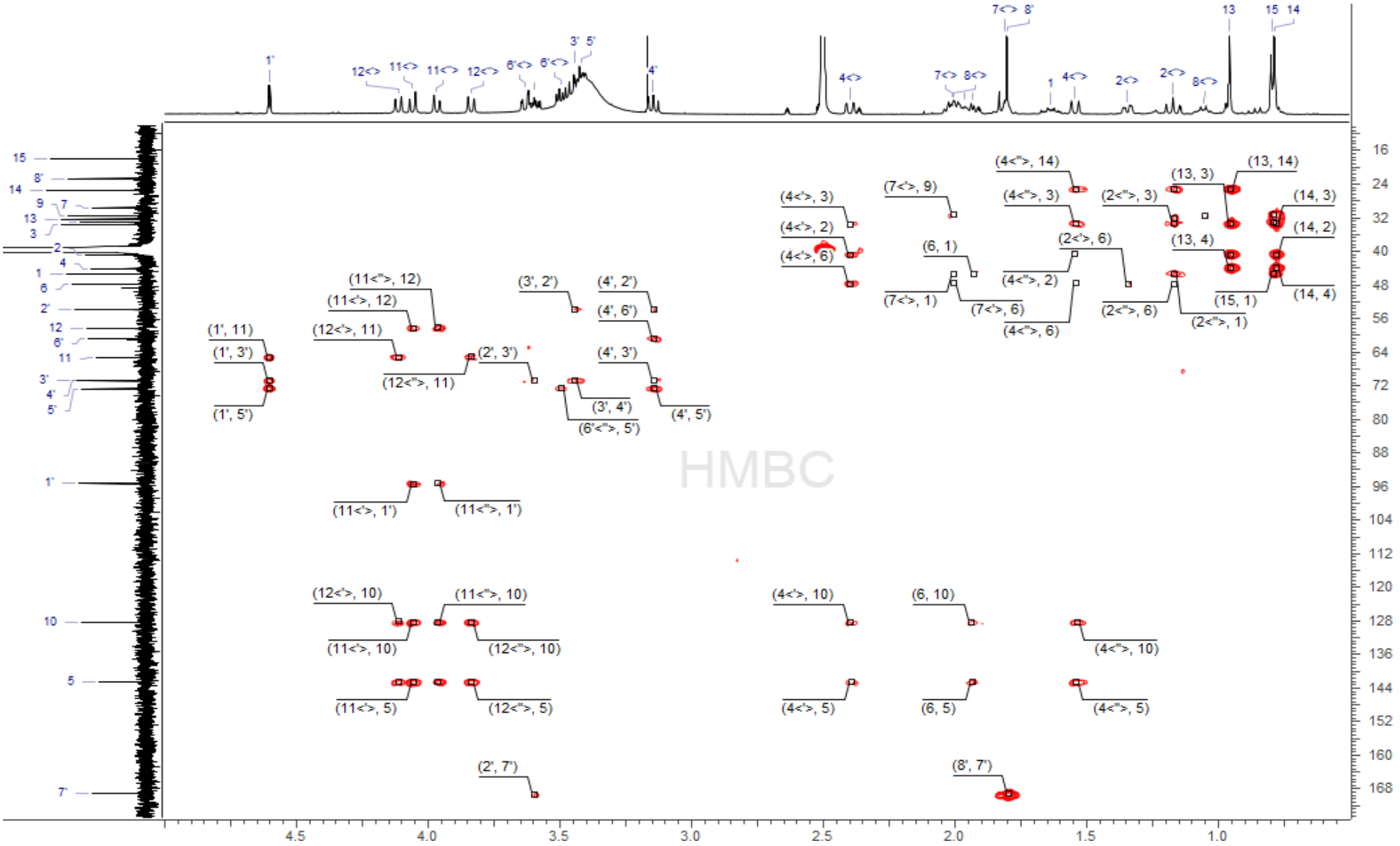

Figure S42 HMBC NMR spectrum (500 MHz, DMSO-d_6) of brasilane D **2**.

S6.4 Brasilane E

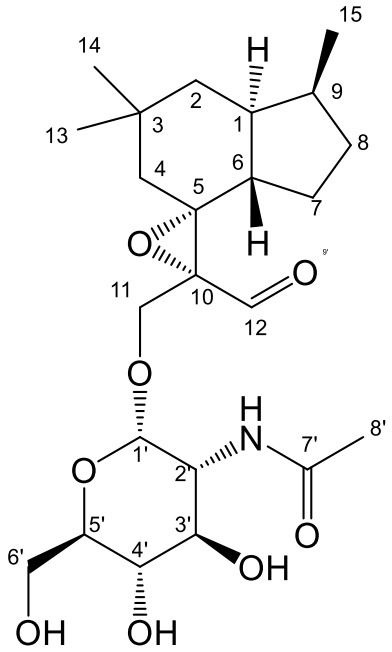

3

amorphous solid; $[\alpha]^{20}_{D}$ +90.0 (c = 0.1, CH_3OH); CD (CH_3OH) λ_{max} ($\Delta\varepsilon$): 195 nm (+4.4), 215 nm (-0.8), 241 (+0.3), 306 (-0.3); ^{1}H NMR (pyridin-d_5; 700 MHz), ^{13}C NMR (pyridin-d_5; 175 MHz) see table S3; ESI-MS *m/z* 456.27 $[M+H]^+$, 500.32 $[M+Na]^+$, 933.47 $[2M+Na]^+$, 454.31 $[M-H]^-$, 500.32 $[M+HCOO]^-$; HR-ESI-MS *m/z* 456.2589 $[M+H]^+$ (calcd. for $C_{23}H_{38}NO_8$, 456.2592), 478.2406 $[M+Na]^+$ (calcd. for $C_{23}H_{37}NO_8Na$, 478.2411).

Atom#	C Shift	H Shift	COSY	N/ROESY	C to H HMBC
1	43.3, CH	1.61, m	2, 2, 6, 9	14, 2, 2, 6, 9	15, 2, 6, 5
2a	40.6, CH_2	0.99, m	14, 13, 2, 1	15, 14, 13, 4, 1, 8, 6	14, 13, 3, 1, 6
2b		1.16, m	2, 4, 1	15, 14, 1, 6	3, 1, 4, 6
3	34.2, C				
4a	45.6, CH_2	1.41, dd (13.8, 1.5)	2, 4	13, 4, 11	14, 7, 13, 3, 2, 6, 5, 10
4b		1.55, d (13.8)	14, 4	13, 2, 4	14, 13, 3, 2, 6, 5, 10
5	71.532				
6	47.791	1.78, m	7, 1	15, 8, 2, 2, 1, 7	8, 7, 2, 1, 5, 4'
7a	30.0, CH_2	1.63, m	7, 8	14, 7, 8, 6, 9, 12	9, 1, 6
7b		0.88, m	7, 6	15, 7, 8, 12	
8a	33.7, CH_2	1.77, m	8, 7, 9	15, 7, 2, 7, 9	15, 7, 1, 6, 5, 4'
8b		0.88, m	8	6, 9	
9	32.6, CH	1.88, m	15, 1, 8	15, 8, 1, 7, 8	
10	73.0, C				
11a	68.3, CH_2	3.89, dd (11.3, 1.2)	11, 12	14, 4, 11	5, 10, 1', 12
11b		5.00, d (11.4)	11	14, 11, 5'	1'
12	201.7, CH	9.85, br s	11	7, 7	11, 10
13	32.4, CH_3	0.84, s	2	2, 4, 4	14, 3, 2, 4, 5
14	25.5, CH_3	0.77, s	2, 4	2, 2, 1, 7, 11, 11	13, 3, 2, 4
15	17.8, CH_3	0.71, d (7.1)	9	7, 2, 2, 8, 6, 9	9, 8, 1
1'	99.0, CH	5.64, d (3.7)	2'		11, 3', 5'
2'	55.6, CH	4.88, ddd (10.9, 8.3, 3.8)	3', 1', 2'NH	4', 2'NH	3', 1', 1Ac
2'NH		9.19, d (8.3)	2'	2Ac, 3', 2'	2', 3', 1Ac
3'	72.7, CH	4.47, dd (10.9, 8.7)	4', 2'	2'NH	2', 4'
4'	72.970	4.27, dd (9.8, 8.5)	5', 3'	6', 2'	6', 3', 5'
5'	75.154	4.35, ddd (9.8, 5.1, 2.4)	4', 6'	11	4'
6'a	62.8, CH_2	4.40, dd (11.8, 5.1)	5', 6'		5'
6'b		4.53, dd (11.8, 2.4)	6'	4'	4', 5'
7'	171.2, CH_2				
8'	23.4, CH_3	2.17, s		2'NH	1Ac

Table S6 NMR data (^{1}H 700MHz, ^{13}C 175 MHz) of brasilane E **3** in pyridin-d_5.

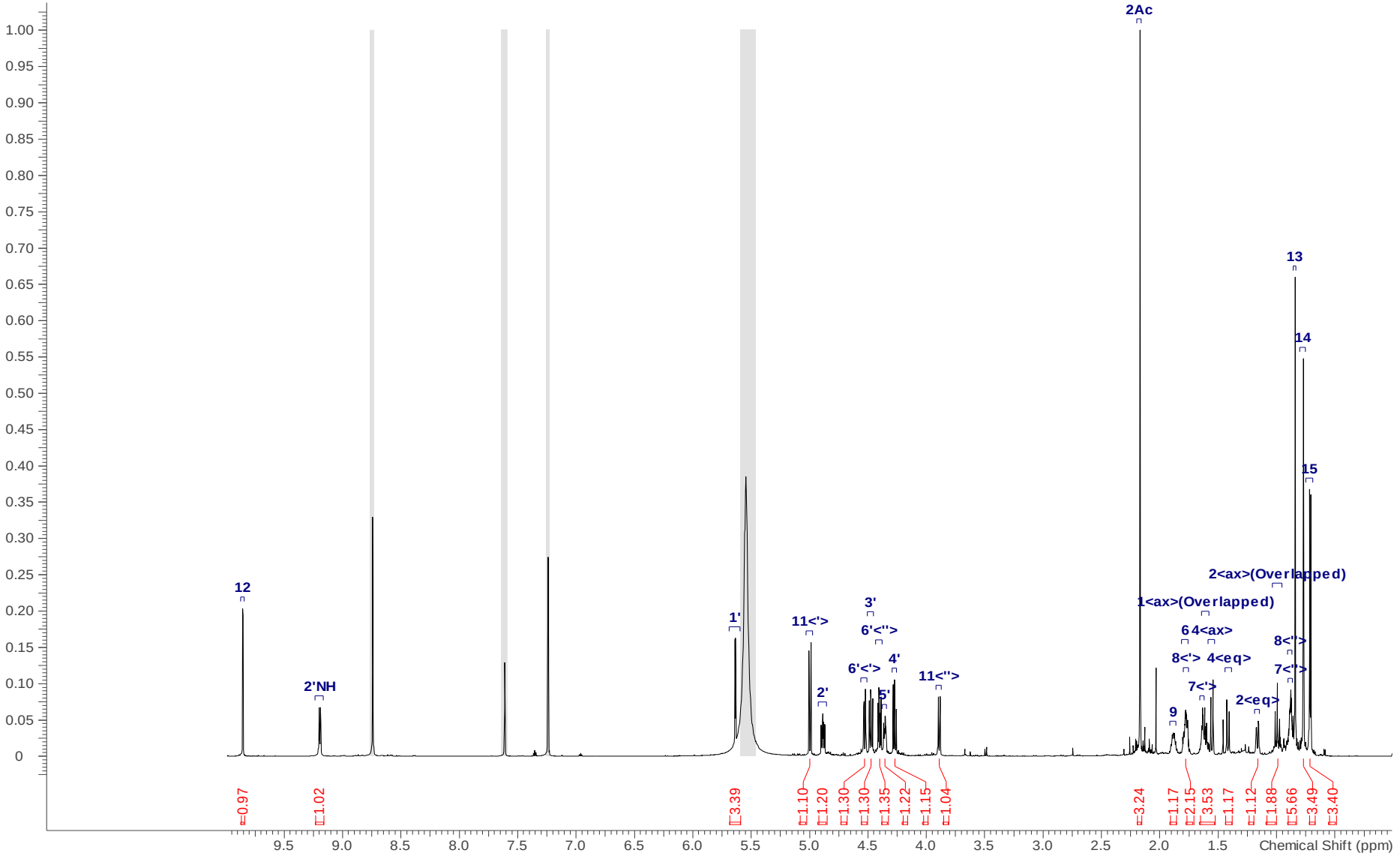

Figure S43 ^{1}H NMR spectrum (700 MHz, pyridin-d_5) of brasilane E **3**.

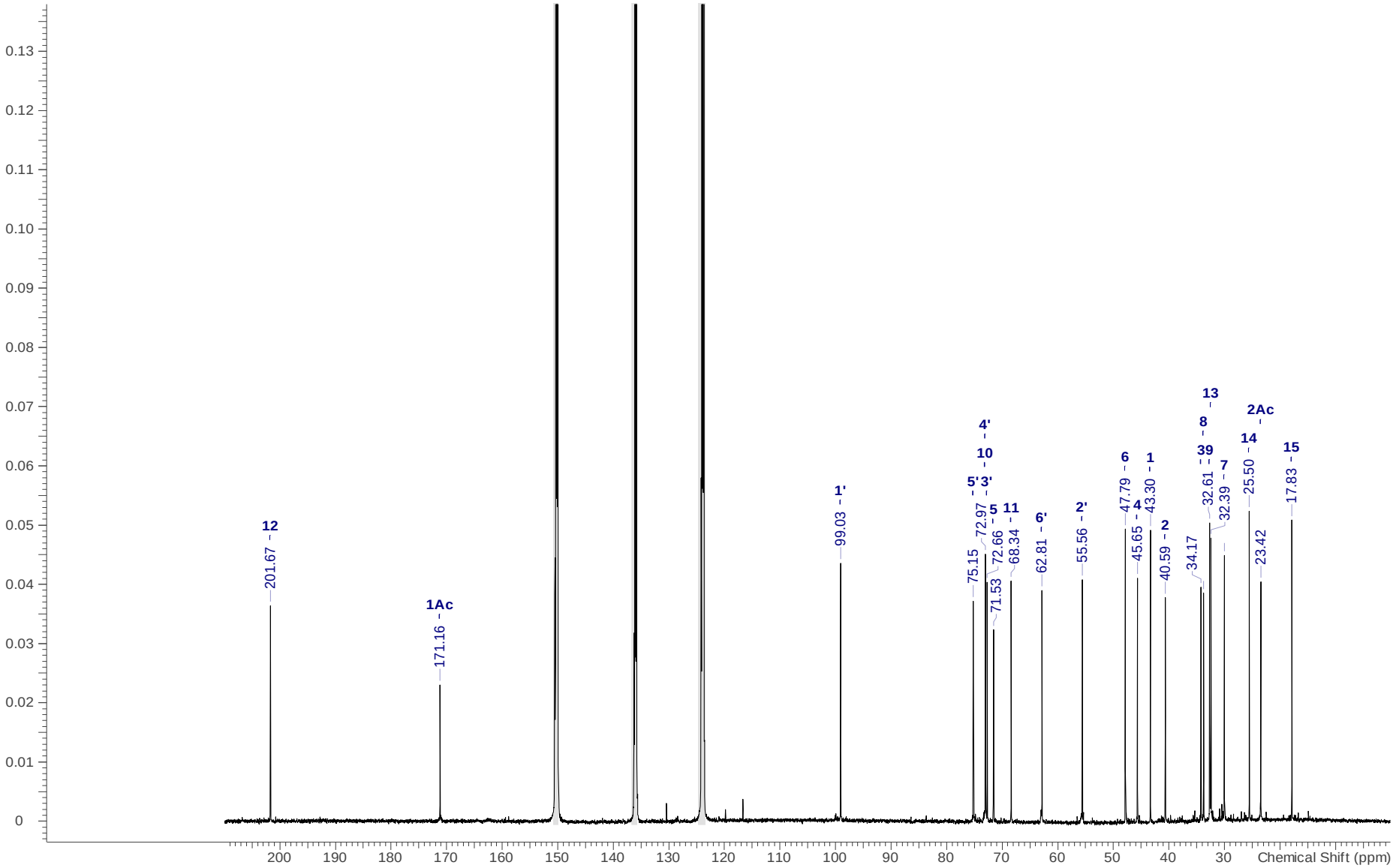

Figure S44 ^{13}C NMR spectrum (175 MHz, pyridin-d_5) of brasilane E **3**.

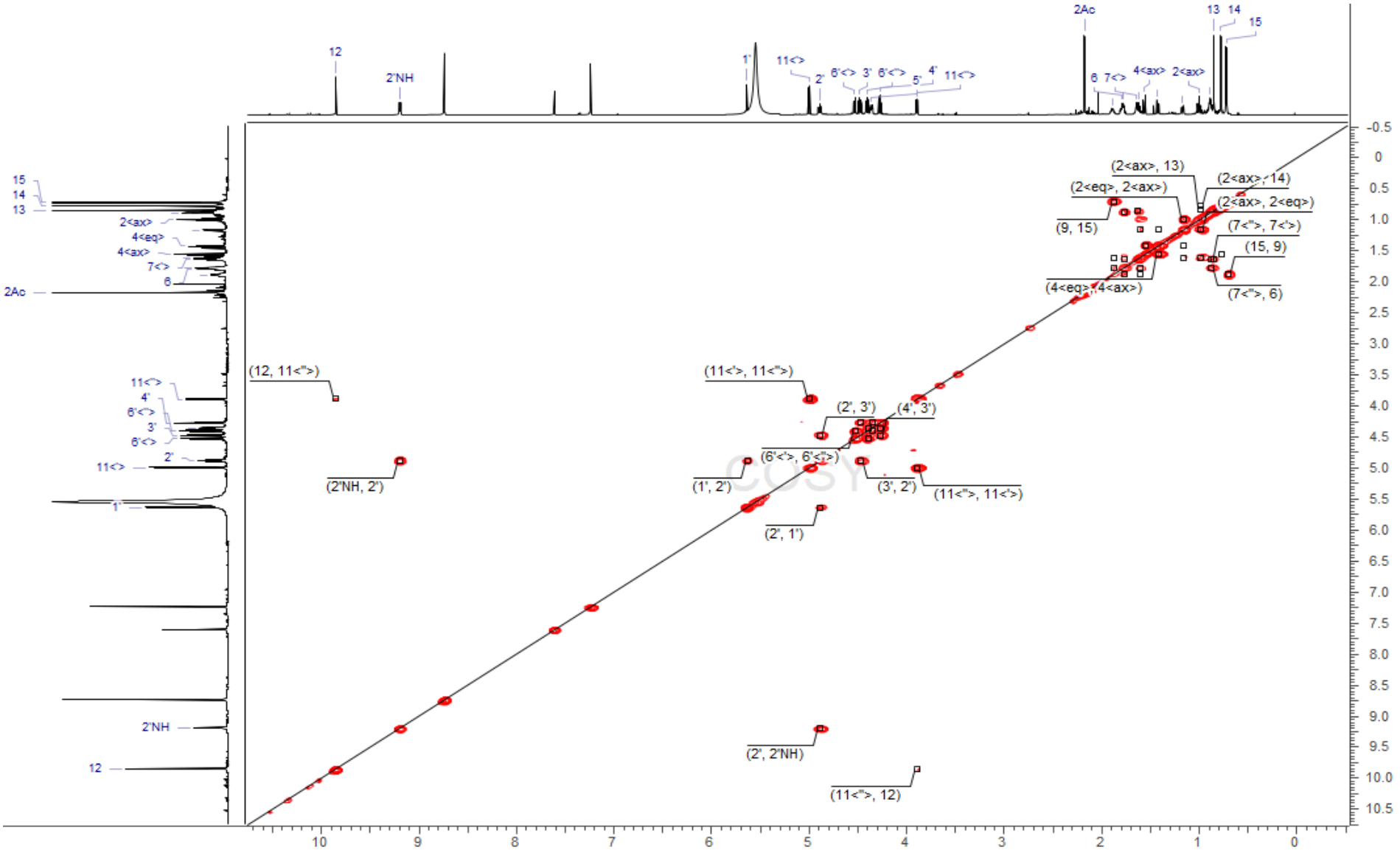

Figure S45 COSY NMR spectrum (700 MHz, pyridin-d_5) of brasilane E **3**.

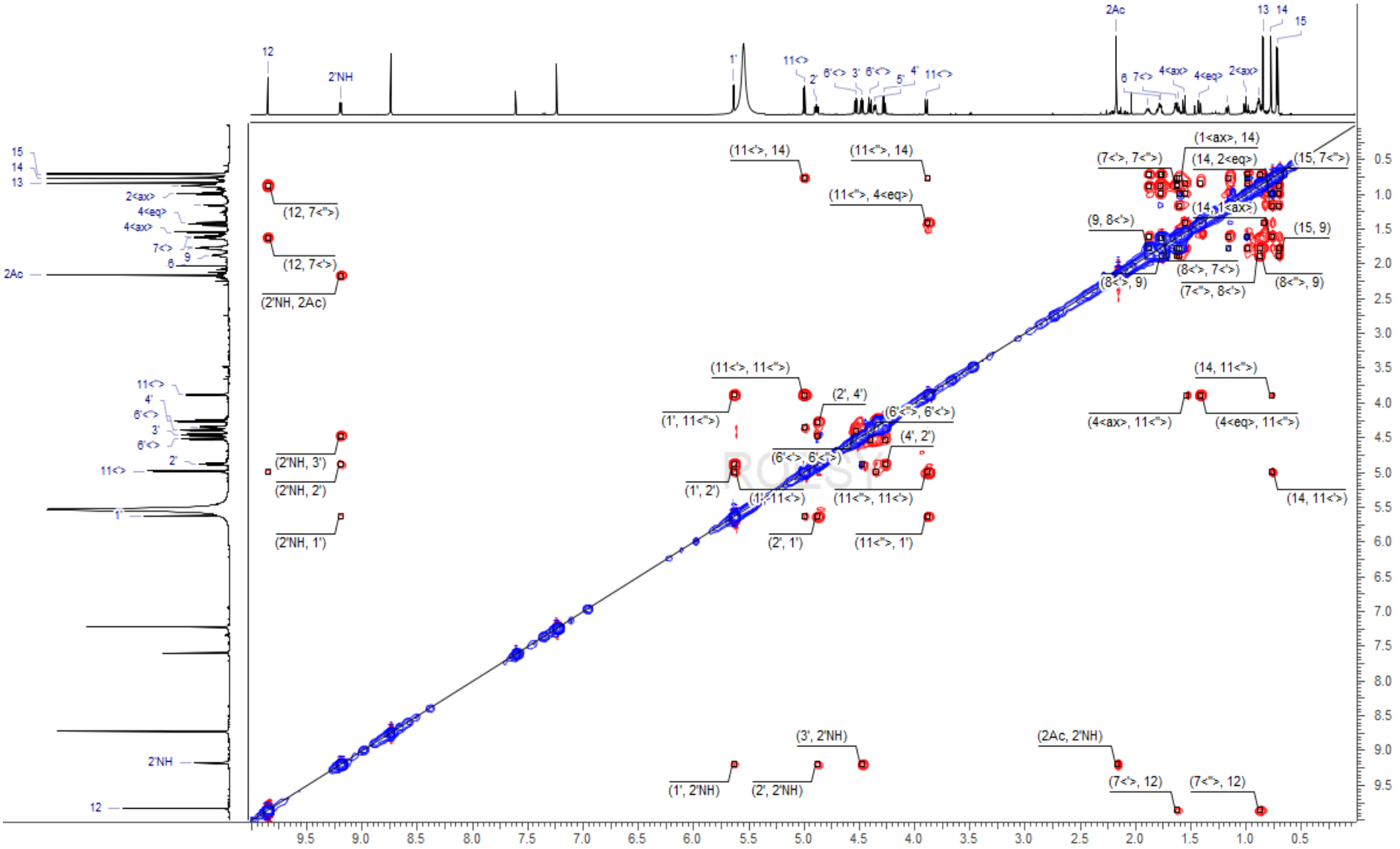

Figure S46 ROESY NMR spectrum (700 MHz, pyridin-d_5) of brasilane E **3**.

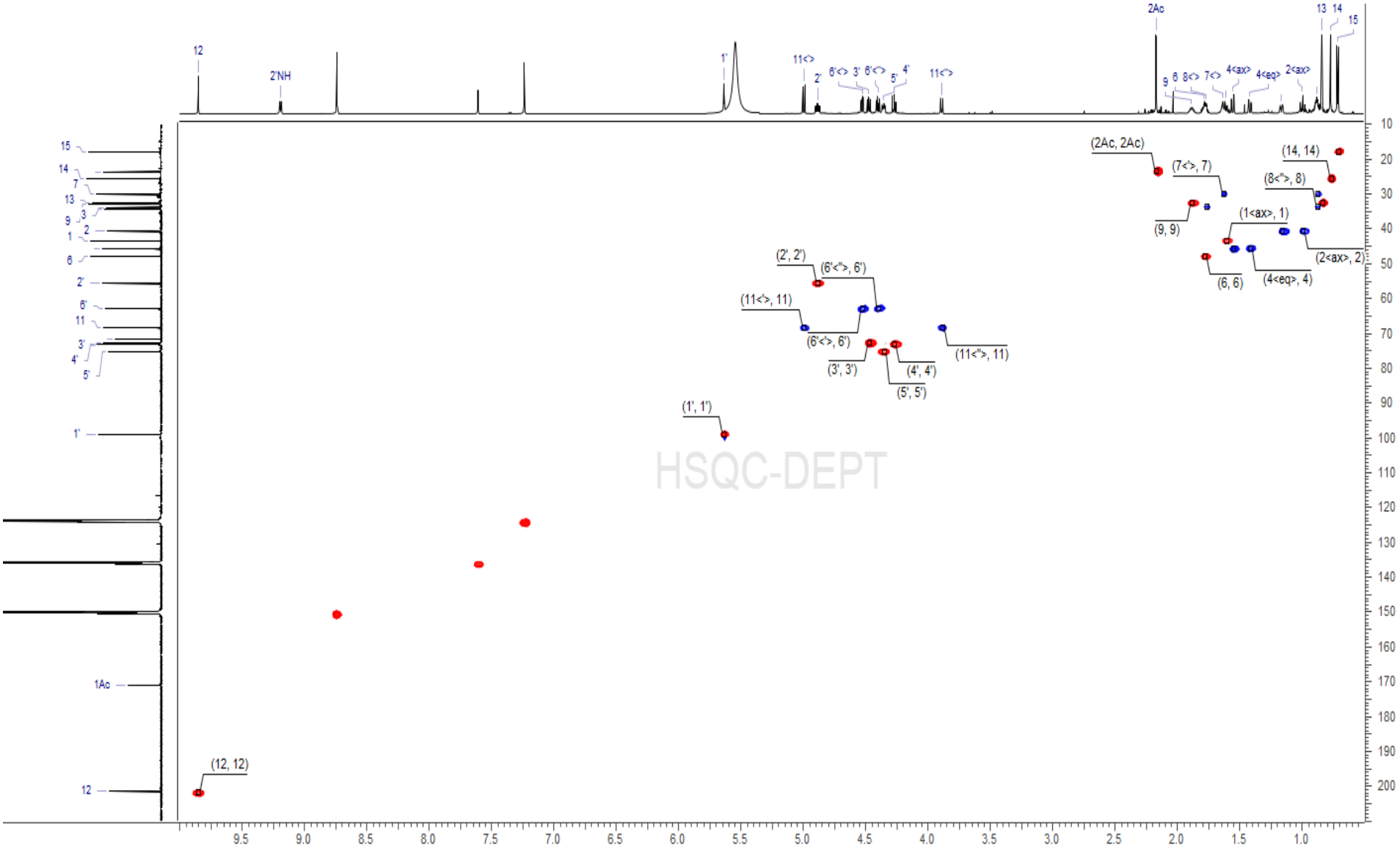

Figure S47 HSQC NMR spectrum (700 MHz, pyridin-d_5) of brasilane E **3**.

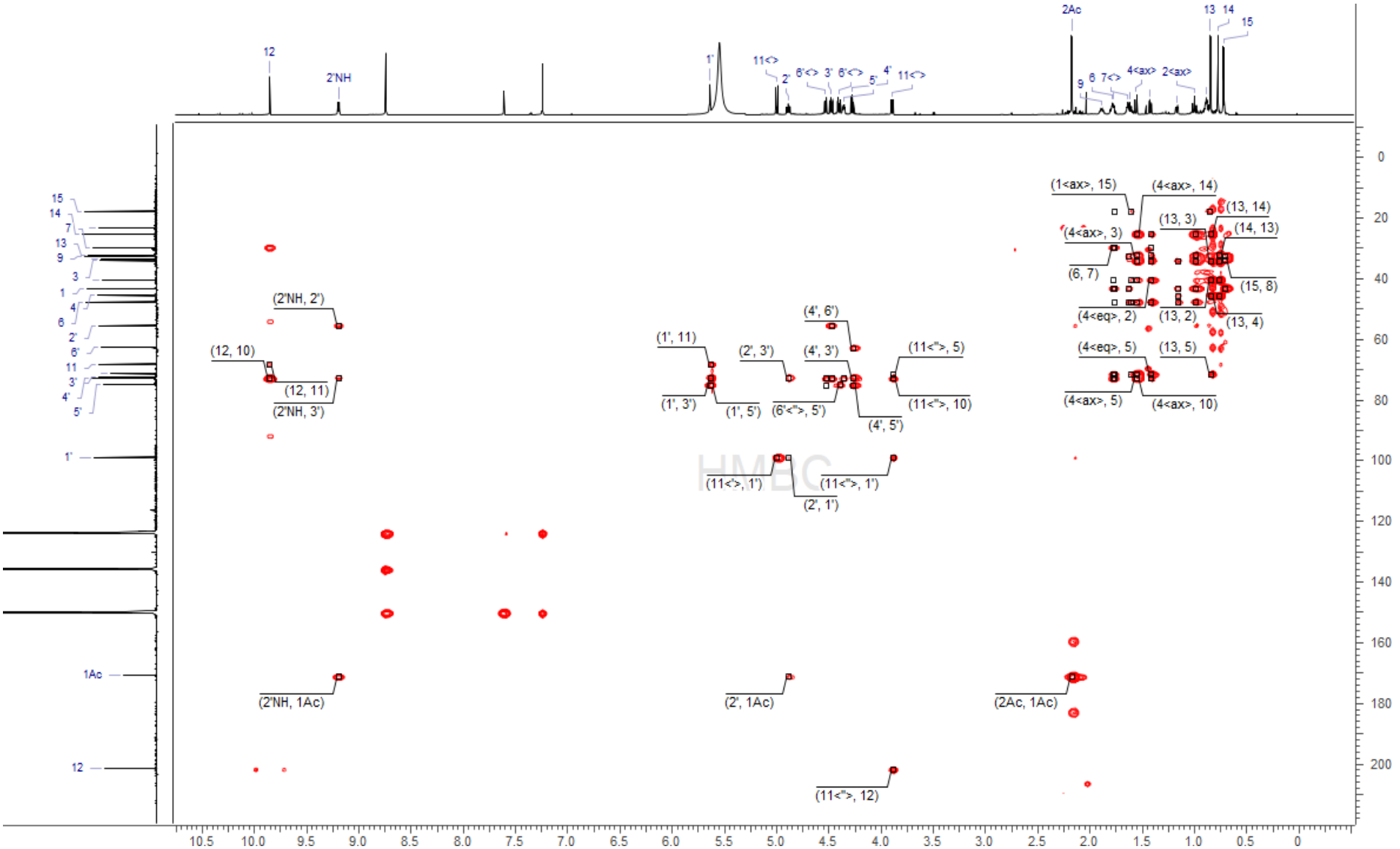

Figure S48 HMBC NMR spectrum (700 MHz, pyridin-d_5) of brasilane E **3**.

S6.5 Brasilane F

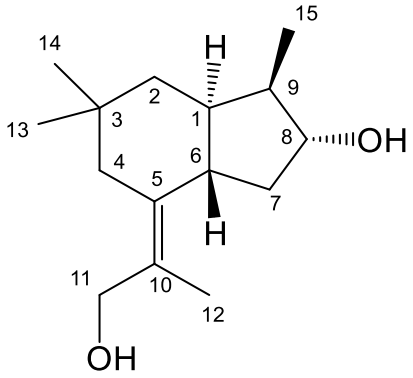

5

amorphous solid; $[\alpha]^{20}_{D}$ -12.0 (c = 0.1, CH_3OH); CD (CH_3OH) λ_{max} (Δ_ε): 197 nm (-2.0), 201 nm (+0.5), 214 (-0.7); ESI-MS *m/z* 221.11 $[M-H_2O+H]^+$, 261.10 $[M+Na]^+$, 237.03 $[M-H]^-$; HR-ESI-MS *m/z* 261.1822 $[M+Na]^+$ (calcd. for $C_{15}H_{26}NaO_2$, 261.1823), 221.1896 $[M-H_2O+H]^+$ (calcd. for $C_{15}H_{25}O$, 221.1900).

Atom#	C Shift	H Shift	COSY	N/ROESY	C to H HMBC
1	44.6, CH	2.05, m	2, 2	8	
2a	41.5, CH_2	1.37, m	2, 1, 6, 4	2	
2b		1.19, br t (12.5)	2, 1	2	14, 13, 3, 1, 6
3	34.0, C				
4a	44.7, CH_2	2.44, dd (13.9, 1.6)	2, 4	14, 13, 4, 11, 11	3, 2, 6, 10, 5
4b		1.60, br d (13.9)	14, 12, 4	6, 4	
5	136.9, C				
6	47.3, CH	2.05, m	2, 7, 7	4, 7	
7a	42.1, CH_2	1.70, m	6, 7, 8	7	6, 8
7b		2.55, ddd (11.9, 6.9, 5.1)	7, 6, 8	7, 12, 6, 8	1
8	81.7, CH	3.70, ddd (7.1, 6.9, 3.2)	7, 9, 7	15, 1, 7	
9	43.1, CH	1.77, m	15, 8		
10	127.8, C				
11a	64.8, CH_2	3.86, d (11.6)	11	12, 4, 11	10, 5
11b		4.21, d (11.6)	11	12, 4, 11	10, 5
12	17.6, CH_3	1.86, s	4	7, 11, 11	11, 10, 5
13	32.6, CH_3	0.97, s		4	14, 3, 2, 4
14	26.4, CH_3	0.88, s	4	4	13, 3, 2, 4
15	14.9, CH_3	0.90, d (7.53)	9	8	9, 1, 8

Table S7 NMR data (^{1}H 700MHz, ^{13}C 175 MHz) of brasilane F **5** in pyridin-d_5

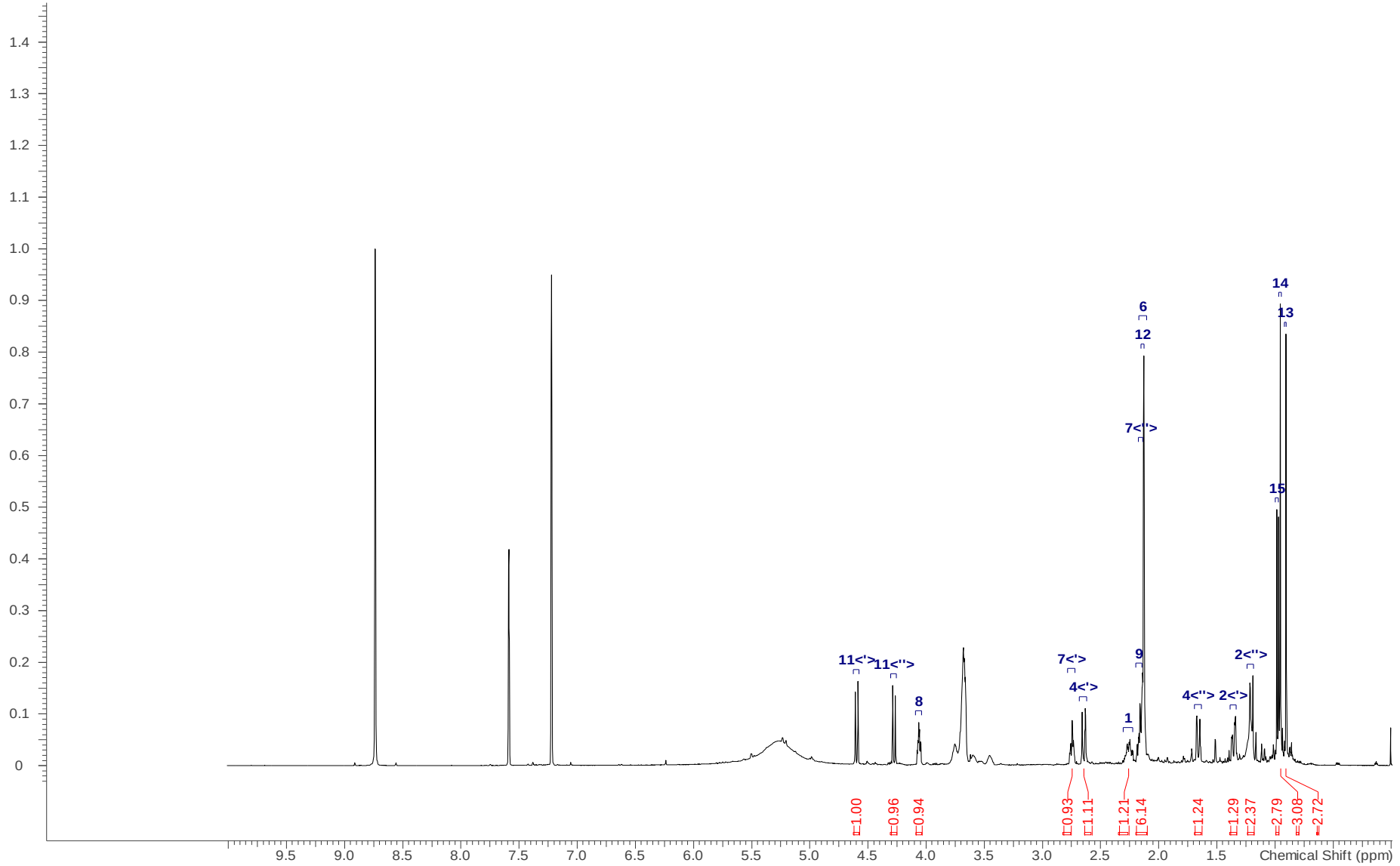

Figure S49 ^{1}H NMR spectrum (500 MHz, pyridin-d_5) of brasilane F **5**.

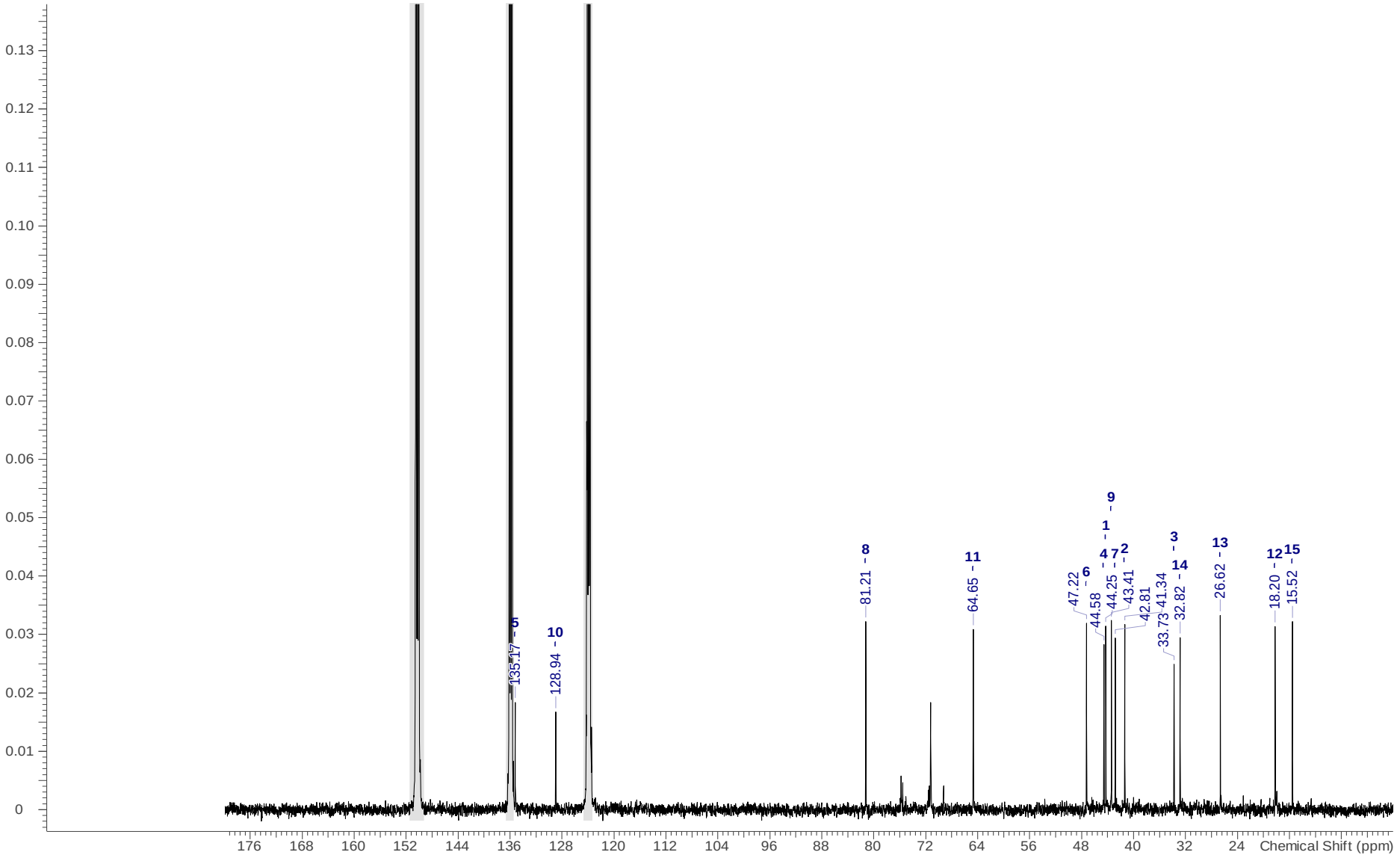

Figure S50 ^{13}C NMR spectrum (125 MHz, pyridin-d_5) of brasilane F **5**.

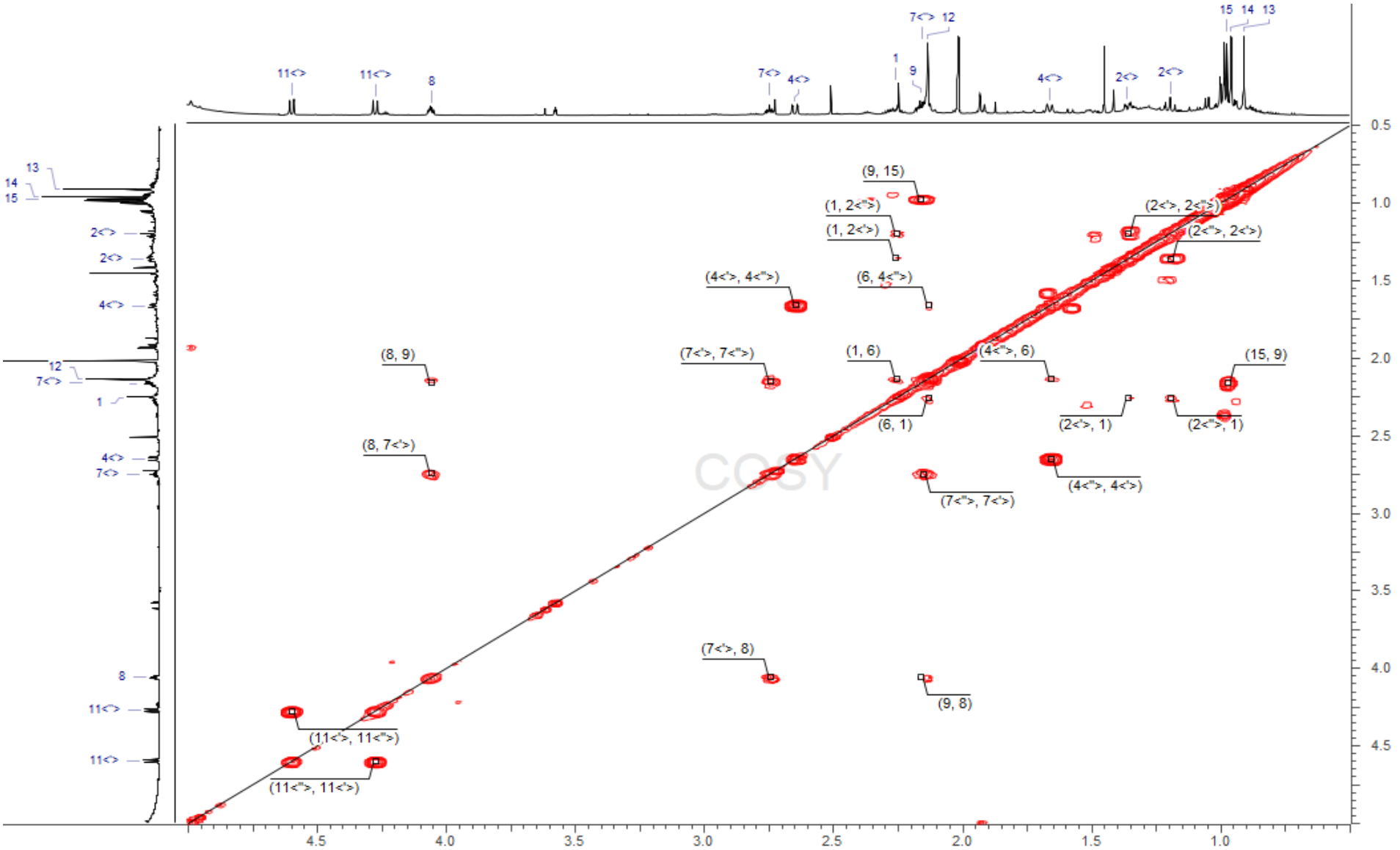

Figure S51 COSY NMR spectrum (500 MHz, pyridin-d_5) of brasilane F **5**.

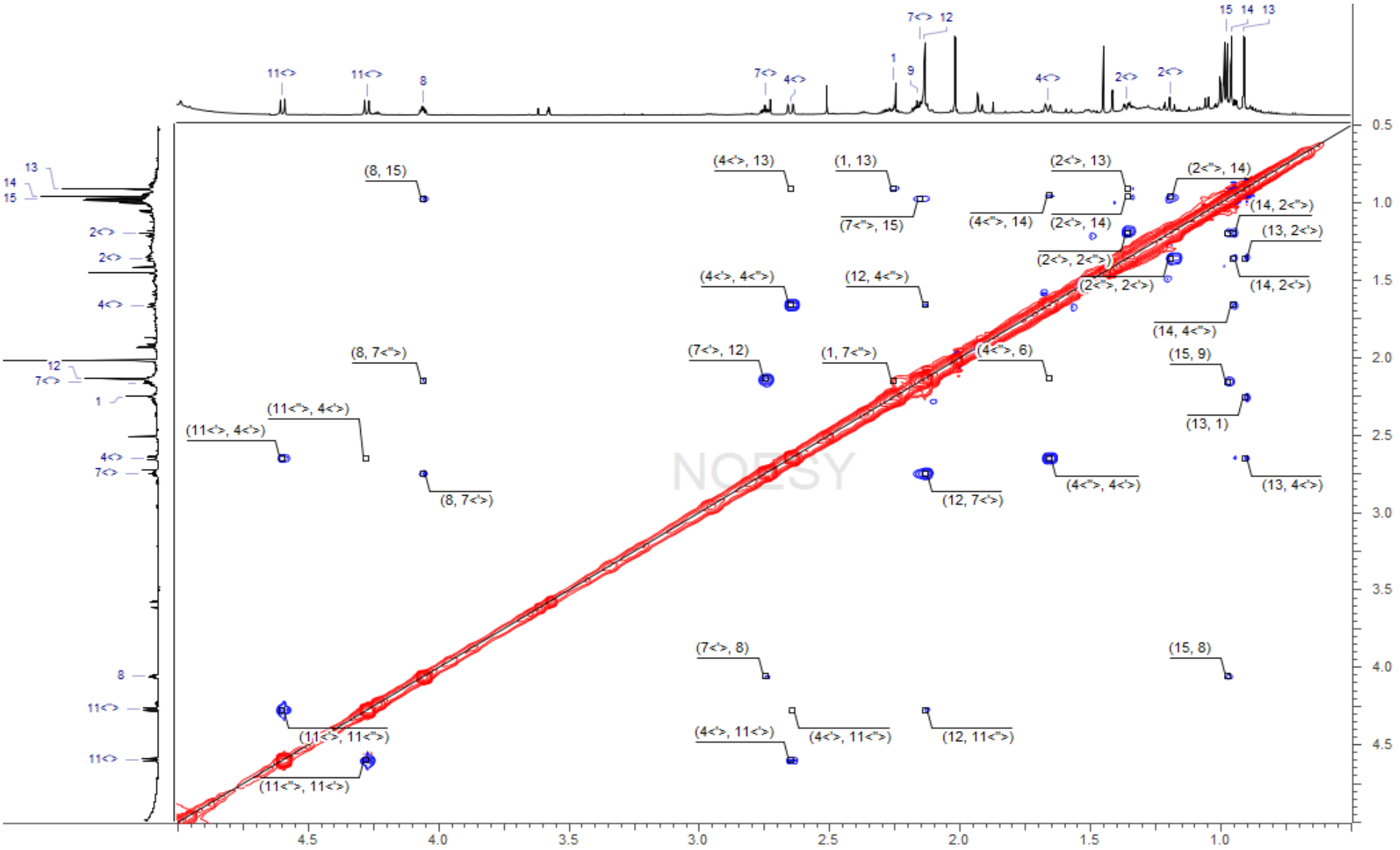

Figure S52 NOESY NMR spectrum (500 MHz, pyridin-d_5) of brasilane F **5**.

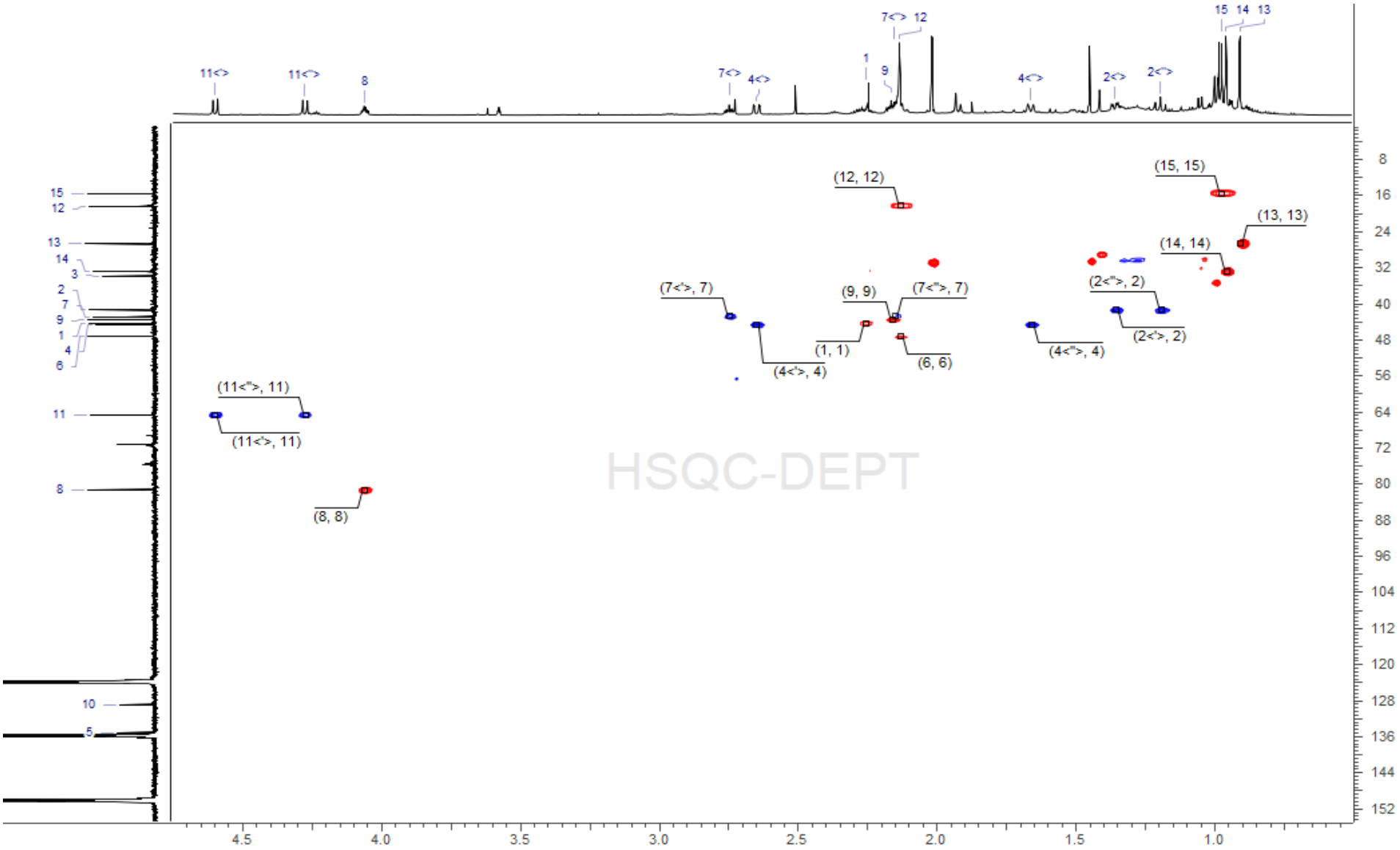

Figure S53 HSQC NMR spectrum (500 MHz, pyridin-d_5) of brasilane F **5**.

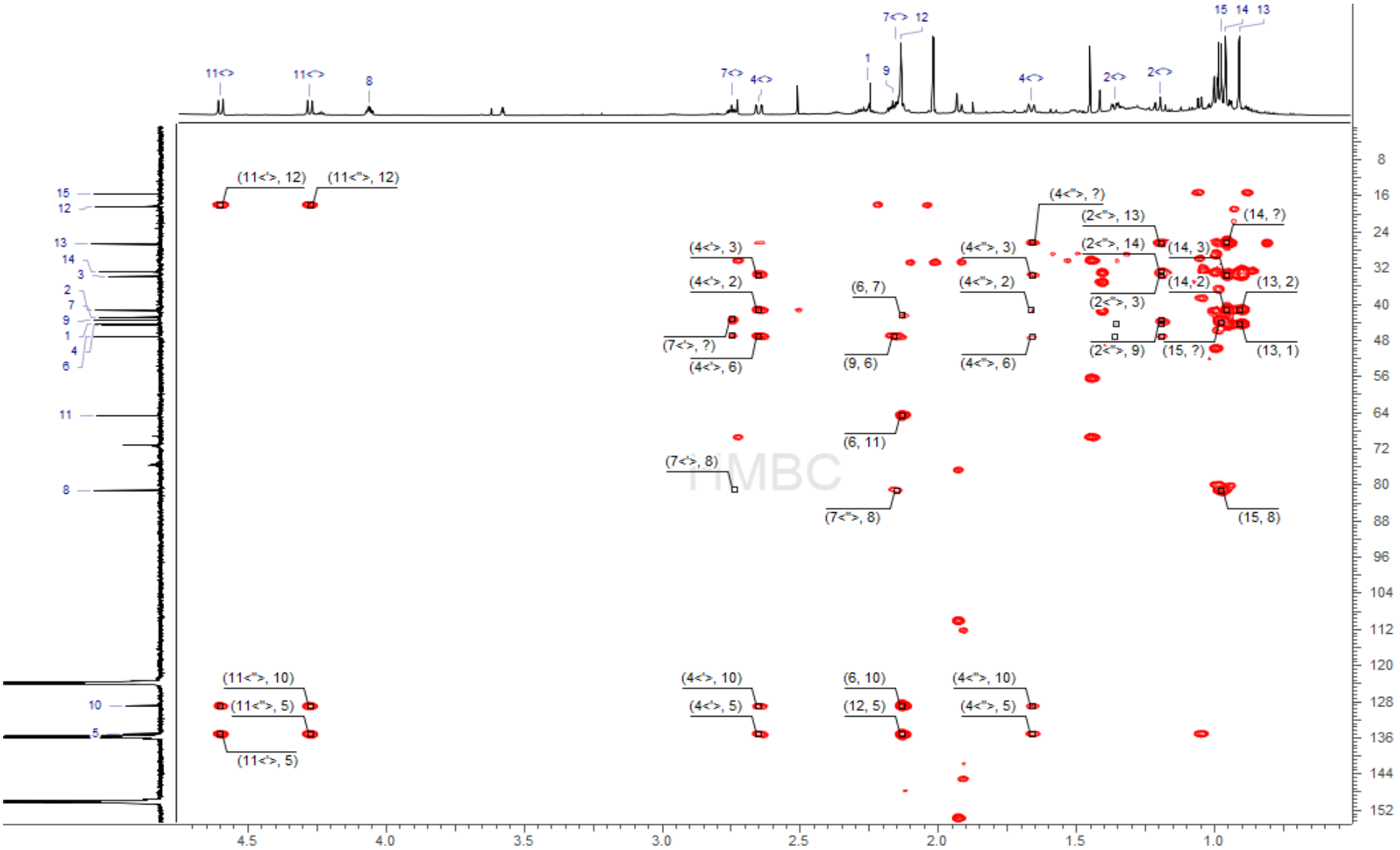

Figure S54 HMBC NMR spectrum (500 MHz, pyridin-d_5) of brasilane F **5**.

S6.6 Xylarenic acid B

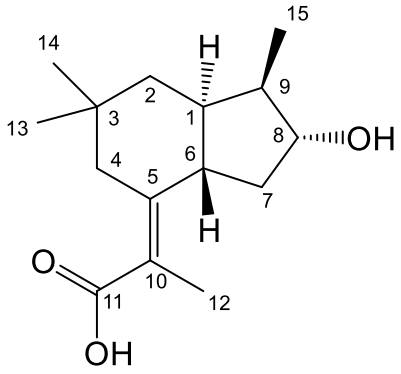

6

amorphous solid; $[\alpha]^{20}_{D}$ -6.0 (c = 0.1, CH_3OH); CD (CH_3OH) λ_{max} (Δ_ε): 197 nm (+1.7), 223 nm (-1.0), 253 (+0.3);); ESI-MS *m/z* 235.09 $[M\text{-}H_2O+H]^+$, 275.11 $[M+Na]^+$, 527.32 $[2M+Na]^+$, 251.06 $[M\text{-}H]^-$, 503.29 $[2M\text{-}H]^-$; HR-ESI-MS *m/z* 253.1797 $[M+H]^+$ (calcd. for $C_{15}H_{25}O_3$, 253.1798), 275.1616 $[M+Na]^+$ (calcd. for $C_{15}H_{24}NaO_3$, 275.1618).

Atom#	C Shift	H Shift	COSY	N/ROESY	C to H HMBC
1	43.7, CH	2.38, m		15, 13, 2, 7, 12, 7, 8	6
2a	40.8, CH_2	1.21, dd (12.8, 12.4)	2	14, 2, 6	13, 14, 3, 1, 4
2b		1.39 dd (12.4, 2.3)	2, 4	14, 2, 1	13, 3, 1, 4
3	33.7, C				
4a	46.4, CH_2	2.99, br d (13.8)	2	14, 13, 4, 12	13, 14, 3, 2, 6, 10
4b		2.01, s		12, 4	13
5	138.6, C				
6	46.3, CH	2.15, m	7	2, 8	7
7a	41.8, CH_2	2.15, m	7, 8	15, 1, 8	6, 8, 5
7b		2.73, m	6, 7, 8	15, 9, 12, 1, 8	9, 6, 8
8	80.7, CH	4.08, m	7, 7	15, 6, 7, 1, 7	15
9	43.1, CH	2.18, m	15	7	15, 6
10	126.7, C				
11	175.8, C				
12	17.0, CH_3	2.24, br s		4, 1, 7, 4	10, 11
13	26.7, CH_3	1.09, s		14, 1, 4	14, 3, 2
14	32.7, CH_3	0.97, d (8.0)		13, 2, 2, 4	13, 3, 2, 4
15	15.1, CH_3	0.98, s	9	7, 1, 7, 8	9, 8

Table S8 NMR data (^{1}H 700MHz, ^{13}C 175 MHz) of xylarenic acid B **6** in pyridin-d_5

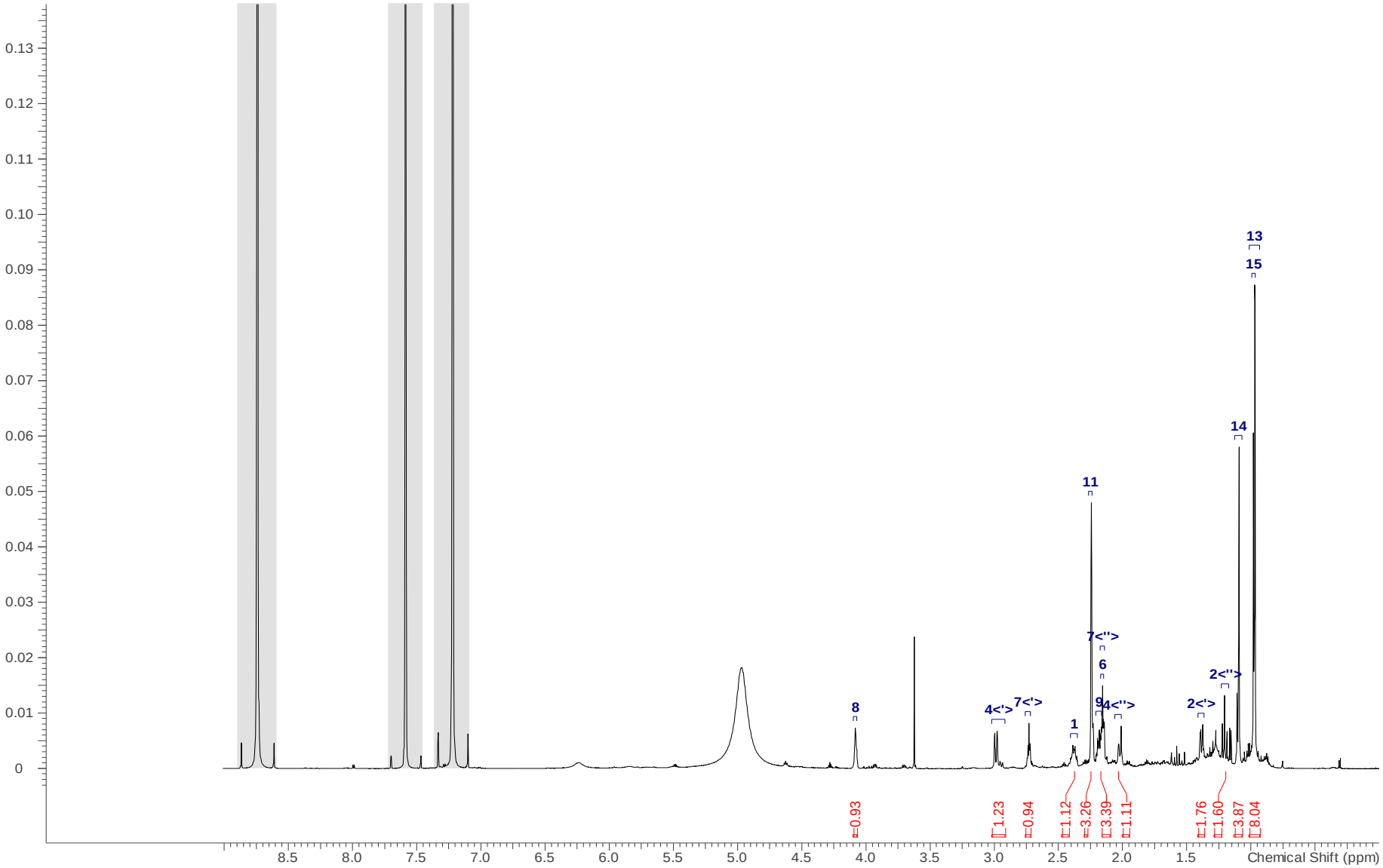

Figure S55 ^{1}H NMR spectrum (700 MHz, pyridin-d_5) of xylarenic acid B **6**.

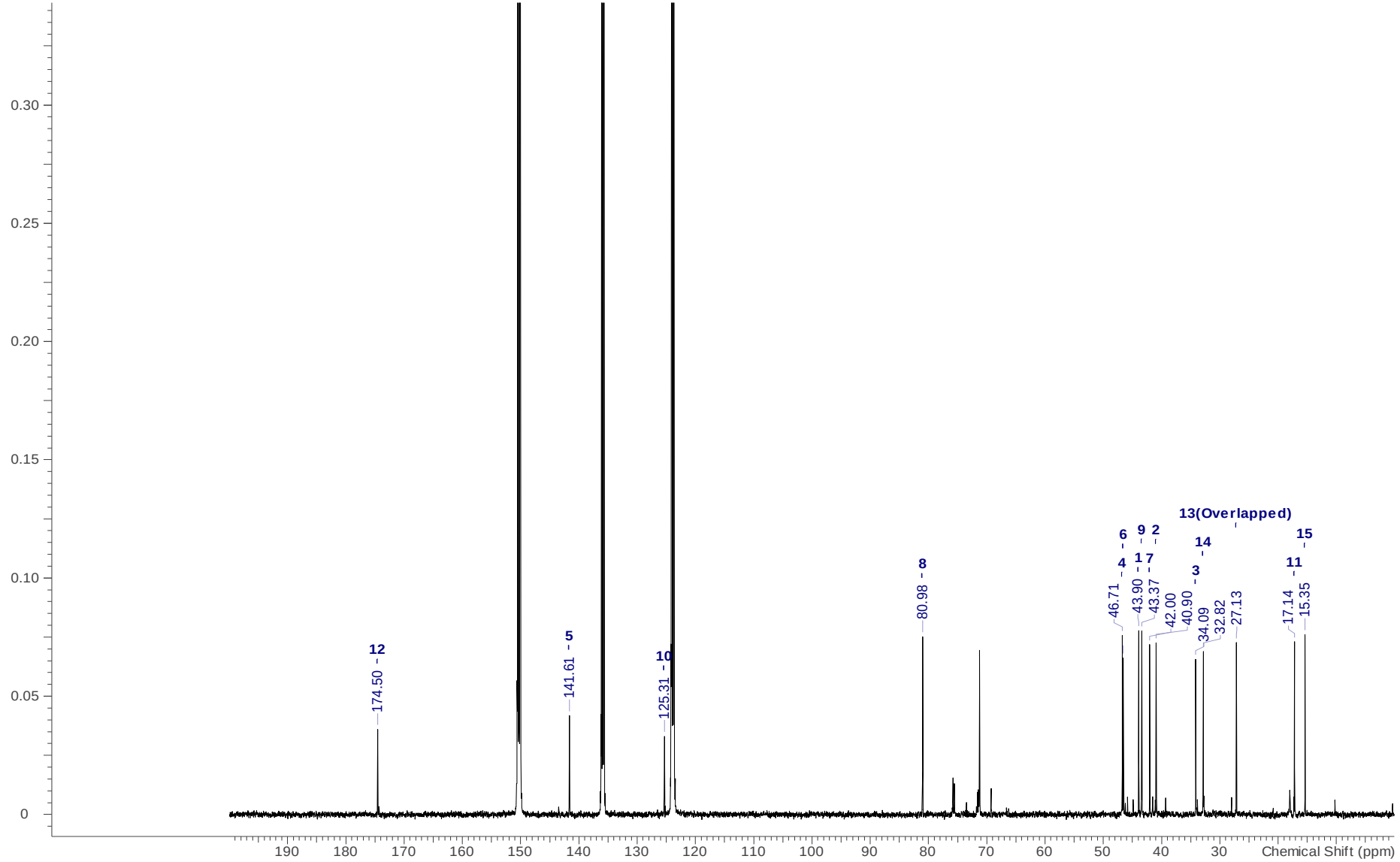

Figure S56 ^{13}C NMR spectrum (125 MHz, pyridin-d_5) of xylarenic acid B **6**.

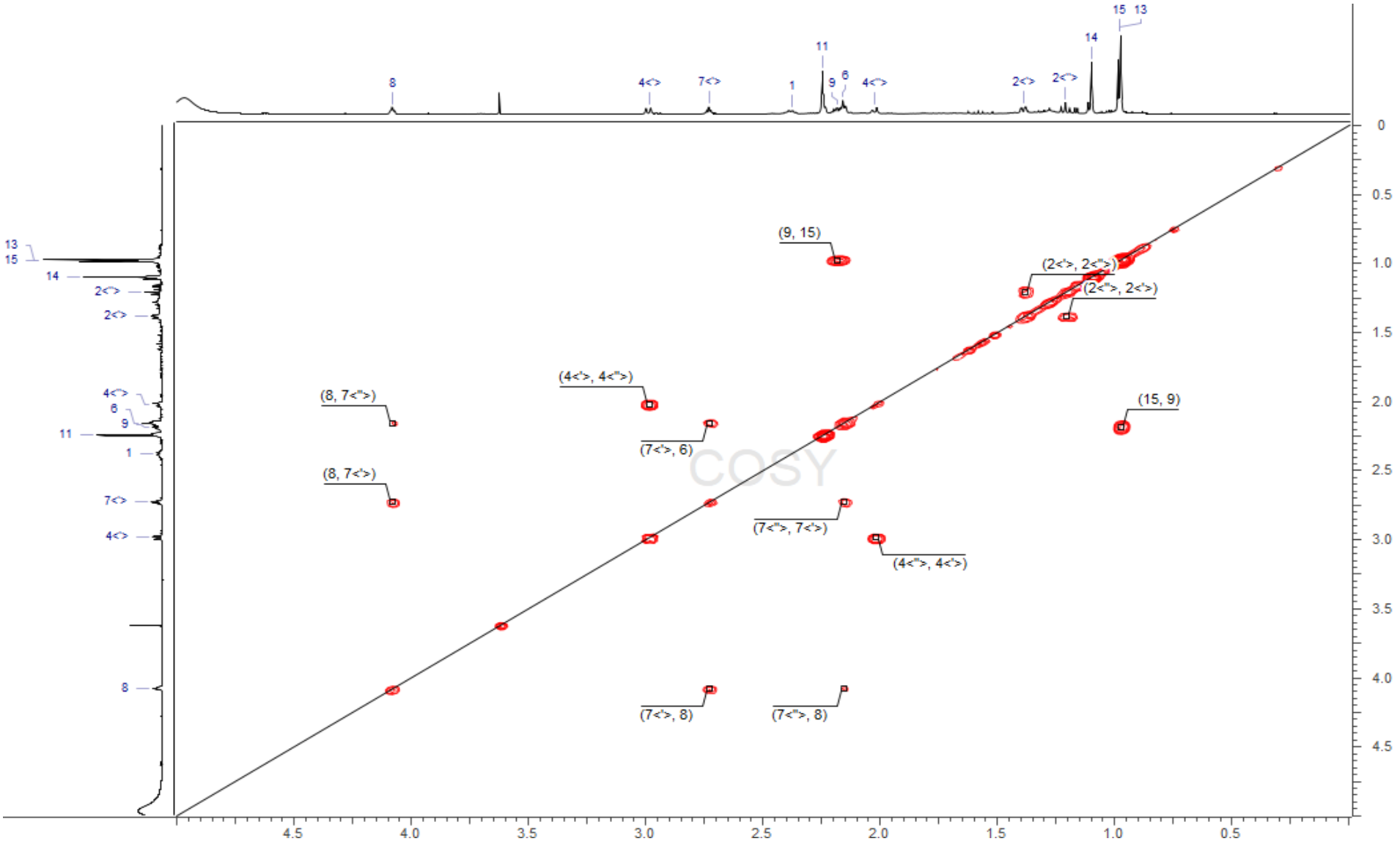

Figure S57 COSY NMR spectrum (700 MHz, pyridin-d_5) of xylarenic acid B **6**.

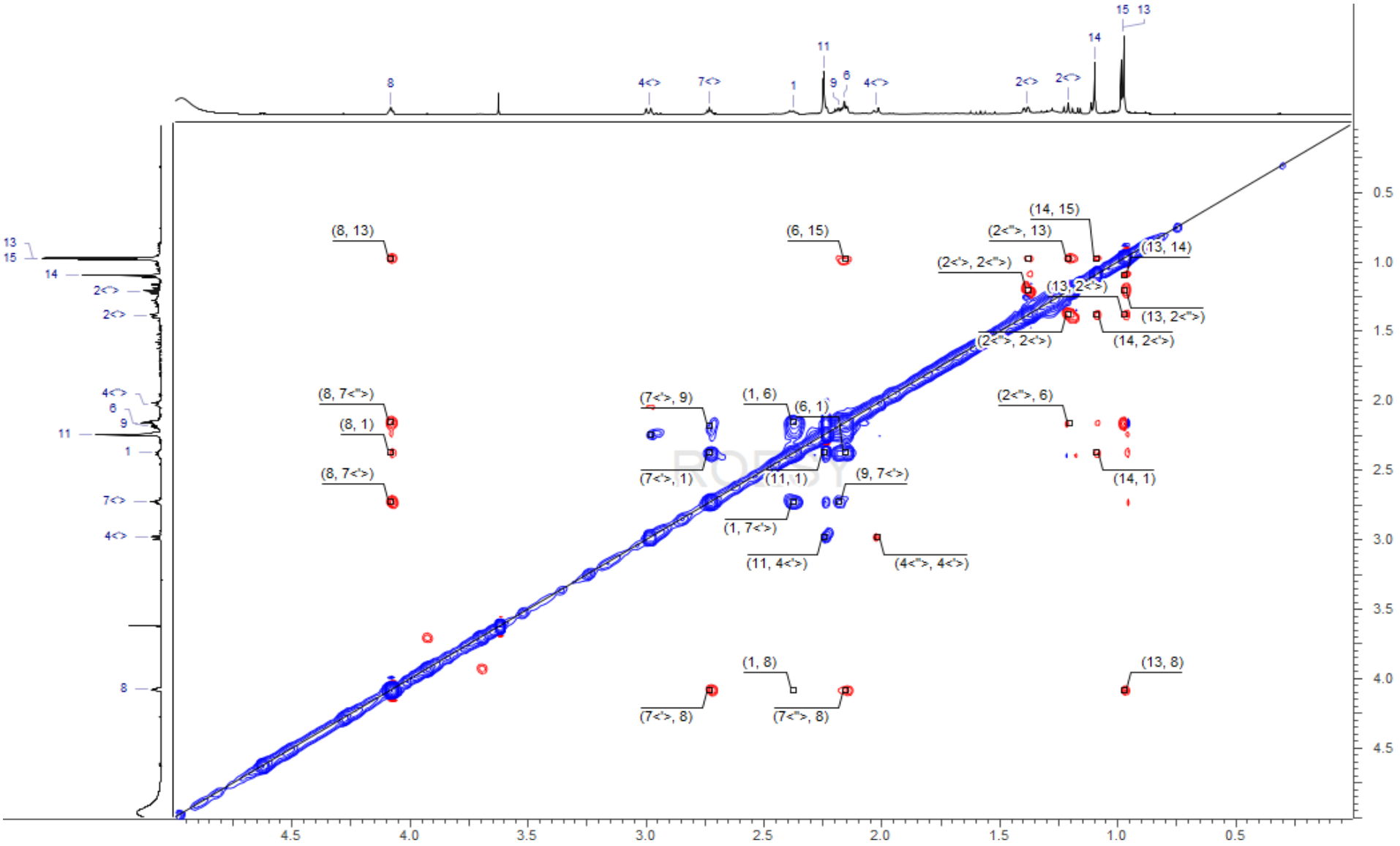

Figure S58 ROESY NMR spectrum (700 MHz, pyridin-d_5) of xylarenic acid B **6**.

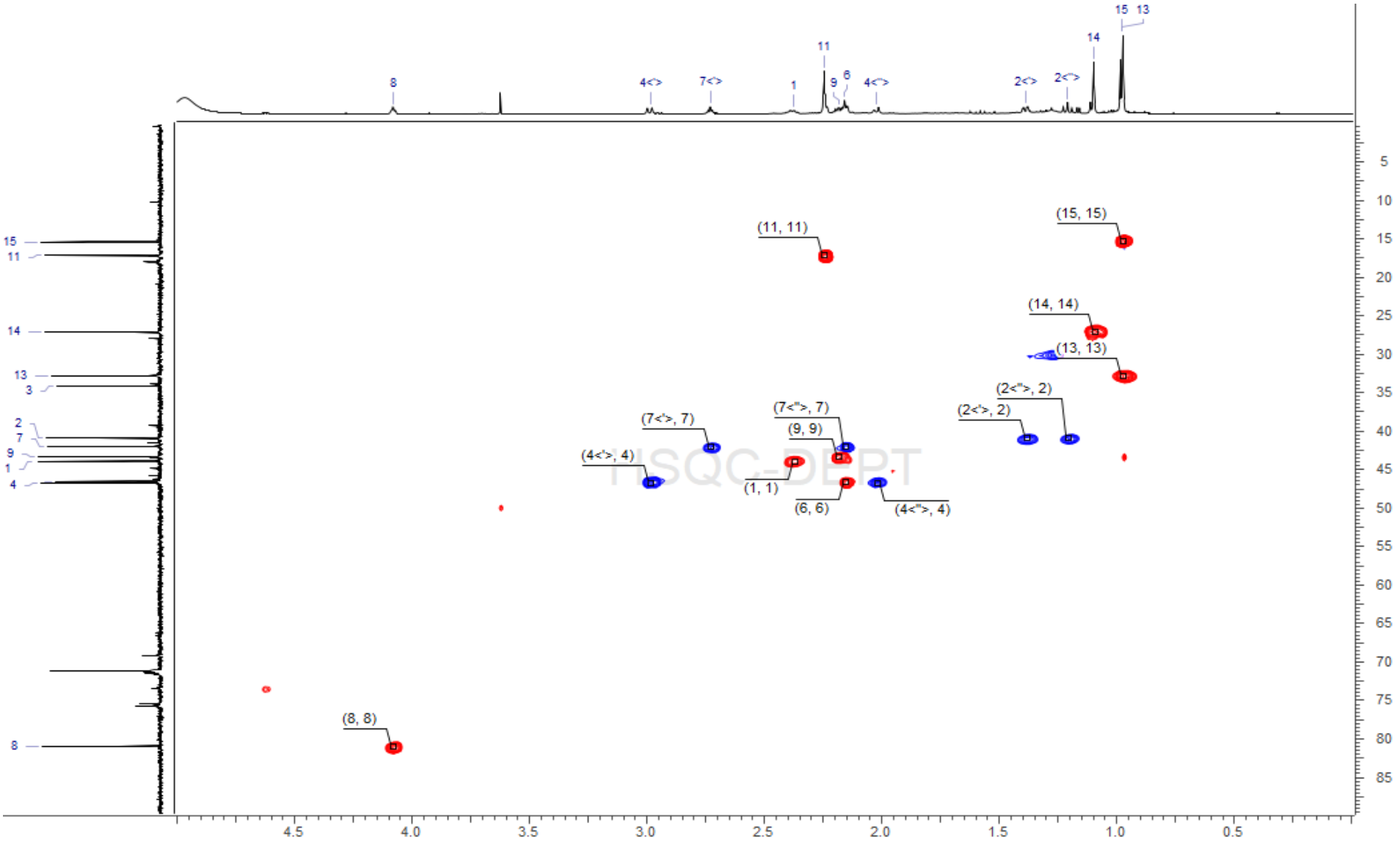

Figure S59 HSQC NMR spectrum (700 MHz, pyridin-d_5) of xylarenic acid B **6**.

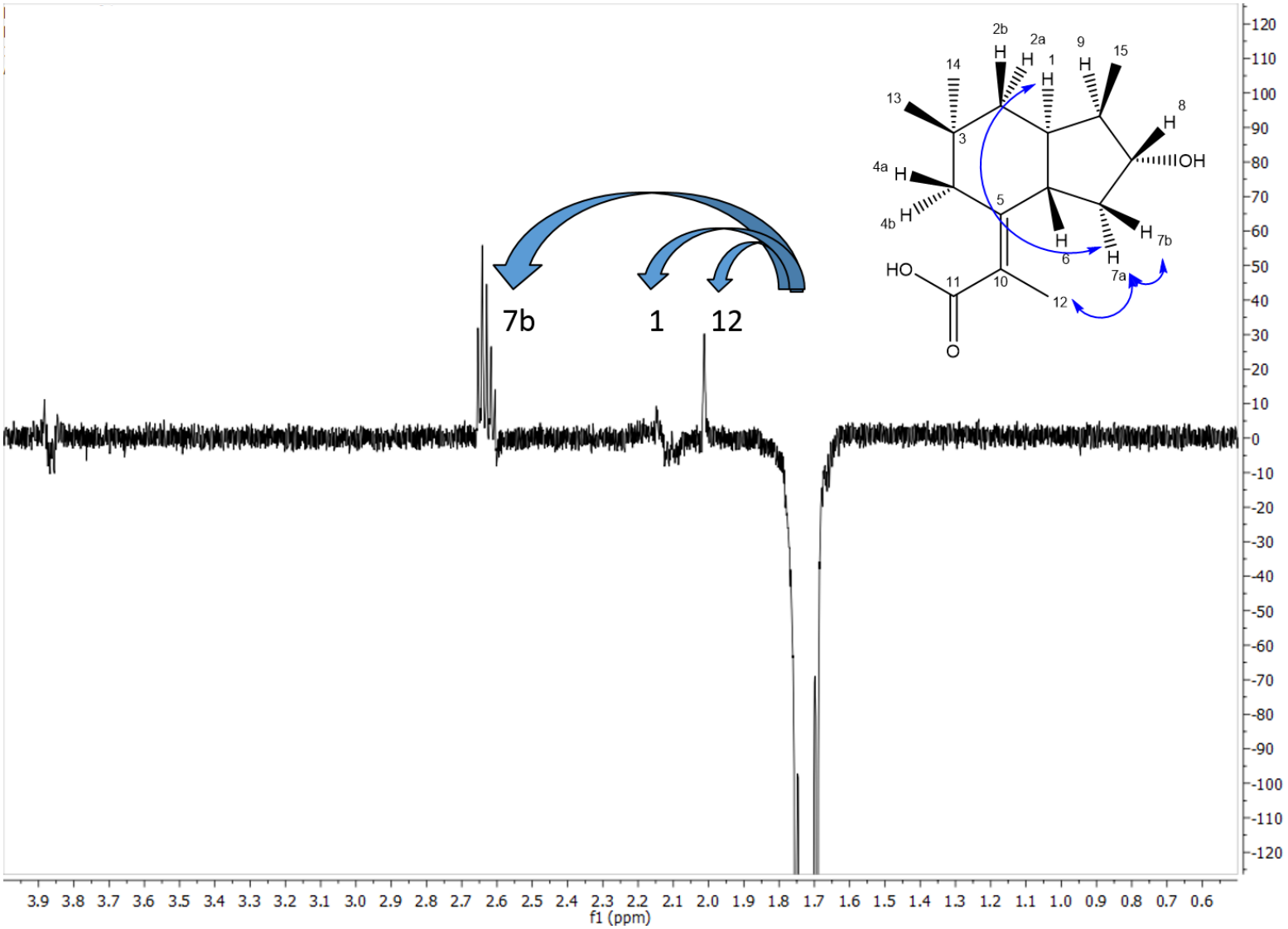

Figure S60 1D-NOE NMR spectrum of xylarenic acid B **6** (500 MHz, chloroform-*d*) excited at 1.73 ppm (H-7a).

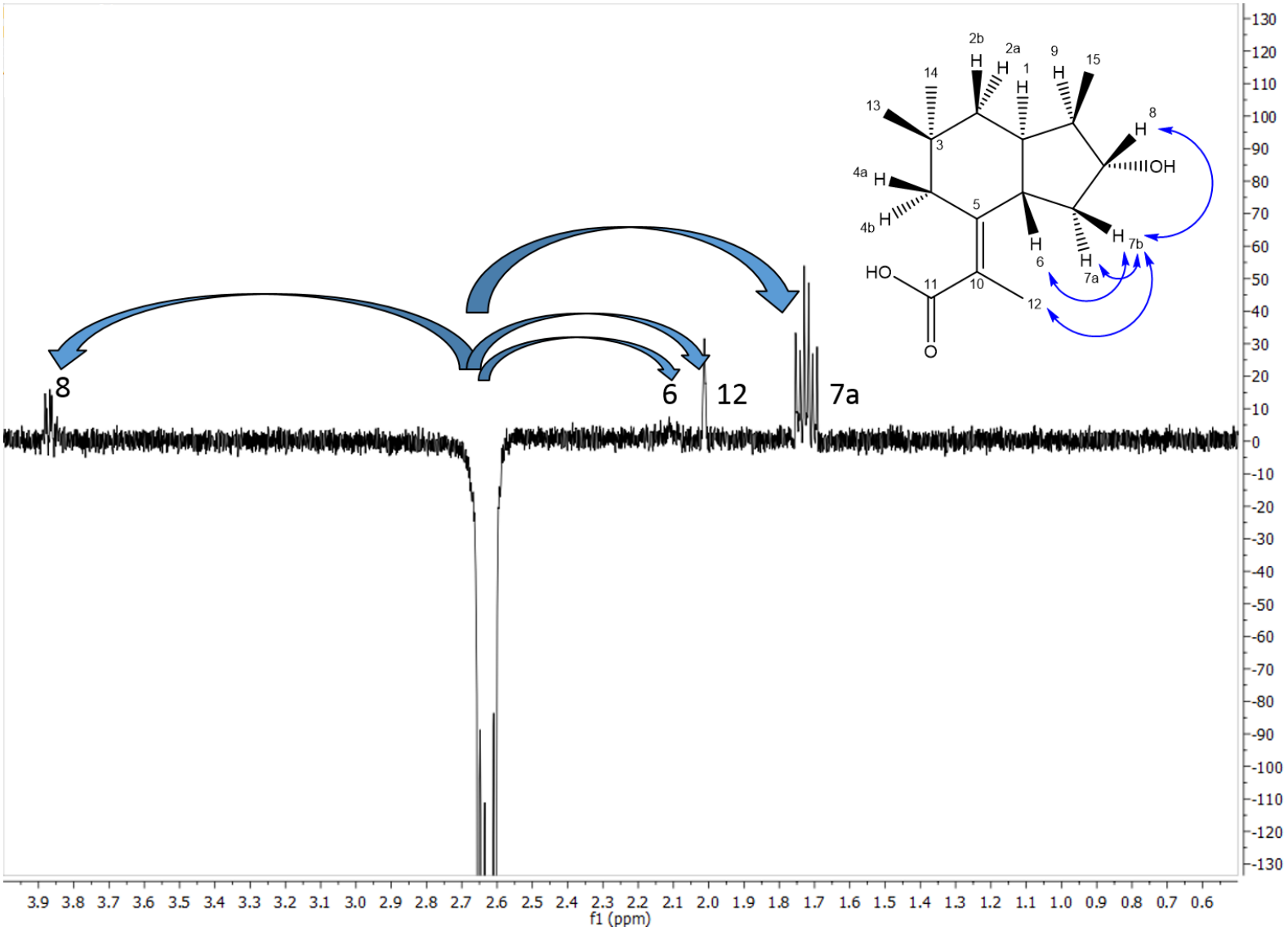

Figure S61 1D-NOE NMR spectrum of xylarenic acid B **6** (500 MHz, chloroform-*d*) excited at 2.63 ppm (H-7b).

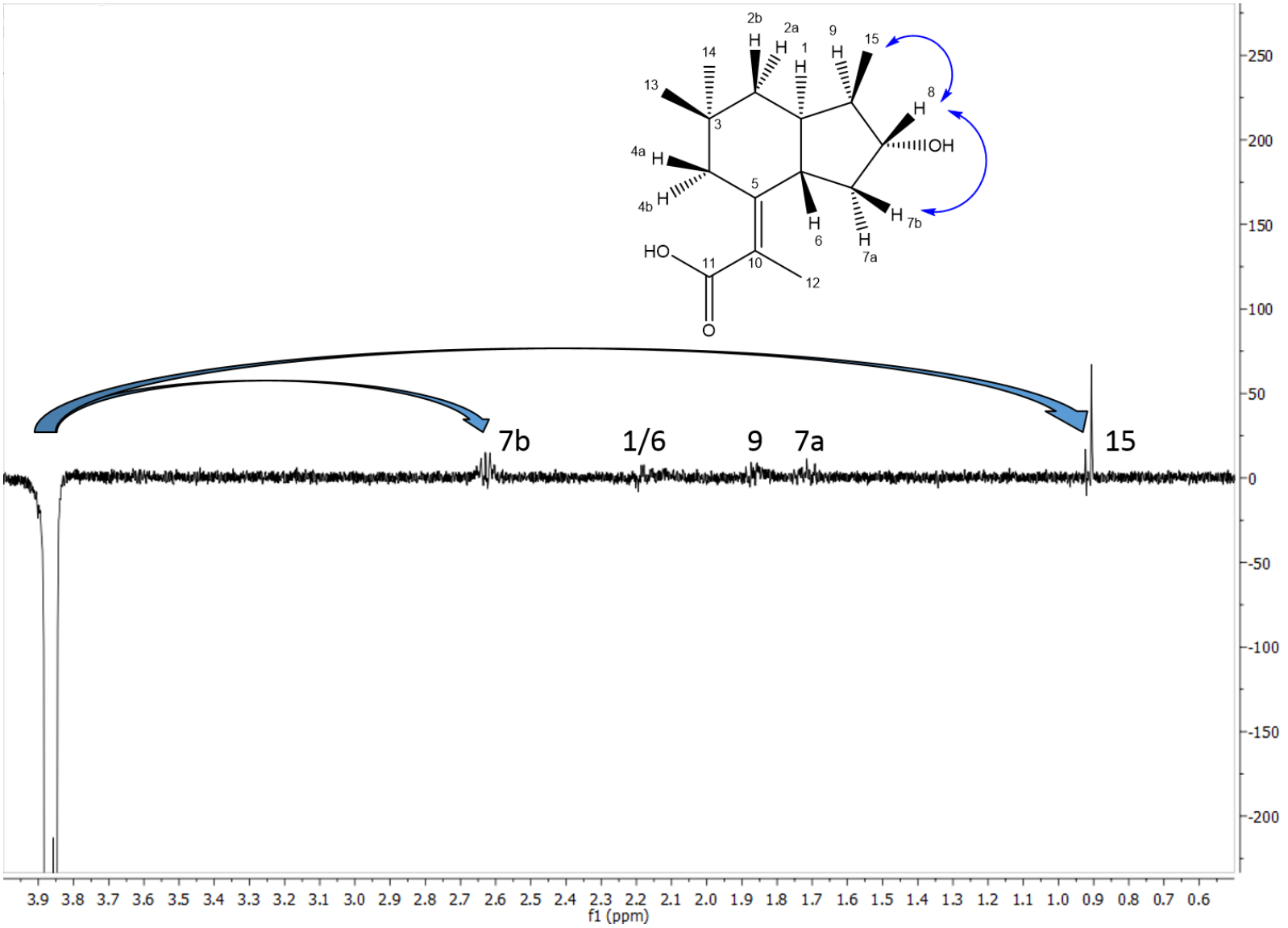

Figure S62 1D-NOE NMR spectrum of xylarenic acid B **6** (500 MHz, chloroform-*d*) excited at 3.87 ppm (H-8).

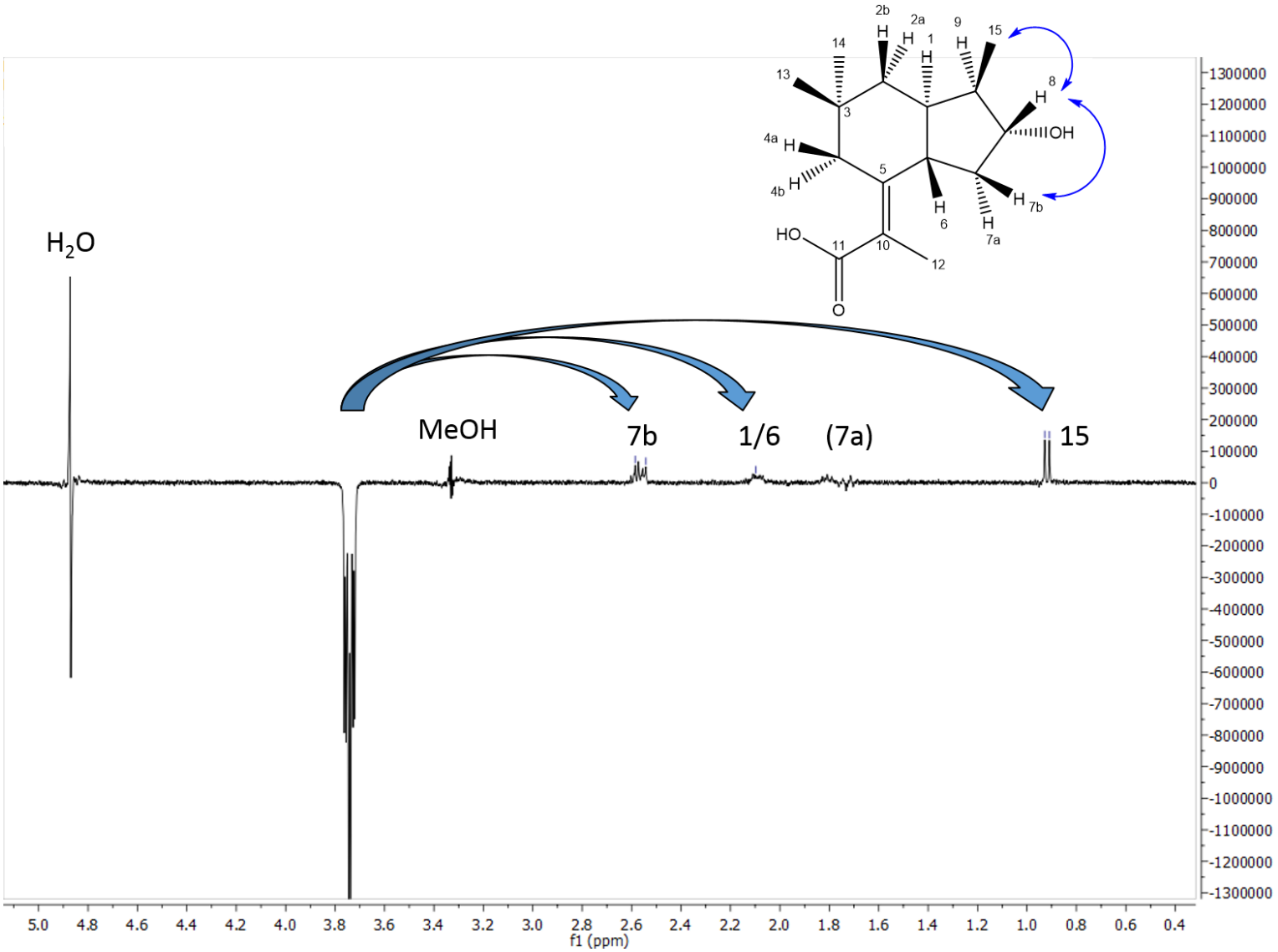

Figure S63 1D-NOE NMR spectrum of xylarenic acid B **6** (500 MHz, methanol-d_4) excited at 3.74 ppm (H-8).

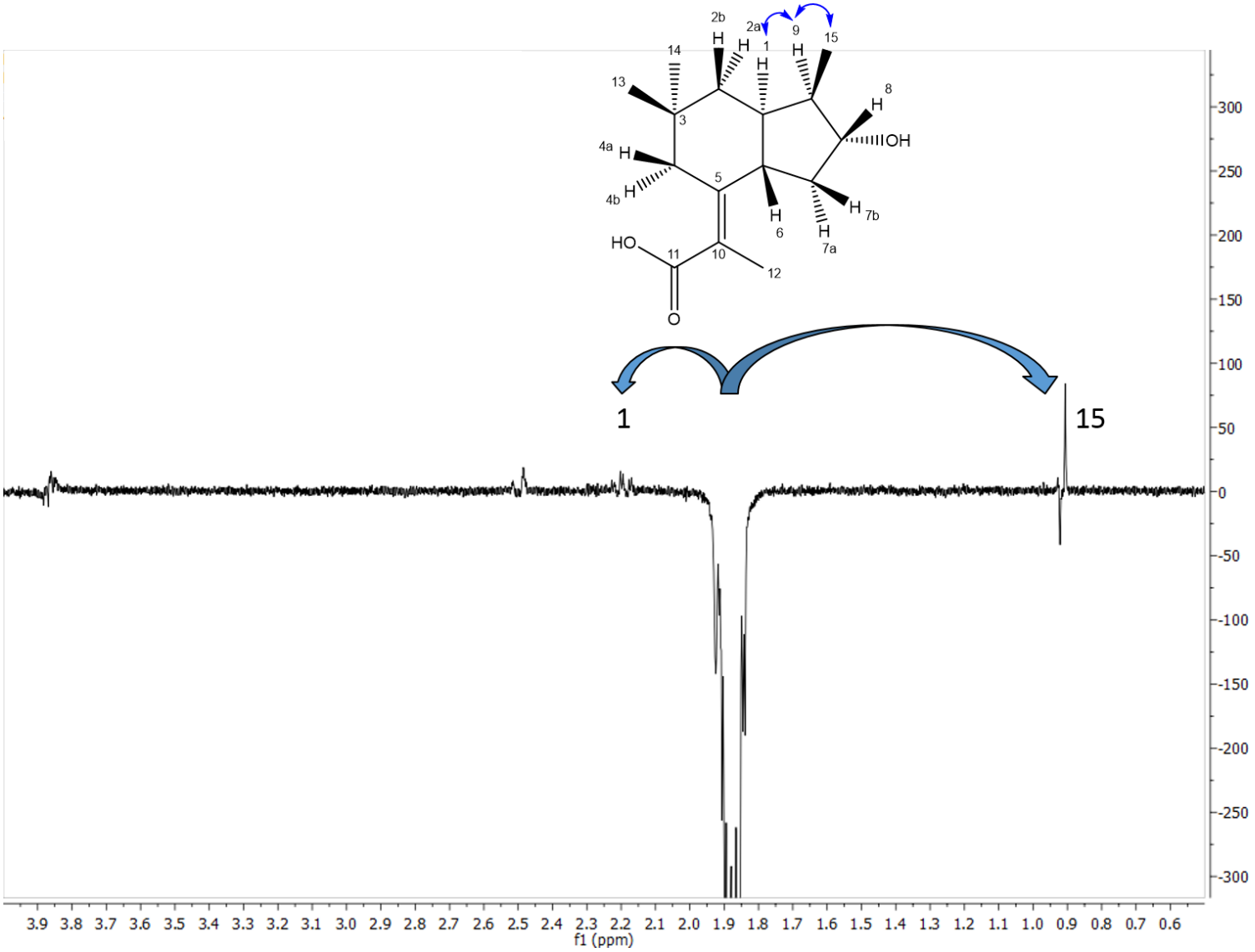

Figure S64 1D-NOE NMR spectrum of xylarenic acid B **6** (500 MHz, chloroform-*d*) excited at 1.87 ppm (H-9).

S6.7 Perillyl glycoside

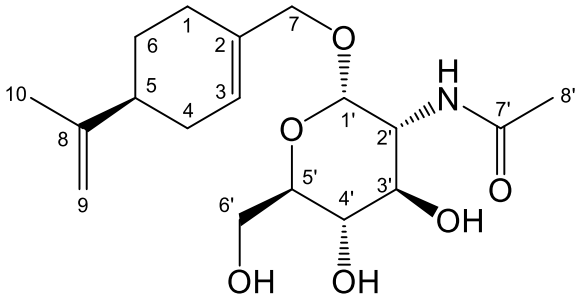

7

amorphous solid; $[\alpha]^{20}_{D}$ +61.0 (c = 0.1, CH_3OH); ESI-MS *m/z* 356.19 $[M+H]^+$, 378.20 $[M+Na]^+$, 733.42 $[2M+Na]^+$, 354.19 $[M-H]^-$, 709.32 $[2M-H]^-$; HR-ESI-MS *m/z* 356.2067 $[M+H]^+$ (calcd. for $C_{18}H_{30}NO_6$, 356.2068), 378.1883 $[M+Na]^+$ (calcd. for $C_{18}H_{29}NNaO_6$, 378.1887).

Atom#	C Shift	H Shift	COSY	C to H HMBC
1a	71.9, CH_2	4.03, d (11.8)	1	1', 3, 2
1b		3.90, d (11.8)	1	7, 1', 3, 2
2	135.3, C			
3	126.8, CH	5.75, m	4	
4a	31.8, CH_2	1.99, m	4, 5	
4b		2.14, m	4, 3	
5	42.6, CH	2.16, m	6, 6, 4	
6a	28.9, CH_2	1.46, m	6, 7, 5, 7	5
6b		1.85, m	6, 7, 5	
7a	27.3, CH_2	2.08, m	6, 6, 7	
7b		2.18, m	6, 7	
8	151.0, C			
9a	109.4, CH_2	4.71, br q (0.9)		5
9b		4.72, m	10	10
10	21.1, CH_3	1.74, br s	9	5, 9, 8
1'	96.5, CH	4.79, d (3.7)	2'	1, 3', 5'
2'	55.6, CH	3.87, dd (10.8, 3.7)	3', 1'	3', 1', 7'
3'	72.8, CH	3.68, m	4', 2'	2', 5'
4'	72.6, CH	3.34, dd (9.8, 9.0)	5', 3'	6', 3', 5'
5'	74.0, CH	3.60, ddd (9.8, 5.7, 2.3)	4', 6', 6'	
6'a	62.9, CH_2	3.69, m	5', 6'	4', 5'
6'b		3.82, dd (11.9, 2.3)	5', 6'	4'
7'	173.6, C			
8'	22.7, CH_3	1.97, s		7'

Table S9 NMR data (^{1}H 500MHz, ^{13}C 125 MHz) of perillyl glycoside **7** in methanol-d_4.

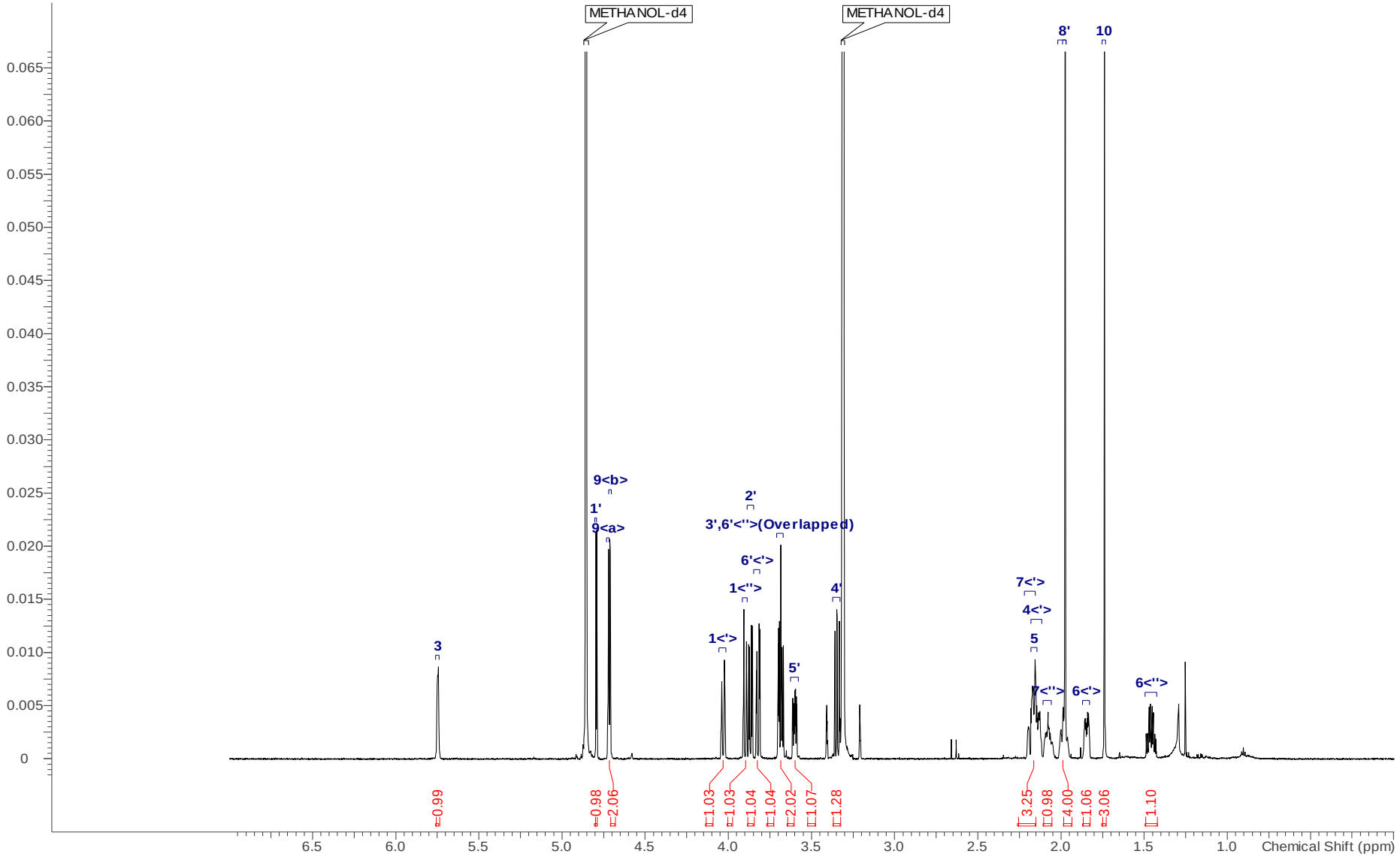

Figure S65 ^{1}H NMR spectrum (500MHz, methanol-d_4) of compound **7**.

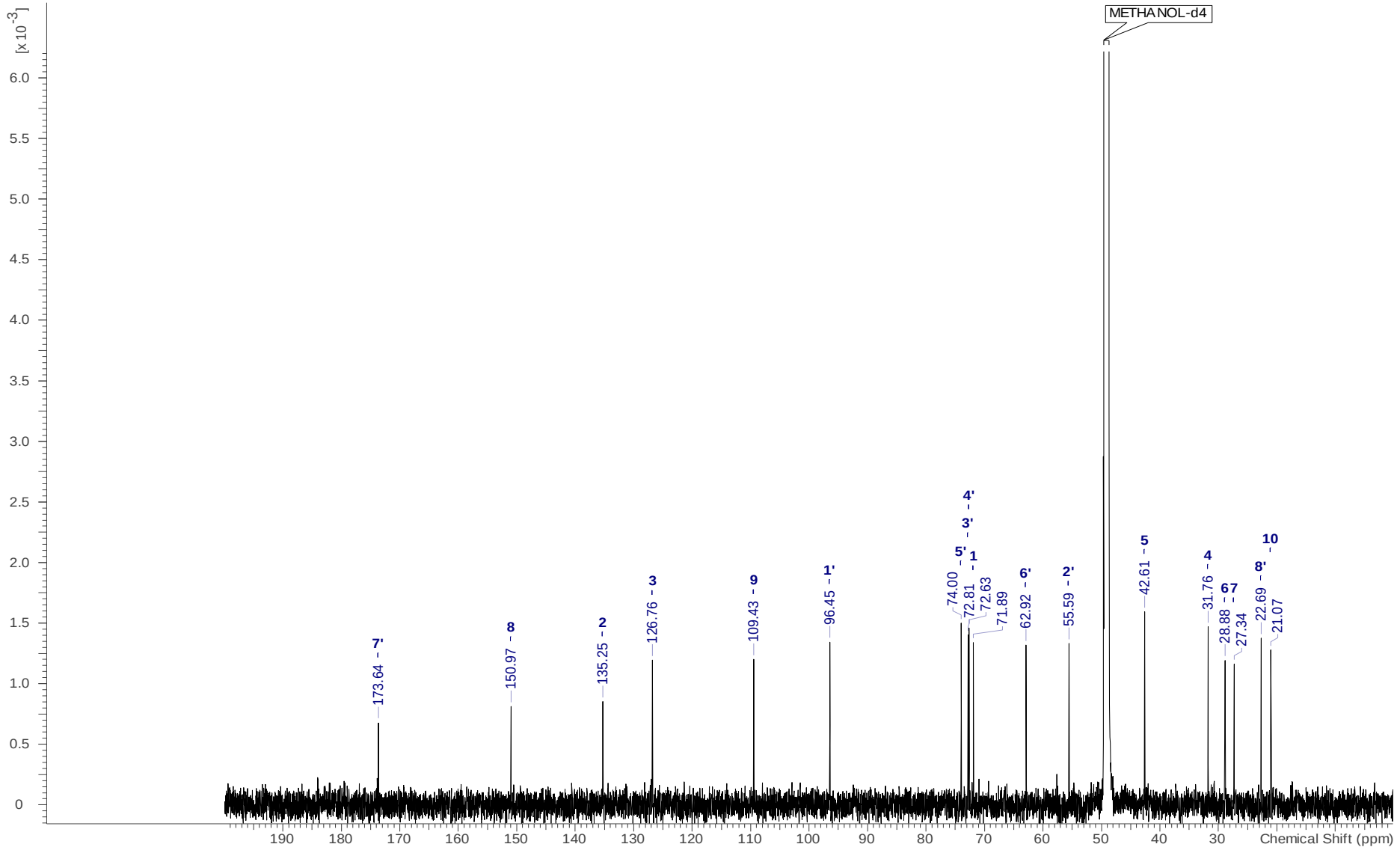

Figure S66 ^{13}C NMR spectrum (175 MHz, methanol-d_4) of compound **7**.

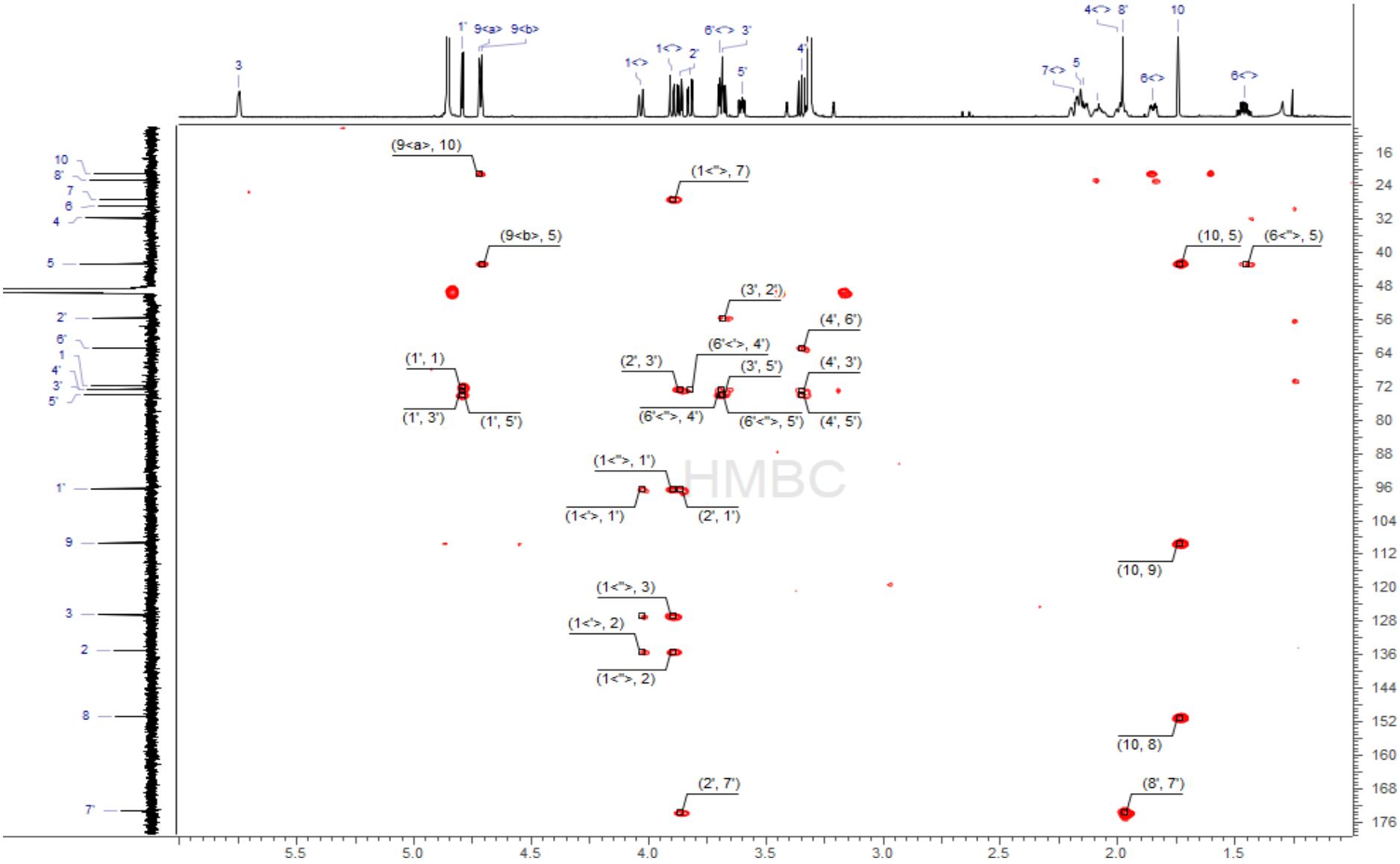

Figure S67 HMBC NMR spectrum (500MHz, methanol-d_4) of compound **7**.

S6.8 MTPA ester

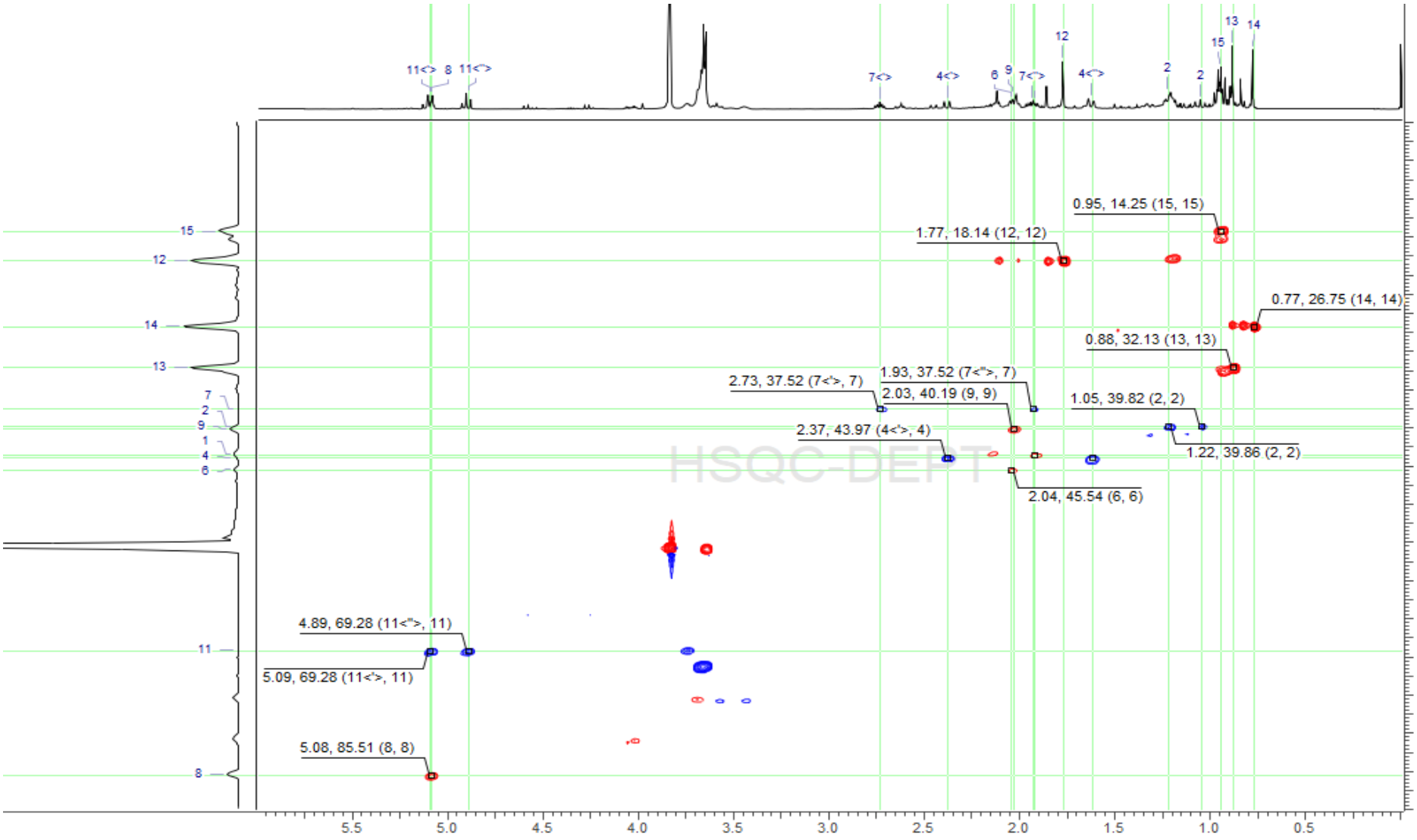

Figure S68 HSQC NMR spectrum (700 MHz, pyridin-d_5) of the *S*-MTPA ester of brasilane F **5**.

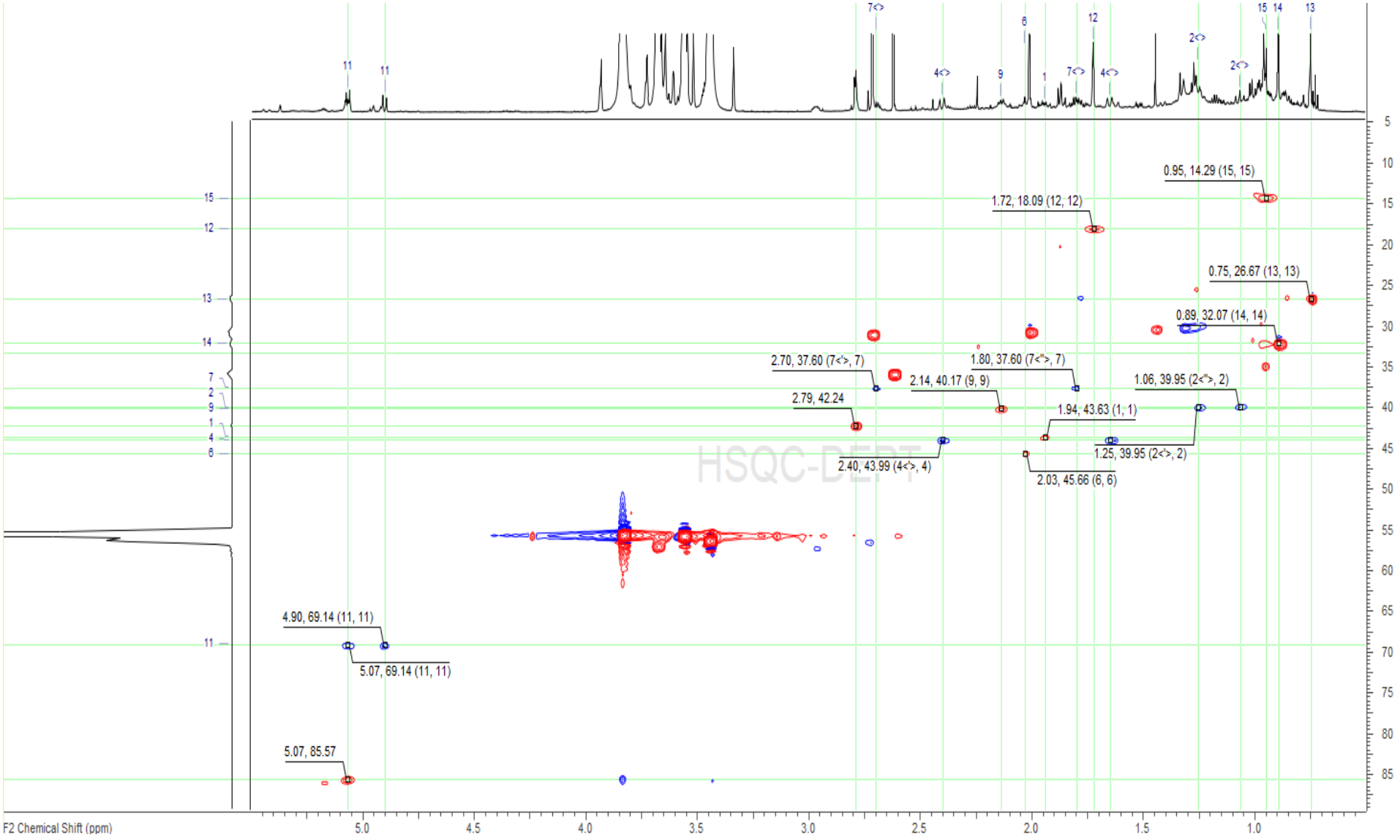

Figure S69 HSQC NMR spectrum (700 MHz, pyridin-d_5) of the *R*-MTPA ester of brasilane F **5**.

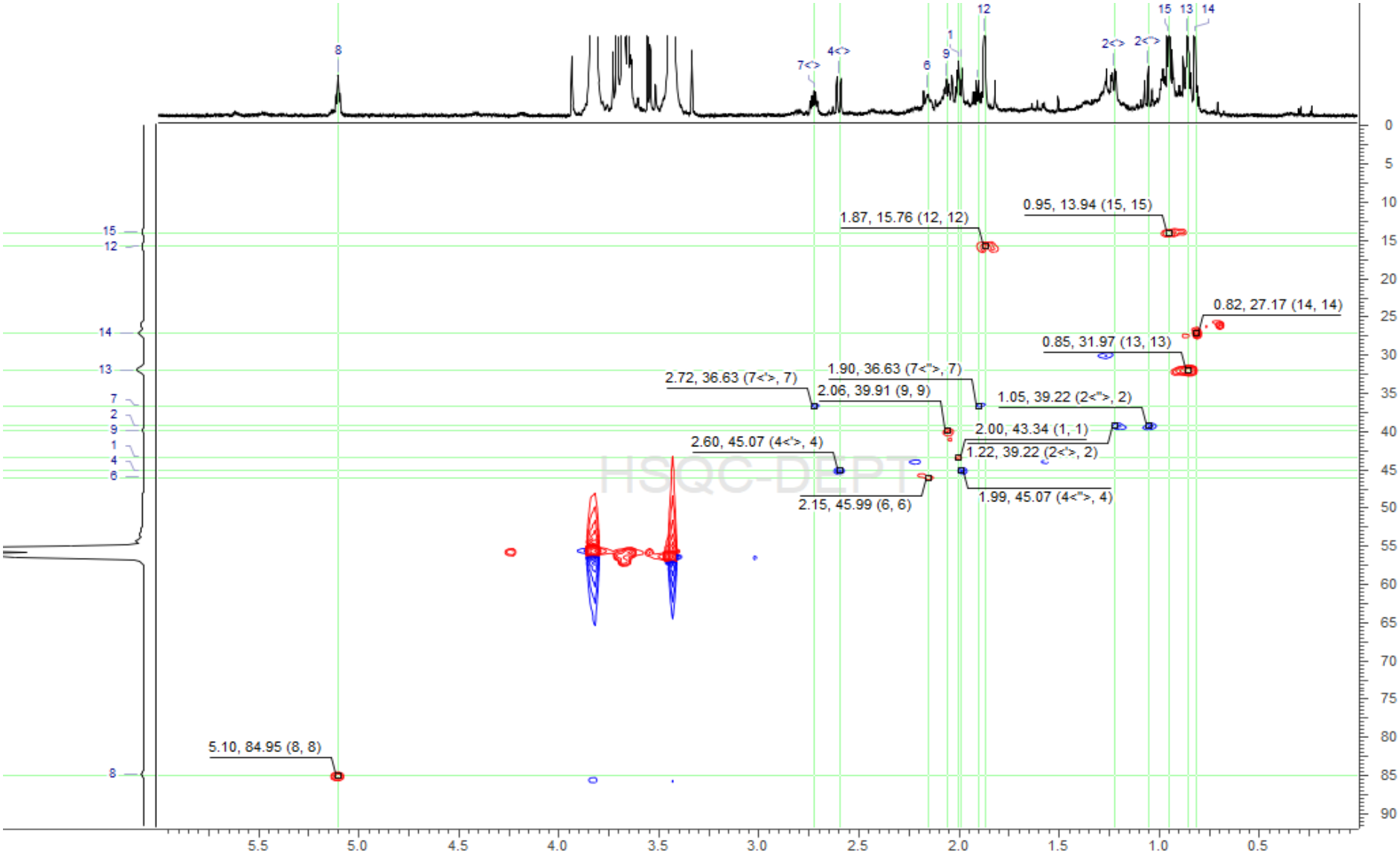

Figure S70 HSQC NMR spectrum (700 MHz, pyridin-d_5) of the *S*-MTPA ester of xylarenic acid B **6**.

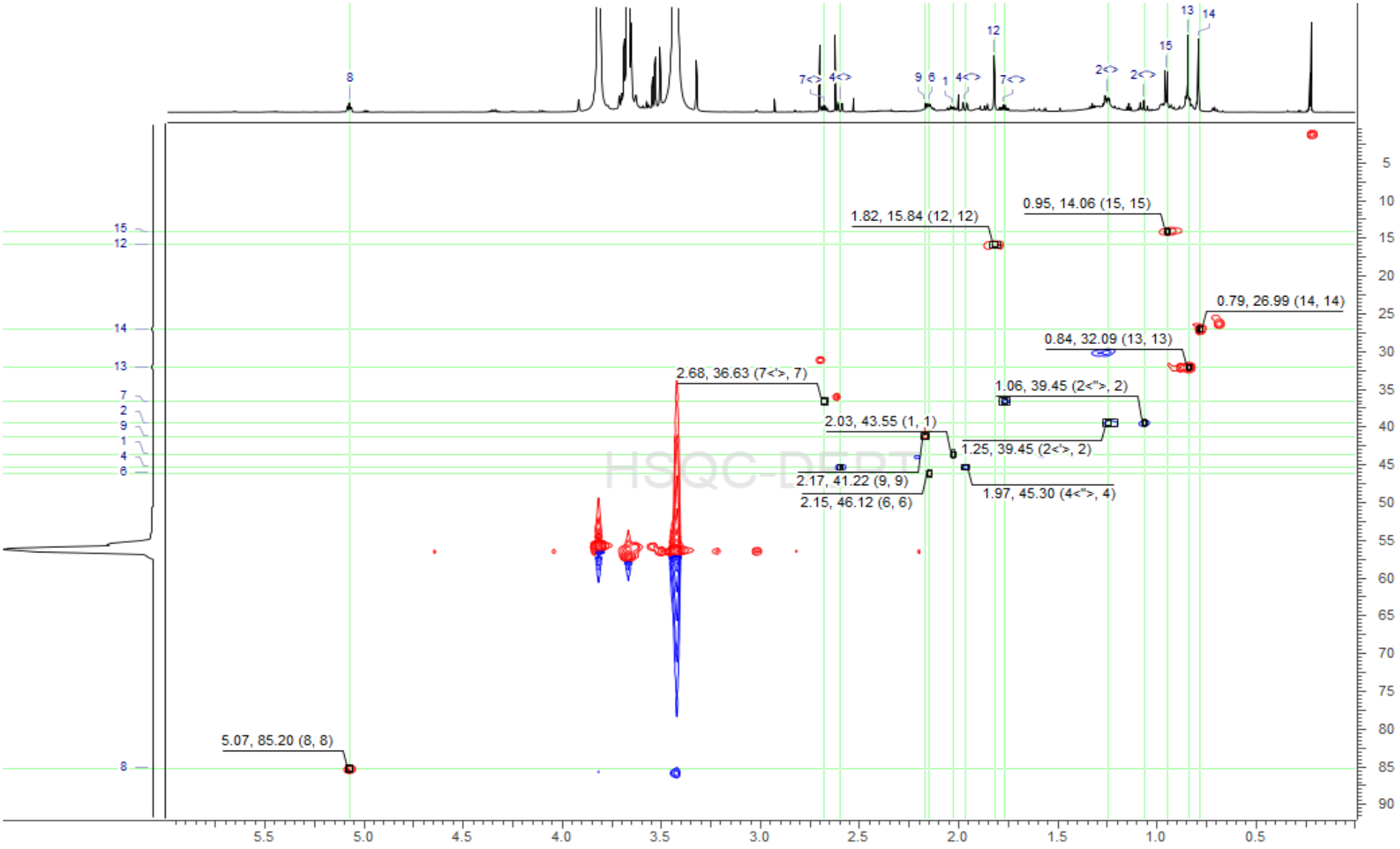

Figure S71 HSQC NMR spectrum (700 MHz, pyridin-d_5) of the *R*-MTPA ester of xylarenic acid B **6**.

References

(1) Kuhnert, E.; Sir, E. B.; Lambert, C.; Hyde, K. D.; Hladki, A. I.; Romero, A. I.; Rohde, M.; Stadler, M. *Fungal Divers.* **2017**, *85* (1), 1–43.

(2) Wibberg, D.; Stadler, M.; Lambert, C.; Bunk, B.; Spröer, C.; Rückert, C.; Kalinowski, J.; Cox, R. J.; Kuhnert, E. *Fungal Divers.* **2020**, https://doi.org/10.1007/s13225-020-00447-5.

(3) Stanke, M.; Diekhans, M.; Baertsch, R.; Haussler, D. *Bioinformatics* **2008**, *24* (5), 637–644.

(4) Ter-Hovhannisyan, V.; Lomsadze, A.; Chernoff, Y. O.; Borodovsky, M. *Genome Res.* **2008**, *18* (12), 1979–1990.

(5) Meyer, F. *Nucleic Acids Res.* **2003**, *31* (8), 2187–2195.

(6) Rupp, O.; Becker, J.; Brinkrolf, K.; Timmermann, C.; Borth, N.; Pühler, A.; Noll, T.; Goesmann, A. *PLoS One* **2014**, *9* (1), e85568.

(7) Sun, X.; Cai, Y.-S.; Yuan, Y.; Bian, G.; Ye, Z.; Deng, Z.; Liu, T. *Beilstein J. Org. Chem.* **2019**, *15*, 2052–2058.

(8) Murai, K.; Lauterbach, L.; Teramoto, K.; Quan, Z.; Barra, L.; Yamamoto, T.; Nonaka, K.; Shiomi, K.; Nishiyama, M.; Kuzuyama, T.; Dickschat, J. S. *Angew. Chemie Int. Ed.* **2019**, *58* (42), 15046–15050.

(9) A. K. Pahirulzaman, K.; Williams, K.; Lazarus, C. M. A Toolkit for Heterologous Expression of Metabolic Pathways in Aspergillus Oryzae. In *Methods in Enzymology*; 2012; pp 241–260.

(10) Kahlert, L.; Bassiony, E. F.; Cox, R. J.; Skellam, E. J. *Angew. Chemie* **2020**, *132* (14), 5865–5871.

(11) Jin, F. J.; Maruyama, J.; Juvvadi, P. R.; Arioka, M.; Kitamoto, K. *FEMS Microbiol. Lett.* **2004**, *239* (1), 79–85.

(12) Hu, D.-B.; Zhang, S.; He, J.-B.; Dong, Z.-J.; Li, Z.-H.; Feng, T.; Liu, J.-K. *Fitoterapia* **2015**, *104*, 50–54.

(13) Basnet, B. B.; Chen, B.; Suleimen, Y. M.; Ma, K.; Guo, S.; Bao, L.; Huang, Y.; Liu, H. *Planta Med.* **2019**, *85* (13), 1088–1097.